

FEDERAL UNIVERSITY OF PARAÍBA
CENTER FOR EXACT AND EARTH SCIENCES
PHYSICS DEPARTMENT

JOÃO PAULO DA MATA ARAÚJO PINHEIRO

PHENOMENOLOGICAL AND THEORETICAL
ASPECTS OF LOW ENERGY SCALE TYPE
II SEESAW MECHANISM

ADVISOR:
PROF. CARLOS ANTÔNIO DE SOUSA PIRES

João Pessoa - PB

July 2021

JOÃO PAULO DA MATA ARAÚJO PINHEIRO

PHENOMENOLOGICAL AND THEORETICAL ASPECTS OF LOW ENERGY SCALE TYPE II SEESAW MECHANISM

Thesis presented to the Graduate Program in
Physics of the Federal University of Paraíba,
as part of the requirements to obtain the De-
gree of Master of Physics.

Advisor: Dr. Carlos Antônio de Sousa
Pires.

João Pessoa - PB

July 2021

Catálogo na publicação
Seção de Catalogação e Classificação

P654p Pinheiro, João Paulo da Mata Araújo.

Phenomenological and theoretical aspects of low energy
scale type II seesaw mechanism / João Paulo da Mata
Araújo Pinheiro. - João Pessoa, 2021.

101 f. : il.

Orientação: Carlos Antônio de Sousa Pires.

Dissertação (Mestrado) - UFPB/CCEN.

1. Neutrinos estéreis leves. 2. Seesaw do tipo II. 3.
Seesaw do tipo II em baixas energias. 4. Modelo 123. 5.
Mecanismo seesaw. 6. Fenomenologia do seesaw do tipo
II. I. Pires, Carlos Antônio de Sousa. II. Título.

UFPB/BC

CDU 539.123(043)

FEDERAL UNIVERSITY OF PARAÍBA
CENTER FOR EXACT AND EARTH SCIENCES
PHYSICS DEPARTMENT

JOÃO PAULO DA MATA ARAÚJO PINHEIRO

PHENOMENOLOGICAL AND THEORETICAL ASPECTS OF LOW ENERGY SCALE TYPE II SEESAW MECHANISM

Comissão Examinadora:

Dr. Carlos Antônio de Sousa Pires (UFPB - Orientador)

Dr. Farinaldo Queiroz (UFPB e UFRN - Membro interno)

Dra. Maria Concepcion Gonzalez-Garcia (Stony Brook University e Universitat de Barcelona
- Membro externo)

João Pessoa - PB

July 2021

Ata da Sessão Pública da Defesa de
Dissertação de **Mestrado** do aluno **João
Paulo da Mata Araujo Pinheiro**, candidato
ao Título de Mestre em Física na Área de
Concentração Física das Partículas
Elementares e Campos.

Aos vinte e oito dias do mês de julho do ano de dois mil e vinte e um, às 10:00, reuniram-se, remotamente, os membros da Banca Examinadora constituída para examinar o candidato ao grau de Mestre em Física na área de Física das Partículas Elementares e Campos, **João Paulo da Mata Araujo Pinheiro**. A comissão examinadora composta pelos professores doutores: Carlos Antônio de Sousa Pires (DF/UFPB), orientador e presidente da banca examinadora, Farinaldo Queiroz (DF/UFPB) e Maria Gonzales-Garcia (Stony Brooke University). Dando início aos trabalhos, o Prof. Carlos Antônio de Sousa Pires comunicou aos presentes a finalidade da reunião. A seguir, passou a palavra o candidato para que o mesmo fizesse, oralmente, a exposição do trabalho de dissertação intitulado "*Phenomenological and Theoretical Aspects of Low Energy Scale Type II Seesaw Mechanism*". Concluída a exposição, o candidato foi arguido pela Banca Examinadora que emitiu o seguinte parecer: **"aprovado"**. Assim sendo, deve a Universidade Federal da Paraíba expedir o respectivo diploma de Mestre em Física na forma da lei. E para constar, eu, José Sérgio Trindade Silva, lavrei esta ata que vai assinada por mim e pelos membros da Banca Examinadora. João Pessoa, **28 de julho de 2021**.

Prof. Dr. Carlos Antônio de Sousa Pires

Orientador - UFPB

Prof. Dr. Farinaldo Queiroz

UFPB

Prof. Dr. Maria Gonzales-Garcia

Stony Brooke University

Link da reunião:

Agradecimentos

A minha (por enquanto) curta jornada na física só foi possível por conta de algumas poucas pessoas. Primeiramente, existem quatro pessoas que me deram os meios necessários para seguir a minha vocação. Meus pais, Ednólia e Júnior, minha querida avó, Eudália e minha tia Áurea. Com eles pude comer, me hospedar e sempre ter um conforto emocional e muitos (muitos mesmo) conselhos de como viver. Existiram outras tantas pessoas que me deram suporte, como a minha irmã, Paula, e minha avó paterna Ana, e o meu tio Tércio.

Não foram anos fáceis, seis anos longe da minha família. Mas essa angústia foi arrefecida pelos meus bons amigos da física, Jefferson, Vinícius e William, com quem tive longas discussões e excelentes comemorações. Não posso esquecer também dos meus bons amigos de Natal, Leandro e Jacinto, que sempre estão dispostos a terem uma boa conversa sobre física.

Não obstante, existem em especial alguns professores que desejo agradecer. Ser aluno da UFPB me fez conhecer pessoas maravilhosas, como o professor Farinaldo, que mesmo sem muito contato, foi um espelho para mim de produção acadêmica, relevância na comunidade, esforço em desenvolver a ciência local e uma honestidade absurda. Outro professor relevante na minha formação e que acima de tudo é um amigo para mim é Paulo Sérgio. Ele foi o primeiro professor a acreditar no meu potencial e me fez aprender muito sobre física de partículas, mas também sobre como ser uma pessoa reta e exigente. Mas o professor que mais me deu formação, mais fez parte da minha vida e que espero estar perto até o fim da vida, é o professor Carlos Pires. Inúmeras reuniões que se estenderam por horas, incontáveis áudios no whatsapp discutindo física, conselhos pessoais, conselhos profissionais, cobranças construtivas. Carlos foi e é o responsável pela minha transição de aluno de física para um pesquisador, e a dívida que tenho com ele é eterna.

Por fim, agradeço ao Cnpq, pelo apoio financeiro.

‘Plato and the neo-Platonists taught that the beauty we see in nature is a reflection of the beauty of the ultimate, the nous. For us, too, the beauty of present theories is an anticipation, a premonition, of the beauty of the final theory. And in any case, we would not accept any theory as final unless it were beautiful. ’

*Dreams of a Final Theory: The Scientist’s
Search for the Ultimate Laws of Nature -
Steven Weinberg*

Resumo

O Modelo Padrão das partículas elementares (MP) fornece a descrição mais acurada do comportamento da matéria nas menores escalas de distância acessíveis. Porém, esse modelo não acomoda neutrinos massivos, como não resolve outros problemas teóricos. Assim, é amplamente aceito que o MP deve ser estendido. Por outro lado, existem três mecanismos canônicos que elucidam a geração de massa leve para neutrinos de forma natural a nível de árvore. Dentre elas, a mais versátil é o tipo II seesaw (iremos explicar o porquê disso nesta tese). Uma simples realização deste mecanismo estende o MP por um tripleto escalar com hipercarga que interage com os dubletos leptônicos, conhecido como Modelo do Tripleto do Higgs (HTM). Depois da quebra espontânea de simetria (SSB), neutrinos de mão-esquerda ganham massa de Majorana. Como qualquer outro mecanismo seesaw, tem um termo que viola o número leptônico por duas unidades e a escala de energia na qual essa violação ocorre nos explica quão pesado são esses escalares. Por exemplo, se o número leptônico é explicitamente quebrado em baixas energias, os componentes do tripleto de escalares adquirem massas próximas a escala de TeV. Assim, é tentador estudar tais modelos fenomenologicamente viáveis e suas consequências nos colisores atuais, já que não é consenso se existe apenas um escalar, que é o Higgs padrão, ou uma realidade mais complexa de vários escalares. Nós discutimos muitos aspectos do HTM, pontuando as implicações fenomenológicas em cada caso. Em particular, procuramos em detalhes por novos processos de violação de sabor leptônico, decaimento em dois fótons de novos bósons de Higgs, decaimento do escalar duplamente carregado e a contribuição destas novas extensões para o espalhamento elétron-neutrino. Nós também discutimos a estabilidade do potencial do Higgs. Argumentamos sobre a possibilidade do vácuo do Higgs se tornar estável em um modelo mais complexo e sob quais configurações do espaço de parâmetros tais modelos precisam obedecer para garantir a estabilidade.

Palavras-Chave: Seesaw do tipo II, Seesaw do tipo II em baixas energias, Modelo 123, Neutrinos estéreis leves, Mecanismo seesaw, Fenomenologia do seesaw do tipo II.

Abstract

The Standard Model (SM) of Particle Physics provides the most accurate description of the behaviour of matter in the smallest accessible distance scales. However, since it does not account for the nonzero neutrino masses and it is also plagued with a number of theoretical, experimental and cosmological issues, it is widely accepted that the SM must be extended. Besides, there are three canonical mechanisms that elucidate naturally neutrino mass smallness at tree-level. Among them, the most versatile one is type II seesaw (in this thesis we will explain why). A simple realization of this mechanism extends SM by a scalar triplet with hypercharge that interacts with leptonic doublets, known as Higgs Triplet Model (HTM). After spontaneous symmetry breaking (SSB), left-handed neutrinos gain masses. As any other seesaw, it has a term that violates lepton number by two units and the energy scale in which this violation occur tell us how heavy are such new scalars. For example, if lepton number is explicitly broken at low energies, the scalar triplet components acquire masses near to TeV scales. Thus, it is tempting to study such phenomenological viable model and its consequences in actual colliders, since it is not settled if there is only the SM Higgs boson or a more complex scalar scheme. We discuss several aspects of HTM, highlighting phenomenological implications in each case. In particular, we searched in detail for new LFV processes, diphoton decay of the new Higgs boson, decay of the doubly-charged scalar and contribution of such extension to the $e - \nu$ scattering process. We also discuss about the stability of the Higgs potential. We argue about the possibility to the Higgs vacuum becomes stable in a more complex model and under what configuration of parametric space such model must obey to ensure stability.

Keywords: Type II seesaw, Low Scale Type II seesaw, 123 model, Light sterile neutrinos, Seesaw Mechanism, Phenomenology of the type II seesaw.

Contents

List of Publications	1
Introduction	1
1 Type II Seesaw Mechanism	12
1.1 Introduction	12
1.2 The Model	12
1.3 The Yukawa Sector	13
1.4 Naturalness principle and explicitly broken $B - L$ symmetry	15
1.5 Spontaneous Symmetry Breaking and Seesaw mechanism	15
1.6 Scalar Mass Spectrum	17
1.6.1 CP-even particles	17
1.6.2 CP-odd	18
1.6.3 Single charged particles	19
1.6.4 Double-charged particles	19
1.7 Potential Stability and Bounded From Below conditions	20
1.8 Discussion	21
2 Low Scale Type II Seesaw	23
2.1 Introduction	23
2.2 ϵ -Parameter and LFV processes	24
2.3 Low scale type II seesaw and Inverse Seesaw mechanism	27
2.4 False Vacuum and Higgs Metastability	30
2.4.1 False Vacuum vs True Vacuum	30
2.4.2 The Callan-Symanzik Equation	32
2.4.3 β -function interpretation	35
2.4.4 $\beta_{\lambda_{SM}}$ -function of the Standard Model	37
2.5 Two problems that cannot be solved simultaneously in this Triplet Extension	38
2.5.1 Vacuum Stability at High Scales	38
2.5.2 One-loop Higgs Mass Correction	39
2.6 Discussion	40

3	Phenomenology of the Low Scale Type II Seesaw Mechanism	41
3.1	Doubly-charged scalar branching ratios	42
3.2	Neutrino-Electron Scattering in Type II Seesaw	45
3.3	CP-odd scalar decay	47
3.4	CP-even scalar decays and diphoton decay	49
3.5	Final Remarks	52
4	123 Model	54
4.1	Introduction	54
4.2	The 1-2-3 model	55
4.3	The Yukawa Sector	56
4.4	Spontaneous Symmetry Breaking	57
4.5	Scalar sector	57
4.5.1	Spectrum of scalars	58
4.5.2	Some constraints	61
4.6	Light Sterile Neutrinos	63
4.7	Vacuum Stability	64
4.7.1	Bounded from below conditions	64
4.7.2	RGE-evolution of the self coupling of the standard-like Higgs	68
4.8	Discussion	69
	Conclusion	71
	Appendices	73
A	Proof that α is limited between $[-1,1]$ interval	74
B	(1PI) and Amputated diagrams - Renormalization conditions	76

List of Figures

1	Dimension-5 operator represented as a Feynman diagram.	6
2	Type I seesaw recovering dimension-5 operator	9
3	Type II seesaw recovering the dimension-5 operator.	10
4	Type III seesaw recovering the dimension-5 operator.	11
1.1	Some possible values for the quartic couplings of the potential using unitarity and BFB conditions.	22
2.1	This plot represents how the vev v_3 changes compared to the ϵ -parameter, supposing that the doubly and singly-charged particles are degenerated in mass.	26
2.2	This figure represents three different ways in which the false vacuum transits to the true vacuum. To transit using Quantum and Thermal fluctuations, the false ground state climbs the potential barrier, going to the true vacuum. However, Tunneling this potential barrier is the most effective way for this transition.	30
2.3	Here we represent a projection of an inclined "mexican hat", in which ϕ_- is the true vacuum of this potential and ϕ_+ is a local minima, but not a global one.	31
2.4	The Green's function $G^{(4)}$ at one-loop perturbation theory. We need to calculate each of these diagrams to find the β -function of the quartic coupling λ	35
2.5	This plot represents the stability of the SM vacuum state in the Higgs and top masses. Ellipses show the 1σ , 2σ , 3σ confidence intervals for m_t and m_h around their central values. In the green region, the current vacuum is absolutely stable, in the yellow region it is metastable, and in the red region it is so unstable that it would not have survived until the present day. These blue and red dotted line are associated with cosmological constraints, assuming values for the Reheating temperature T_{RH} . This ξ parameter is associated with gravitational corrections in the vacuum state of the universe. More detailed explanation in the cited paper.	38

2.6	The dashed blue line represents the SM prediction. In the triplet model, the red thick line, $\lambda_4 = 0.5$. Commonly the other parameters are taken as $\lambda_1 = \lambda_2 = \lambda_3 = 0.1$. We have observed that this model can have a stable vacuum at high scales.	39
3.1	For $v_3 = 1 \text{ eV}$, leptonic decays are totally predominant in the doubly charged scalar channel. We have fixed $m_{\nu 1} = 0$ in Normal Hierarchy, using Eq. 2.3.	43
3.2	For $v_3 = 100 \text{ eV}$, leptonic decays are predominant in the doubly charged scalar channel. We have fixed $m_{\nu 1} = 0$ in Normal Hierarchy, using Eq. 2.3.	43
3.3	For $v_3 = 1 \text{ keV}$, W boson decays are predominant in the doubly charged scalar channel. We have fixed $m_{\nu 1} = 0$ in Normal Hierarchy, using Eq. 2.3.	43
3.4	For $v_3 = 10 \text{ keV}$, W boson decays are totally predominant in the doubly charged scalar channel. We have fixed $m_{\nu 1} = 0$ in Normal Hierarchy, using Eq. 2.3.	44
3.5	Feynman Diagrams responsible for the neutrino-electron scattering.	46
3.6	New Feynman diagram that predominantly contributes for the $e - \nu$ scattering.	46
3.7	Here we can see that r becomes irrelevant for current experiments, if triplet scalar masses are high above TeV scales.	48
3.8	Total diphoton decay of the Heavy Higgs.	50
3.9	Here we divided in two regions to understand completely the behavior of the R_W parameter.	52
4.1	Running of $\lambda_\Phi \approx \lambda_1$ at one-loop level as a function of the energy scale μ for $\lambda_5 = \lambda_3 = \beta_2 = 0.001$ with $y_t = 0.9965$, $g_Y = 0.4627$ and $g = 0.6535$. The dotted line represents the expectation of Standard Model and the red line represents the expectation for our model for two values of κ	68
4.2	Running of $\lambda_\Delta \approx \lambda_2 + \lambda_4$ at one-loop level as a function of the energy scale μ for $\lambda_5 = \lambda_3 = \beta_2 = 0.001$ with $y_t = 0.9965$, $g_Y = 0.4627$ and $g = 0.6535$. The dotted lines represents the expectation for our model for three values of κ . The coupling β_3 is important in the same level as κ for this running.	69
4.3	Running of $\lambda_\sigma \approx \beta_1$ at one-loop level as a function of the energy scale μ for $\lambda_5 = \lambda_3 = \beta_2 = 0.001$ with $y_t = 0.9965$, $g_Y = 0.4627$ and $g = 0.6535$. The dotted lines represents the expectation for our model for three values of β_3	69
B.1	The left diagram is ($1PI$), while the right diagram is not, because we can trace a (red)line that can divide this diagram in two.	76
B.2	The sum of $1PI$ diagrams for the simple scalar theory.	77

- B.3 Now, the total contribution is simply all combinations of $1PI$. Then, we must use the geometric series well know result, for the case in which higher orders of perturbation theory contributes less than lower orders. 77
- B.4 The definition of an amputated 4-point diagram. We cut-off the legs of this diagram, representing this with the red lines. Then, an amputated diagram is the irreducible four-point correction. 79
- B.5 Here we define an amputated diagram for the simple ϕ^4 -theory. 79

List of Tables

- 2.1 This table represent different neutrino Yukawa coupling values after fixing the triplet vev in the values 3 eV , 6 eV and 9 eV . After looking at how these Yukawa couplings evolves, it became clear that it is important to keep v_3 small as possible if it is wanted natural Yukawa couplings. 27

- 3.1 Here we have some values for the parameters a and b for each process that contributes for the $e - \nu$ scattering 46

List of publications

The original content of this thesis was based on the following publication:

J. P. Pinheiro and C. A. de S. Pires, “Vacuum stability and spontaneous violation of the lepton number at a low-energy scale in a model for light sterile neutrinos,” *Phys. Rev. D* **102**, no.1, 015015 (2020) doi:10.1103/PhysRevD.102.015015 [arXiv:2003.02350 [hep-ph]].

A non related pre-print, developed during my master and submitted to JHEP journal was:

J. P. Pinheiro, C. A. d. S. Pires, F. S. Queiroz and Y. S. Villamizar, “Confronting the inverse seesaw mechanism with the recent muon $g-2$ result,” [arXiv:2107.01315 [hep-ph]].

Introduction

According to the Merriam-Webster Dictionary, *a standard is something established by authority, custom, or general consent as a model or example*. The Standard Model of particle physics (SM) is, in fact, a well defined framework for particle physics modeling upon which we can test our understanding of the fundamental structure of matter. But standard is also of *recognized authority, competence, or excellence*; the SM has provided, since its proposal, an accurate description of most experimental results and precisely predicted a wide variety of phenomena.

The Standard Model is build as a quantum field theory that describes interactions between fermionic (as quarks and leptons) and bosonic fields (as the photon)[1, 2, 3, 4, 5]. Such interactions are represented in a mathematical object called Lagrangian that encodes all main aspects of a model. In general, there are some criteria that a Lagrangian needs to obey in order to describe a consistent quantum field theory of fundamental forces. One well known is that any interaction between fields must respect Lorentz invariance. However, such principle is general and do not specify a dynamics, but only ensure that a quantum observable must not depend on a specific time or position in space-time. Aside from this criterion, the most important one is the principle of local gauge invariance, which tells us that the interactions of vector bosons are associated with a global symmetry group. The form of these interactions is uniquely specified by the group structure. Therefore, from the knowledge of the basic symmetry group, we can write down the Lagrangian or the equations of motion. Specifying the group to be $U(1)$, we derive electromagnetism, for example.

Thus, a Lagrangian can only remain invariant if the forces interacts in a particular way. Thereby, one can relate a local gauge symmetry in a Lagrangian, a pure mathematical construction, with the dynamics of quantum particles, measured by experiments. Although a mathematical elegance has thus been achieved, the results of such construction are incomplete in several important aspects. First, the gauge principle has led us to theories in which all the interactions are mediated by massless vector bosons, whereas only a single massless vector boson, the photon, is directly apparent in nature. Second, the construction of gauge theories reacquires a exact symmetric Lagrangian, whereas nature exhibits numerous symmetries that are only approximate. Thereby, including in such framework the famous Higgs mechanism it is vital, since it is a way to deal with symmetries that are not exact or not manifest, evading the conclusion that interactions must be

mediated by massless gauge bosons.

Hence, the Standard Model can be associated with the following global symmetric group,

$$SU(3)_C \otimes SU(2)_L \otimes U(1)_Y,$$

and after Spontaneous Symmetry Breaking (SSB) lead by the Higgs mechanism, the invariance by

$$SU(3)_C \otimes U(1)_{EM},$$

predicting the existence of the massless photon, at the same time it describes short range interactions by massive gauge bosons W^\pm and Z^0 , and hadronic physics explained by $SU(3)_C$ symmetry. A last piece to solve this puzzle was the renormability of the SM[6, 7, 8]. t'Hooft and others successfully proved that Standard Model is renormalizable, avoiding ultraviolet divergences, and this really was the icing on the cake[9, 10, 11].

Nevertheless, after discussing some general principles about dynamics and short range interactions, one can ask what is the particle content of the SM? In short: The gauge bosons and its interactions: Electromagnetism has one source, electric charge, and one boson, the photon; the weak force has two weak charges and three mediators, W^\pm and Z^0 ; the strong force has three strong charges and eight bosons (gluons). The Higgs boson is responsible to generate particles masses. Fermionic content: three generations of charged and neutral leptons. Since quarks have color charges, there are three generations of up and down quarks and each of them has three colors.

After the Higgs boson detection at the LHC, all proposed SM particles were discovered and well understood. Experiments described their interactions precisely, very similar to theoretical expectations only with small deviations. However, there are many open questions of different nature that the SM cannot answer. There are questions that comes from theoretical, cosmological and experimental points of view. Example of cosmological questions are, *what is the nature of the dark matter that constitutes 80% of the matter in the Universe?* and *There is some CP violation beyond the SM that may explain the dominance of matter over antimatter in the Universe today?* There is no SM candidate for the dark matter, but there are good arguments that it might appear at TeV scale. Moreover, quark sector is not sufficient source to generate the correct pattern of CP violation that solves matter-antimatter problem.

From a theoretical point of view, one natural question that appear is *What is the origin of particle masses?* This work aims to answer this question for neutrino particles. However, to understand it deeply, we need to ask ourselves how SM generate masses for fermions. In the SM framework, fermionic masses are generated at tree-level by the SSB of the following Yukawa interaction,

$$\mathcal{L}_{Yukawa} = (y_{ij} h^0 \bar{\psi}_i \psi_j + H.c.) \xrightarrow{\text{EWSB}} (y_{ij} \frac{v}{\sqrt{2}} \bar{\psi}_i \psi_j + H.c.), \quad (1)$$

where $v \approx 246 \text{ GeV}$. These dimensionless couplings y_{ij} are arbitrary and one needs only to find experimentally the mass of some particle (as the mass of the electron, that is close to 0.5 MeV) and divide this value by 174 GeV to find the correct value for the Yukawa couplings ($y_e \approx 3 \times 10^{-6}$). There is none fundamental principle that guide our understanding in *how particles have exact the measured values?* or *Why an electron do not have a mass close to 0.5 keV ?*

Experimentally, there are mainly two facts that are a direct probe that the SM is an incomplete representation of the fundamental structure of matter. Recently, the $g - 2$ anomaly requires non SM interactions to explain its actual measured value[12, 13], but we will not dig too much about this. The other and more well known are experiments related to neutrino oscillations[14, 15, 16, 17, 18], establishing that active neutrinos are massive, their masses are much smaller than those of the other SM fermions and weak flavor neutrinos states maximally mix with each other. But, why Standard Model cannot explain neutrino masses?

We have saw that in Eq. 1, fermionic masses are generated in the Yukawa sector. For an arbitrary fermion ψ we always can write its field as a linear combination of its chiral states ψ_R and ψ_L as

$$\psi = \psi_R + \psi_L$$

and its mass Lagrangian can be written as[19]

$$\mathcal{L}_{mass} = m(\bar{\psi}_R \psi_L + H.c.), \quad (2)$$

known as a Dirac mass term.

Then, one must have simultaneously Right-handed and Left-handed states in order to generate fermionic masses. Since the SM do not have a right-handed state for neutrinos, then clearly cannot generate masses for neutrinos in the usual way, without an extension. However, there is another way to generate neutrino masses, in which one needs one chiral state. But, we can reproduce such type of mass in the SM?

Following the discussions in [20, 21], there is only one way to write a mass term for the neutrinos using ν_L that is Lorentz invariant. Nonetheless, it can be shown that such chiral term is written as

$$\nu_{L(R)}^C = C \bar{\nu}_{L(R)}^T,$$

where C is the charge conjugation operator. ν_L^C and ν_R^C are left and right-handed fields, respectively ($P_{R(L)} \nu_{L(R)}^C \neq 0$). Therefore the coupling $\bar{\nu}_{L(R)}^C \nu_{L(R)}$ does not vanish [20][21]. These references shows that $\nu_{L(R)}^C$ has the correct properties to be used in place of $\nu_{R(L)}$ in the Dirac mass term, leading to the Majorana mass term

$$\mathcal{L}_{mass}^M = -\frac{1}{2} m \bar{\nu}_{L(R)}^C \nu_{L(R)} + H.c., \quad (3)$$

and clearly violates lepton number by two units.

After establishing Majorana mass term, we can answer if it is possible to have an interaction in the SM that reproduces this Lagrangian for left-handed neutrinos. At tree-level the answer is negative, because left-handed neutrino field has a third component I_3 of the weak isospin equal to $1/2$ and hypercharge Y equal to -1 . Then, it follows that the mass term

$$\bar{\nu}_L^C \nu_L$$

has the SM quantum numbers $I_3 = 1$ and $Y = -2$. Since the SM does not contain any weak isospin triplet with $Y = 2$, it is not possible to have a renormalizable Lagrangian term which can generate a Majorana neutrino mass at tree-level.

When we go beyond simple tree-level approximation, one cannot generate a Majorana term in the SM simply because there is no broken lepton number interaction in the SM Lagrangian, even after EWSB. This means that a Majorana mass term cannot be generated to all orders in perturbation theory in the SM framework, which imply that neutrinos are massless even beyond tree-level in the SM.

Then, as usual in any scientific procedure, one must build a framework that accommodates our previous successful results and at the same time explains the new facts. The most trivial way is extending the Standard Model. As we will discuss, a simple extension is sufficient to accommodate neutrino masses. We have saw that fermions needs RH and LH states in order to generate masses by the trivial Higgs mechanism. So, is it possible to add in the SM a right-handed neutrino? Saying the truth, there is no fundamental reason why there is no right-handed states for neutrinos (RHNs) in the fermionic content of SM, as one does for all other fermions. The ν_R state was not introduced just because there was no conclusive experiments that states the existence of masses for the neutrinos. Nonetheless, one can just as well arrange things in some other way. Another SM massless particle is the photon. However, its masslessness is a consequence of a local $U(1)$ gauge symmetry which governs the dynamics of the electromagnetic interaction. For neutrinos, we see no such symmetry principle in the SM.

Naturally, introducing RHNs fields in the SM will not only generate masses for neutrinos, but the asymmetry in the SM between the lepton and quark sectors due to the absence of RHNs is eliminated. To accommodate neutrino masses one can extent the SM adding to it three RHNs N_{Ri} and allowing them to interact in the following way

$$\mathcal{L}_\nu = Y'_D \bar{L}' \tilde{\Phi} N'_R + H.c. \xrightarrow{\text{EWSB}} \mathcal{L}_\nu = Y'_D \frac{v}{\sqrt{2}} \bar{N}'_R \nu'_L + H.c.,$$

such that Φ is the standard doublet scalar, L' is the left-handed leptonic doublet and $N'_R \equiv (N'_{eR}, N'_{\mu R}, N'_{\tau R})^T$. Nevertheless, after Electroweak Symmetry Breaking (EWSB), neutrinos gain masses in the same way as up-quarks. Such new interaction is invariant by gauge transformations, since RHNs are sterile under SM gauge group, $L' \sim (\mathbf{1}, \mathbf{2}, -1)$ and $\tilde{\Phi} \sim (\mathbf{1}, \mathbf{2}, -1)$. Such model is sometimes called the minimally extended Standard

Model. The matrix Y'_D of neutrino Yukawa couplings can be diagonalized as

$$V_L^{\nu\dagger} Y'_D V_R^\nu = Y_D, \quad \text{with } Y_{Dkj} = y_k^D \delta_{kj} \quad (k, j = 1, 2, 3), \quad (4)$$

with real and positive y_k^D . Here V_L^ν and V_R^ν are two appropriate 3×3 unitary matrices. Defining the chiral massive neutrino arrays

$$n_L = V_L^\nu \nu'_L, \quad n_R = V_R^\nu N'_R, \quad (5)$$

the diagonalized neutrino mass Lagrangian reads

$$\mathcal{L}_\nu = \frac{y_k^D v}{\sqrt{2}} \bar{n}_{kR} n_{kL} + H.c., \quad (6)$$

and neutrino masses are given by

$$m_k = \frac{y_k^D v}{\sqrt{2}}, \quad (7)$$

such that $v \approx 246 \text{ GeV}$ is the EW vacuum.

For usual Dirac mass term, the total lepton number is conserved. This is so because the Dirac mass Lagrangian is invariant under the global $U(1)$ gauge transformations. Noether's theorem implies that there is a conserved current and consequently a conserved charge. In this case, it can be proved[20][21] that neutrinos and negatively charged leptons have $L = +1$, whereas antineutrinos and positively charged leptons have $L = -1$, as in SM. Therefore, leptonic quantum numbers are different for neutrinos and antineutrinos. Such distinction between neutrinos and antineutrinos is important for classification of the states describing physical systems with one or more neutrinos and antineutrinos. Hence, Dirac character of massive neutrinos, implying that neutrinos and antineutrinos are different particles, is closely related to the invariance of the total Lagrangian under the global $U(1)$ gauge transformation.

It is important to note that neutrino masses that we have obtained with such mechanism are proportional to the standard EW vev as the masses of another charged leptons. However, it is known that the masses of neutrinos are much smaller than those of charged fermions, in such a way that the ratio between the lightest charged fermion mass (at MeV scales) and the heaviest neutrino mass (at eV scales) is near to 10^{-6} . In the mechanism that we have just described, thus, there is no theoretical explanation of the very small values of the eigenvalues y_k^D of the Higgs-neutrino Yukawa coupling matrix that are needed.

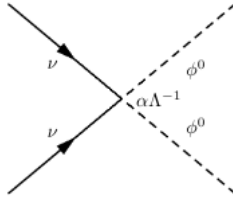


Figure 1: Dimension-5 operator represented as a Feynman diagram.

Introducing a small coupling constant as $y_k \sim 10^{-11}$ into a theory is generally considered unnatural and a powerful theory must find a symmetry reason for such smallness[22]. Then, one can imagine a theoretical framework where neutrino masses are due a perturbation of some symmetry, in which such small asymmetry is totally related with a tiny masses for the neutrinos as in [23][24]

$$\mathcal{L} = \mathcal{L}_0 + \delta\mathcal{L}.$$

As we will discuss, such small asymmetry has a connection between the global $B - L$ number violation and a Majorana mass term[25]. The lowest dimensional term which could generate a Majorana neutrino mass that one can construct with the SM fields, respecting SM symmetries, is the lepton number violation term [26]

$$\mathcal{L}_5 = \frac{\alpha}{\Lambda}(L'^T \sigma_2 \Phi) C^\dagger (\Phi^T \sigma_2 L') + H.c., \quad (8)$$

such that σ_i are well known Pauli matrices, Λ is a effective mass coupling and α is a dimensionless coupling coefficient.

After EWSB, such interaction generates the following masses of the neutrinos

$$M_{\nu ij} \bar{\nu}_{L i}^C \nu_{L j} \rightarrow M_{\nu ij} = \alpha_{ij} \Lambda^{-1} v^2. \quad (9)$$

The Lagrangian term \mathcal{L}_5 is not acceptable in the framework of the SM because it contains a product of fields with energy dimension five, which is not renormalizable [27].

To include \mathcal{L}_5 as a perturbative Lagrangian of the total symmetric Lagrangian \mathcal{L}_0 that conserves $B - L$ symmetry, one must fix Λ to be sufficiently large. Therefore, this choice naturally encompass tiny masses for neutrinos, counterbalancing the Higgs vev and generating neutrino masses at eV . As draw in Fig. 1, it can be seen as a contact interaction whose the contact point is given by $\alpha\Lambda^{-1}$. This way to counterbalance different energy scales to give the correct neutrino mass pattern is generally known as "Seesaw Mechanism".

Therefore, we can extend the SM to recover the same structure of the dimension-5 operator using many well motivated renormalizable models. Such models always encom-

passes lepton number violation and consequently imposes that all neutrinos are Majorana fermions. As shown by [28] there is only three of these constructions that recovers minimally such operator at tree-level, known as canonical Type I [29, 25, 30, 31], Type II [32, 33, 34, 35, 36] and Type III [37] seesaw mechanisms.

Canonical Type I: Since the RHNs are invariant under $SU(2)_L \otimes U(1)_Y$, so must be their conjugate field,

$$N_{Ri} \sim (1, 1, 0) \rightarrow \bar{N}_{Ri}^C \sim (1, 1, 0).$$

Thus, one can form gauge invariant mass terms

$$\mathcal{L}_{Maj} = \frac{1}{2} M_{Rij} \bar{N}_{Ri}^C N'_{Rj} + H.c..$$

These terms must be present if we write down the most general gauge-invariant Lagrangian involving the particles in the model. Therefore, such term is a Majorana mass term and consequently violates lepton number by 2 units. If we imposes $B - L$ symmetry, then such interaction vanishes and we go back to the model with Dirac neutrinos. The total Lagrangian that give masses for neutrinos can be written as

$$\mathcal{L}_\nu = Y_D \bar{L}' \tilde{\Phi} N'_R + \frac{1}{2} M_R \bar{N}'^C_R N'_R + H.c. \xrightarrow{\text{EWSB}} \mathcal{L}_\nu = m_D \bar{N}'_R \nu'_L + \frac{1}{2} M_R \bar{N}'^C_R N'_R + H.c.. \quad (10)$$

Now, it is convenient to define the column matrix of $N = 3 + 3$ left-handed fields

$$N'_L \equiv \begin{pmatrix} \nu'_L \\ N'^C_R \end{pmatrix}. \quad (11)$$

In this way, the Dirac-Majorana mass term can be written in the compact form

$$\mathcal{L}_\nu = \frac{1}{2} N'^T_L C^\dagger M^{D+M} N'_L + H.c., \quad (12)$$

with the 6×6 symmetric mass matrix

$$M^{D+M} = \begin{pmatrix} 0 & m_D \\ m_D^T & M_R \end{pmatrix}. \quad (13)$$

Now, the diagonalization of the Dirac-Majorana mass term is formally written by

$$N'_L = V_L^\nu n_L, \quad \text{with} \quad n_L = \begin{pmatrix} \nu_{1L} \\ \nu_{2L} \\ \nu_{3L} \\ \nu_{4L} \\ \nu_{5L} \\ \nu_{6L} \end{pmatrix}. \quad (14)$$

The unitary matrix V_L^ν is chosen in order to diagonalize the symmetric mass matrix

$$(V_L^\nu)^T M^{D+M} V_L^\nu = M, \quad \text{where} \quad M_{kj} = m_k \delta_{kj}, \quad (15)$$

with real and positive masses m_k . After this diagonalization, one must define the neutrino fields as mass eigenstates and discovers that they are Majorana fields [20][21].

Since M_R is not constrained by the SM symmetries, it is natural to choose it to be at a scale much higher than the weak scale. Then, imposing that $M_R \gg m_D$, the mass matrix can be diagonalized by blocks, up to corrections of the order $(M_R)^{-1} m_D$:

$$W^T M^{D+M} W \approx \begin{pmatrix} M_{light} & 0 \\ 0 & M_{heavy} \end{pmatrix}, \quad (16)$$

with

$$W \approx \begin{pmatrix} 1 - \frac{1}{2} m_D^\dagger (M_R M_R^\dagger)^{-1} m_D & [(M_R)^{-1} m_D]^\dagger \\ -(M_R)^{-1} m_D & 1 - \frac{1}{2} (M_R)^{-1} m_D m_D^\dagger (M_R^\dagger)^{-1} \end{pmatrix}. \quad (17)$$

The light 3×3 mass matrix M_{light} and the heavy 3×3 mass matrix M_{heavy} are given by

$$M_{light} \approx -m_D^T (M_R)^{-1} m_D, \quad M_{heavy} \approx M_R. \quad (18)$$

The heavy masses are given by the eigenvalues of M_R , whereas the light masses are given by the eigenvalues of M_{light} , whose elements are suppressed with respect to the elements of the Dirac mass matrix m_D by the small matrix factor $m_D^T (M_R)^{-1}$. As a matter of fact, after fixing the EW scale mass to be close to the EWSB energy scale, $m_D \sim 10^2 \text{ GeV}$, to recover neutrinos tiny masses, it requires that $M_R \sim 10^{14} - 10^{15} \text{ GeV}$. Here, we have recovered the same physics of the dimension-5 operator as a renormalizable model with the Feynman diagram in Fig. 2. In this case, M_R does the same role of Λ . Since sterile neutrinos have masses proportional to M_R , their masses are undetectable in actual and near future experiments.

Canonical Type II: As discussed in the beginning of this section, to generate Majorana masses for left-handed neutrinos at tree-level in a renormalizable way, without adding right-handed neutrinos, one must extent the SM by a colorless triplet scalar with

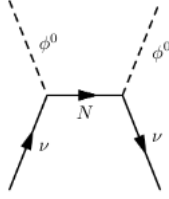


Figure 2: Type I seesaw recovering dimension-5 operator

hypercharge $Y = 2$. Then, the interaction

$$\Delta^0 \bar{\nu}_L^C \nu_L \quad (19)$$

becomes $SU(2)_L \times U(1)_Y$ invariant. Then, after SSB of the field Δ^0 , such interaction becomes a Majorana mass term. The triplet scalar field is fully represented by $\Delta = (\Delta^0, \Delta^+, \Delta^{++})^T$ and has six degrees of freedom, the same as if we introduce three RHNs. In $SU(2)_L$, there is many representations for this scalar field, but we will adopt here the following one

$$\Delta = \begin{pmatrix} \Delta^+/\sqrt{2} & -\Delta^{++} \\ \Delta^0 & -\Delta^+/\sqrt{2} \end{pmatrix} \sim (\mathbf{1}, \mathbf{3}, \mathbf{2}). \quad (20)$$

The full invariant form of Eq. (19) is written as

$$\mathcal{L}_\nu = \frac{1}{\sqrt{2}} Y_{ij}^L \bar{L}_i^c i \sigma_2 \Delta L_j + H.c.. \quad (21)$$

Here it is clear that the triplet scalar field carries lepton number $L_\Delta = 2$. After SSB masses of the neutrinos are given by

$$m_{\nu ij} = \frac{v_\Delta}{\sqrt{2}} Y_{ij}^L,$$

such that v_Δ is the Δ^0 vev. Then, after SSB of the triplet neutral field, this Yukawa interaction breaks lepton number by two units and leads to Majorana mass for the neutrinos. However, if one maintain exact lepton number symmetry in the model and generate the triplet vev via the usual “mexican hat” potential, then it leads to the triplet Majoron which has been ruled out by actual experimental data and in the same time in such framework we do not naturally understood smallness of the neutrino masses.

The seesaw relation can be generated only after introducing the following trilinear interaction in the scalar sector,

$$\mu \Phi^T \Delta \Phi,$$

that clearly violates explicitly $B - L$ symmetry by 2 units.

When establishing the minimum conditions of the potential, the lepton number

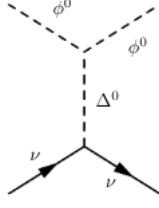


Figure 3: Type II seesaw recovering the dimension-5 operator.

violation energy scale, μ , leads to a seesaw-like relation,

$$v_\Delta \sim \mu v^2 / M_\Delta^2.$$

Masses for the neutrinos follows from the combination of these three different energy scales: explicitly violation of the lepton number μ , EW scale vev v and the mass of the triplet field M_Δ .

Then, the smallness of neutrinos masses are naturally explained if the relation μ/M_Δ^2 is large enough to counterbalance EW vev. However, since these two energy scales are not necessarily related, we have freedom to choose the best way to fit neutrino masses. For example, we can fix these two energy scales to be at GUT scales, $\mu \sim 10^{14} \text{ GeV}$ and $M_\Delta \sim 10^{14} \text{ GeV}$, and consequently recovering $v_\Delta \sim 0.1 \text{ eV}$. After we will discuss other interesting choices to naturally explain neutrino mass smallness in such framework. A last comment is about recovering the Feynman diagram in Fig.(1). The neutral field Δ^0 as a mediator it is responsible to generate the dimension-5 operator at tree-level in such model, as given by Fig. (3). Here, the effective coupling $\alpha\Lambda^{-1}$ is given by $Y^L \mu M_\Delta^{-2}$.

Canonical Type III: In the canonical type III seesaw one needs to introduce a fermionic triplet Σ_L that transforms as $\Sigma_L \sim (1, 3, 0)$ under the SM gauge group

$$\Sigma_L = \begin{pmatrix} \Sigma^0/\sqrt{2} & \Sigma^+ \\ \Sigma^- & \Sigma^0/\sqrt{2} \end{pmatrix}, \quad (22)$$

and interacts in the following way

$$\mathcal{L}_\nu = -\frac{1}{2} \text{Tr} [\bar{\Sigma} M_\Sigma \Sigma^c + \bar{\Sigma}^c M_\Sigma^* \Sigma] - \tilde{\Phi}^\dagger \bar{\Sigma} \sqrt{2} Y_\Sigma L. \quad (23)$$

We can associate a lepton number for this fermionic triplet in such a way that the Dirac mass term is invariant by any global phase symmetry. Neutrino masses can be approximated by the following relation if we impose that $M_\Sigma \gg v$,

$$m_\nu \sim Y_\Sigma^2 v^2 M_\Sigma^{-1}$$

and the heavy neutral fermions have masses proportional to M_Σ , similar to type I seesaw. As a last comment, to recover the Feynman diagram of the Fig. 1, one needs to write Σ^0

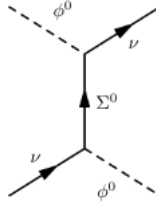


Figure 4: Type III seesaw recovering the dimension-5 operator.

as the propagator, as in Fig. 4. The contact point in this case is proportional to $Y_\Sigma^2 M_\Sigma^{-1}$.

Protagonism of the Canonical Type II Seesaw : To generate the right pattern for tiny masses for the neutrinos, one needs to introduce a very heavy particle that links neutrinos with standard-like Higgs, as indicated by Figs. 2, 3 and 4. Such link, after EWSB, reproduces neutrinos masses in the same way as in Eq. 9. As we pointed out, the effective mass coupling Λ needs to be sufficiently large to counterbalance v^2 in order to reproduce eV neutrinos masses.

Nonetheless, type I and III seesaw mechanisms mix chiral states and the introduced lepton number violation scales M_R and M_Σ are directly responsible for reproducing small masses for the neutrinos. Then, one needs to associate M_R and M_Σ with Λ . This is a crucial difference between type II seesaw and these two. Thus, type II seesaw has two interesting features. First, one do not need right-handed neutral fermions in order to reproduce neutrino mass pattern. Second, the seesaw relation $v_\Delta \sim \mu v^2 / M_\Delta^2$ relates not only two energy scales, but three. One of them is fixed, the EWSB scale. However, in principle we are free to choose any value for M_Δ and μ . As explained before, one can associate μ and M_Δ to be at GUT scales and successfully reproduces neutrino mass pattern. Therefore, if lepton number is violated at low energies, $\mu \sim v_\Delta$, then the mass scale of the triplet scalar should be close to the EWSB energies, $M_\Delta \sim v$. Such mass scale is fully accessible to current experiments, unlike the two previous types of seesaw. Making such mechanism the most phenomenologically viable among them. The versatility of type II seesaw fully justifies its complete study. Then, in the next chapters we will develop its main phenomenological and theoretical aspects.

1 Type II Seesaw Mechanism

1.1 Introduction

At first, we will analyse some general aspects of the type II seesaw and its constraints, as bounded from below inequalities and the ρ -parameter. Another relevant aspect that will be understood more deeply in this chapter is the lepton number explicitly violation energy scale μ and its theoretical justifications. This chapter is organized as follows. In sections 1.2 and 1.3 we develop the main aspects of the model including neutrino masses. In section 1.4 we discuss naturalness principles in type II seesaw, while in sections 1.5 and 1.6 we develop the scalar sector. In section 1.7 we discuss the stability of the vacuum. In section 1.8 we present our final remarks.

1.2 The Model

The scalar sector is composed by the standard Higgs doublet, plus one scalar triplet,

$$\Delta = \begin{pmatrix} \frac{\Delta^+}{\sqrt{2}} & -\Delta^{++} \\ \Delta^0 & -\frac{\Delta^+}{\sqrt{2}} \end{pmatrix} \sim (\mathbf{1}, \mathbf{3}, \mathbf{2}); \quad \Phi = \begin{pmatrix} \phi^+ \\ \phi^0 \end{pmatrix} \sim (\mathbf{1}, \mathbf{2}, \mathbf{1}), \quad (1.1)$$

where the content in parenthesis means the transformation by the SM gauge group.

These particles are described by the following Lagrangian,

$$\mathcal{L}_s = (D^\mu \Phi)^\dagger (D_\mu \Phi) + Tr[(D^\mu \Delta)^\dagger (D_\mu \Delta)] - V(\Phi, \Delta), \quad (1.2)$$

where the covariant derivative is the same as the Standard Model one,

$$D_\mu = \partial_\mu - ig\hat{T}^a W_\mu^a - i\frac{g_y}{2}\hat{Y}_Y V_\mu. \quad (1.3)$$

This triplet scalar representation interacts with the group operators as

$$\begin{aligned}
\hat{T}^a \Delta &= \frac{1}{2}[\sigma^a, \Delta] \\
\hat{Y}_Y \Delta &= 2\Delta,
\end{aligned} \tag{1.4}$$

recovering $\hat{T}^0 \Delta^0 = -\Delta^0$.

The most general potential that conserves Lepton Number explicitly is given by,

$$\begin{aligned}
V(\Phi, \Delta) &= -\mu_2^2 \Phi^\dagger \Phi + \frac{\lambda}{4}(\Phi^\dagger \Phi)^2 + \mu_3^2 \text{Tr}[(\Delta^\dagger \Delta)] \\
&\quad + \lambda_1(\Phi^\dagger \Phi) \text{Tr}[(\Delta^\dagger \Delta)] + \lambda_2(\text{Tr}[(\Delta^\dagger \Delta)])^2 + \lambda_3 \text{Tr}[(\Delta^\dagger \Delta)^2] \\
&\quad + \lambda_4 \Phi^\dagger \Delta \Delta^\dagger \Phi.
\end{aligned} \tag{1.5}$$

However, as we have saw before, we need to include a Lepton Number explicitly violation interaction that is responsible for neutrinos masses. This new term can be written as

$$\mu(\Phi^T i \sigma^2 \Delta^\dagger \Phi) + H.c.$$

The requirement that the potential be hermitian implies that the parameters μ_2^2 , μ_3^2 , λ_1 , λ_2 , λ_3 , λ_4 and λ_5 are real numbers, while μ is in general complex. Nonetheless, μ could be a source of CP violation if was imaginary. For this work, we are considering μ as a real number, too.

1.3 The Yukawa Sector

The Yukawa interactions involving Δ and the standard lepton doublet, $L = (\nu, e)_L^T \sim (\mathbf{1}, \mathbf{2}, -\mathbf{1})$ is

$$\mathcal{L}_Y = \frac{1}{\sqrt{2}} Y_{ij}^L \bar{L}_i^c i \sigma_2 \Delta L_j + H.c.. \tag{1.6}$$

When Δ develops vacuum expectation value (vev), we obtain the following general neutrino mass matrix

$$m_\nu = Y_L v_3. \tag{1.7}$$

The neutrino mass matrix in the flavor basis is related to the physical mass matrix, m_ν^D , through a 3×3 unitarity mixing matrix U in the following way

$$m_\nu^D = U m_\nu U^\dagger, \tag{1.8}$$

where $m_\nu^D = \text{diag}(m_1, m_2, m_3)$ and U is the neutrino mixing matrix, which may be

parametrized in the general way by

$$U = \begin{pmatrix} c_{12}c_{13} & s_{12}c_{13} & s_{13} \\ -s_{12}c_{23} - c_{12}s_{23}s_{13} & c_{12}c_{23} - s_{12}s_{23}s_{13} & s_{23}c_{13} \\ s_{12}s_{23} - c_{12}c_{23}s_{13} & -c_{12}s_{23} - s_{12}c_{23}s_{13} & c_{23}c_{13} \end{pmatrix}, \quad (1.9)$$

where $c_{ij} = \cos \theta_{ij}$ and $s_{ij} = \sin \theta_{ij}$, while in this work we neglect CP violation phases, since they are not too relevant in normal hierarchy mass ordering ($m_1 < m_2 < m_3$)[38]. Thus, on inverting the Eq. (1.8) we obtain

$$m_\nu = U^\dagger m_\nu^D U, \quad (1.10)$$

Combining equations (1.7) and (1.10), we obtain

$$Y_{ij}^L = \frac{1}{v_\Delta} U_{ik}^\dagger m_{\nu_{kk}}^D U_{kj}. \quad (1.11)$$

Explicitly, these Yukawa entries are expressed as

$$\begin{aligned} Y_{11}^L &= \frac{1}{v_3} (c_{12}^2 c_{13}^2 m_1 + m_3 (c_{12} c_{23} s_{13} - s_{12} s_{23})^2 + m_2 (c_{23} s_{12} + c_{12} s_{13} s_{23})^2), \\ Y_{12}^L &= \frac{1}{v_3} (c_{12} c_{13}^2 m_1 s_{12} + m_3 (c_{23} s_{12} s_{13} + c_{12} s_{23}) (c_{12} c_{23} s_{13} - s_{12} s_{23}) - \\ &\quad m_2 (c_{23} s_{12} + c_{12} s_{13} s_{23}) (c_{12} c_{23} - s_{12} s_{13} s_{23})), \\ Y_{13}^L &= \frac{1}{v_3} (c_{13} (c_{23} (-m_2 + m_3) s_{12} s_{23} + c_{12} s_{13} (m_1 - c_{23}^2 m_3 - m_2 s_{23}^2)), \\ Y_{22}^L &= \frac{1}{v_3} (c_{13}^2 m_1 s_{12}^2 + m_3 (c_{23} s_{12} s_{13} + c_{12} s_{23})^2 + m_2 (c_{12} c_{23} - s_{12} s_{13} s_{23})^2), \\ Y_{23}^L &= \frac{1}{v_3} (c_{13} ((m_1 - c_{23}^2 m_3) s_{12} s_{13} + c_{12} c_{23} (m_2 - m_3) s_{23} - m_2 s_{12} s_{13} s_{23}^2), \\ Y_{33}^L &= \frac{1}{v_3} (m_1 s_{13}^2 + c_{13}^2 (c_{23}^2 m_3 + m_2 s_{23}^2)). \end{aligned} \quad (1.12)$$

The experimental values of these angles are, for the normal ordering[38]

$$s_{12}^2 = 0.306_{-0.012}^{+0.012}, \quad s_{23}^2 = 0.441_{-0.021}^{+0.027}, \quad s_{13}^2 = 0.02166_{-0.00075}^{+0.00075} \quad (1.13)$$

and the masses[38]

$$\Delta m_{21}^2 = 7.50_{-0.17}^{+0.19} \times 10^{-5} eV^2, \quad \Delta m_{31}^2 = 2.524_{-0.040}^{+0.039} \times 10^{-3} eV^2. \quad (1.14)$$

Many experiments have been limited the values for the mixing angles and neutrino masses. Fixing $m_1 = 0$, it can be associated $m_2 = \sqrt{\Delta m_{21}^2}$ and $m_3 = \sqrt{\Delta m_{31}^2}$. Now, Y_{Lij} depends exclusively from v_3 value. We will explore this in detail in Chapter 2.

1.4 Naturalness principle and explicitly broken $B - L$ symmetry

Analysing the new Yukawa interaction, Eq. (1.6), one can attribute a lepton number for this triplet field. Therefore, in type II seesaw, these scalars only interacts with leptons and the Higgs doublet. Then, to conserve explicitly $B - L$ symmetry in the Yukawa term we attribute a lepton number 2 for the triplet scalar ($N_{B-L}^\Delta = -2$). After SSB, this interaction generate Majorana masses for the LHNs and in this interaction $B - L$ symmetry will be spontaneously broken. In chapter 3 we will explore an extension of such model with a complex singlet scalar. In that extension, μ parameter only appears after Spontaneous Symmetry Breaking of the introduced scalar field and lepton number is explicitly conserved.

In Eq. (4.3), there is a term that explicitly violates $B - L$ symmetry[39]. Therefore, such trilinear interaction $\mu(\Phi^T i\sigma^2 \Delta^\dagger \Phi)$ can reveal a link between hidden gauge symmetries and new scale physics. Another symmetry that is explicitly broken in such trilinear interaction is custodial symmetry [40]. Such global symmetry links the left (right) chirality fermions in the SM, transforming them accordingly to the global symmetry $SU(2)_{L(R)}$. Nonetheless, the Higgs doublet is a bidoublet under this global symmetry. Before EWSB, the Higgs potential and the Yukawa interactions in the SM has a $SU(2)_L \otimes SU(2)_R$ global symmetry which reduces to $SU(2)_V$ when the symmetry is broken. However, in the case of type II seesaw, it is clear that the triplet scalar Δ only interacts with left-handed fermions and breaks this symmetry. Then, representing them as Δ_L , the trilinear scalar interaction represents the explicit symmetry breaking energy scale of the custodial symmetry. In fact, there is a possibility of associating such custodial and $B - L$ explicitly breaking symmetries with spontaneously broken gauge theory $SU(2)_L \otimes SU(2)_R \otimes U(1)_{B-L}$, known as Left-Right gauge symmetry[41].

Nonetheless, the μ parameter is expected to be small and natural in the t'Hooft sense [42], inasmuch as μ is the energy scale at which this symmetry is broken. If μ tends to zero, would increase symmetry of the system. Therefore, we must associate this trilinear coupling with a low energy scale parameter that can be a reminiscent of new physics in another scale. On the other hand, GUT scale μ could be a remnant of $SO(10)$ or $SU(5)$ symmetries [43][44] .

1.5 Spontaneous Symmetry Breaking and Seesaw mechanism

The Spontaneous Symmetry Breaking occurs when the triplet and the doublet scalars acquire nonzero vevs. As the vacuum must be invariant under $U(1)_{em}$ transformations, only the neutral scalars can develop vevs. Thus, if the triplet scalar is not inert,

one can expand these fields as,

$$\begin{aligned}\phi^0 &= \frac{v_2}{\sqrt{2}} + \frac{R_2 + I_2}{\sqrt{2}}, \\ \Delta^0 &= \frac{v_3}{\sqrt{2}} + \frac{R_3 + I_3}{\sqrt{2}}.\end{aligned}\tag{1.15}$$

The conditions that minimize such potential for $\mu_2^2 > 0$ and $\mu_3^2 > 0$ imposes to us the following equations,

$$\begin{aligned}\mu_2^2 &= \frac{1}{4}(\lambda v_2^2 - 4\sqrt{2}\mu v_3 + 2\lambda_1 v_3^2 + 2\lambda_4 v_3^2), \\ \mu_3^2 &= \frac{1}{2v_3}(\sqrt{2}\mu v_2^2 - \lambda_1 v_2^2 v_3 - \lambda_4 v_2^2 v_3 - 2\lambda_2 v_3^3 - 2\lambda_3 v_3^3).\end{aligned}\tag{1.16}$$

Back to the gauge interactions with the scalars, v_3 is constrained in order to reproduce the mass for the physical gauge bosons Z and W . With the additional triplet, the Lagrangian for the gauge boson masses is, after standard Weinberg Rotation,

$$\mathcal{L}_{gauge\ mass} = \frac{1}{4}g^2(v_2^2 + 2v_3^2)W^+_\mu W^{-\mu} + \frac{1}{4}g^2(v_2^2 + 4v_3^2)Z_\mu Z^\mu,\tag{1.17}$$

and the W and Z bosons masses are

$$m_W^2 = \frac{g^2}{4}(v_2^2 + 2v_3^2), \quad m_Z^2 = \frac{g^2}{4c_W^2}(v_2^2 + 4v_3^2).\tag{1.18}$$

This change in the mass values of gauge bosons has a directly influence in the tree-level ρ -parameter[45],

$$\rho = \frac{m_W^2}{c_W^2 m_Z^2}.\tag{1.19}$$

This parameter in the SM framework is exactly one. Experimental evidences points toward one, too, with small deviations. In type II seesaw, the ρ -parameter is given by

$$\rho = \frac{v_2 + 2v_3}{v_2 + 4v_3} < 1.\tag{1.20}$$

Experimental values for the ρ -parameter are converging at 3σ to 1.002[46]. Due to experimental errors, we cannot conclusively state that ρ is greater than one. Then, after these considerations, one can limit superiorly the value of v_3 as

$$v_3 < 2.3 \text{ GeV}. \quad (1.21)$$

The small value of v_3 , constrained by the ρ -parameter, combined with the minimal conditions in Eq. (1.16), are the key to understand neutrino mass smallness in this framework. Thus,

$$v_3 \approx \frac{\mu v_2^2}{2\mu_3^2 + v_2^2(\lambda_1 + \lambda_4)}, \quad (1.22)$$

implies that $v_3 \sim (\mu/\mu_3^2)v_2^2$, a seesaw relation, since (μ/μ_3^2) must suppress v_2^2 in order to have a low value for v_3 . Neutrino mass consequently obeys the same seesaw relation, since it has a v_3 dependence in its mass $m_\nu = y v_3 \sim y(\mu/\mu_3^2)v_2^2$.

1.6 Scalar Mass Spectrum

1.6.1 CP-even particles

The neutral CP-even mixing matrix after using the minimum conditions, in $(R_2, R_3)^T$ basis reads

$$m_{R_2, R_3}^2 = \begin{pmatrix} \frac{1}{2}\lambda v_2^2 & v_2(-\sqrt{2}\mu + (\lambda_1 + \lambda_4)v_3) \\ v_2(-\sqrt{2}\mu + (\lambda_1 + \lambda_4)v_3) & \frac{1}{2v_3}(\sqrt{2}\mu v_2^2 + 4(\lambda_2 + \lambda_3)v_3^3) \end{pmatrix}. \quad (1.23)$$

This mass matrix can be expressed in the following way

$$m_{R_2, R_3}^2 = \begin{pmatrix} m_{R_2}^2 & m_{R_2 R_3}^2 \\ m_{R_2 R_3}^2 & m_{R_3}^2 \end{pmatrix}. \quad (1.24)$$

Imposing the hierarchy $v_3 \ll v_2$, these two CP-even scalars decouples from each other, since non-diagonal terms are perturbative compared to diagonal terms. Then, the exact form for these masses can be written as

$$m_{H, h}^2 = \frac{1}{2}(m_{R_2}^2 + m_{R_3}^2 \pm \sqrt{(m_{R_2}^2 - m_{R_3}^2)^2 + 4(m_{R_2 R_3}^2)^2}). \quad (1.25)$$

We can approximate these exact values inducing some limits. As our case, if the non-diagonal elements are much minor than the diagonal ones,

$$m_{R_2 R_3}^2 \ll m_{R_2}^2, m_{R_3}^2, \quad (1.26)$$

then, these masses can be approximated in first order by,

$$\begin{aligned} m_h^2 &= m_{R_2}^2 - \frac{(m_{R_2 R_3}^2)^2}{m_{R_3}^2 - m_{R_2}^2}, \\ m_H^2 &= m_{R_3}^2 + \frac{(m_{R_2 R_3}^2)^2}{m_{R_3}^2 - m_{R_2}^2}. \end{aligned} \quad (1.27)$$

At this limit, these masses have become

$$\begin{aligned} m_H^2 &\approx \frac{\mu v_2^2}{\sqrt{2} v_3}, \\ m_h^2 &\approx \frac{\lambda}{2} v_2^2. \end{aligned} \quad (1.28)$$

In this approximation, the scalar h has a mass value very close to the standard Higgs. After diagonalization, we have obtained the following mixing between these fields

$$\begin{aligned} H &= c_\alpha R_3 - s_\alpha R_2, \\ h &= s_\alpha R_3 + c_\alpha R_2, \\ \tan 2\alpha &= \frac{-2\sqrt{2}v_2\mu + 2(\lambda_1 + \lambda_4)v_2v_3}{\frac{\lambda}{2}v_2^2 - \frac{\mu v_2^2}{\sqrt{2}v_3} - 2(\lambda_3 + \lambda_2)v_3^2}. \end{aligned} \quad (1.29)$$

1.6.2 CP-odd

Here, after SSB, we obtain the mass matrix of the CP-odd scalars,

$$m_{I_2, I_3}^2 = \begin{pmatrix} 2\sqrt{2}\mu v_3 & -\sqrt{2}\mu v_2 \\ -\sqrt{2}\mu v_2 & \frac{1}{\sqrt{2}}v_2^2 \frac{\mu}{v_3} \end{pmatrix}. \quad (1.30)$$

One of these scalars, after diagonalization, becomes the neutral Goldstone boson, G^0 . The other CP-odd scalar mass is heavy in the same order as H

$$\begin{aligned} m_A^2 &= \frac{\mu}{\sqrt{2}v_3}(v_2^2 + 4v_3^2), \\ m_{G^0}^2 &= 0. \end{aligned} \quad (1.31)$$

The mixing states are

$$\begin{aligned} A &= c_{\beta'} I_3 - s_{\beta'} I_2, \\ G^0 &= s_{\beta'} I_3 + c_{\beta'} I_2, \\ tg\beta' &= \frac{2v_3}{v_2}, \end{aligned} \quad (1.32)$$

and these scalars are decoupled, since $c_{\beta'} \approx 1$. It is notable that if this μ -parameter is set to be zero, the CP-odd particle A would not have mass and become a Goldstone Boson. This means that $B - L$ explicitly conservation leads to a Majoron.

1.6.3 Single charged particles

For the singly charged scalars we have the following mass matrix

$$m_{\Delta^\pm, \phi^\pm}^2 = \begin{pmatrix} \sqrt{2}\mu v_3 - \frac{1}{2}\lambda_4 v_3^2 & \frac{1}{4}(-4\mu v_2 + \sqrt{2}\lambda_4 v_2 v_3) \\ \frac{1}{4}(-4\mu v_2 + \sqrt{2}\lambda_4 v_2 v_3) & \frac{1}{4}v_2^2(-\lambda_4 + \frac{2\sqrt{2}\mu}{v_3}) \end{pmatrix}. \quad (1.33)$$

One of these scalars, after diagonalization, become the charged Goldstone boson, G^\pm . The other charged scalar mass is heavy in the same order as H and A

$$\begin{aligned} m_{H^\pm}^2 &= \frac{1}{4v_3}(2\sqrt{2}\mu - \lambda_4 v_3)(v_2^2 + 2v_3^2), \\ m_{G^\pm}^2 &= 0. \end{aligned} \quad (1.34)$$

Mixing among these charged fields are given by

$$\begin{aligned} H^\pm &= c_\beta \Delta^\pm - s_\beta \phi^\pm, \\ G^\pm &= s_\beta \Delta^\pm + c_\beta \phi^\pm, \\ tg\beta &= \frac{\sqrt{2}v_3}{v_2}. \end{aligned} \quad (1.35)$$

As before, this mixing angle is very close to zero and consequently $c_\beta \approx 1$. This means that H^\pm is predominantly a triplet particle.

1.6.4 Double-charged particles

For the doubly charged scalar there is no mix among other particles. Then, the mass of this scalar is simply

$$m_{\Delta^{\pm\pm}}^2 = -\frac{1}{2}\lambda_4 v_2^2 + \frac{\mu v_2^2}{\sqrt{2}v_3} - \lambda_3 v_3^2. \quad (1.36)$$

1.7 Potential Stability and Bounded From Below conditions

We have discussed in section (1.5) how SSB generates gauge invariant masses for some bosons and fermions of the model. Any potential to develop vev, i.e., the lowest energy state or the ground state of the scalar field, needs to be Bounded From Below (BFB). This minimum value is the stationary value of the neutral scalar fields, $\langle\phi^0\rangle$ and $\langle\Delta^0\rangle$, and consequently the effective interaction at low energies between the Higgs fields and another particles and gauge fields. This ground state is proportional to what we measure as the mass of the fundamental particles at tree-level. Exciting a Higgs field from this ground state is generally manifested as a Higgs particle transition, i.e., several new Higgs particles will be generated and these particles will decay into lighter particles, until at some point the Higgs by-product are stable particles and will no longer decay.

As with the inflaton models, the Higgs field will oscillate around its vacuum dissipating energy with Higgs emission (like excited electrons in the atomic orbit that emit photons and return to the ground state). If this potential is at the global minimum value, after a while, this field will return to its ground state. However, there is serious issues if this field doesn't rest in its minimum value. We will investigate what type of problem it is in the next chapter.

Here, we will suppose that the potential is BFB, guarantying that the ground state, or the vev, exists. This means that, by construction, the potential has a global minimum. To ensure this, if the potential is polynomial, the coefficient of the highest order it is mandatory to be positive. In the SM case, we have explicitly the potential, for the complex doublet field Φ

$$V(\phi) = \frac{\mu^2}{2}\Phi^\dagger\Phi + \frac{\lambda}{4}(\Phi^\dagger\Phi)^2. \quad (1.37)$$

It is necessary to ensure that $\lambda > 0$. Then, the global minimum of this potential exists. The value of this minimum depends on whether μ^2 is positive or negative. If $\mu^2 > 0$ it is clear that $\langle\phi^0\rangle = 0$. If $\mu^2 < 0$, then $\langle\phi^0(\theta)\rangle = e^{i\theta}\sqrt{\frac{-\mu^2}{\lambda}}$. In the last case, all possible values for the vev have the same magnitude (multiplied by a complex phase), meaning that all these vev's are global minima. We will discuss in the next chapter an arbitrary case where the vacuum rests in a local minima, but it is not a global one.

However, for scalar extensions of the SM, it is not so easy to find the conditions

to the potential to be BFB. This is so because the quartic interactions between scalars generally mixes different fields. In the potential (1.5), there is five quartic couplings, but we can shrink it in only three effective couplings for the neutral scalars

$$V^4(\phi^0, \Delta^0) = \lambda_H(\phi^{0\dagger}\phi^0)^2 + \lambda_{HT}(\phi^{0\dagger}\phi^0)(\Delta^{0\dagger}\Delta^0) + \lambda_T(\Delta^{0\dagger}\Delta^0)^2, \quad (1.38)$$

and it is sufficient if these three couplings are positive, but not necessary. The necessary conditions are

$$\lambda_H > 0, \quad \lambda_T > 0, \quad \lambda_{HT} + 2\sqrt{\lambda_H\lambda_T} > 0. \quad (1.39)$$

To make a complete treatment of these parameters generally it is used the method called Spherical Parametrization, detailed in Chapter 4. Directly we can find, after Spherical Parametrization, the following conditions for the potential to be BFB

$$\begin{aligned} \lambda > 0, \quad \lambda_2 + \lambda_3/2 > 0, \quad \lambda_2 + \lambda_3 > 0, \quad \lambda_1 + 2\sqrt{\lambda(\lambda_2 + \lambda_3/2)} > 0, \\ \lambda_1 + 2\sqrt{\lambda(\lambda_2 + \lambda_3)} > 0, \quad \lambda_1 + \lambda_4 + 2\sqrt{\lambda(\lambda_2 + \lambda_3/2)} > 0, \\ \lambda_1 + \lambda_4 + 2\sqrt{\lambda(\lambda_2 + \lambda_3)} > 0. \end{aligned} \quad (1.40)$$

Analysing these inequalities it is viable to infer the parametric space for these couplings. These are the conditions for the potential to be BFB at low energies. At high energies quantum effects are relevant, via loop contributions. Then, in the next chapter we will discuss BFB conditions at high energies. Nonetheless, we present some possible values for the quartic coupling constants in Fig. (1.1).

1.8 Discussion

In this Chapter, we have discussed how the minimal type II seesaw is versatile and can either explicitly break lepton number at GUT scales or at low energy scales. Then, we have found the tree-level mass expressions and mixings for the scalars and neutrinos at tree-level of this model after SSB. We will use these expressions for scalars masses in the next chapters, when studying the phenomenology of this model. Finally, we have studied the stability of the potential and the conditions for the potential to be BFB and some solutions for its quartic couplings. In the next chapter, we will study the low energy scale type II seesaw and its main features.

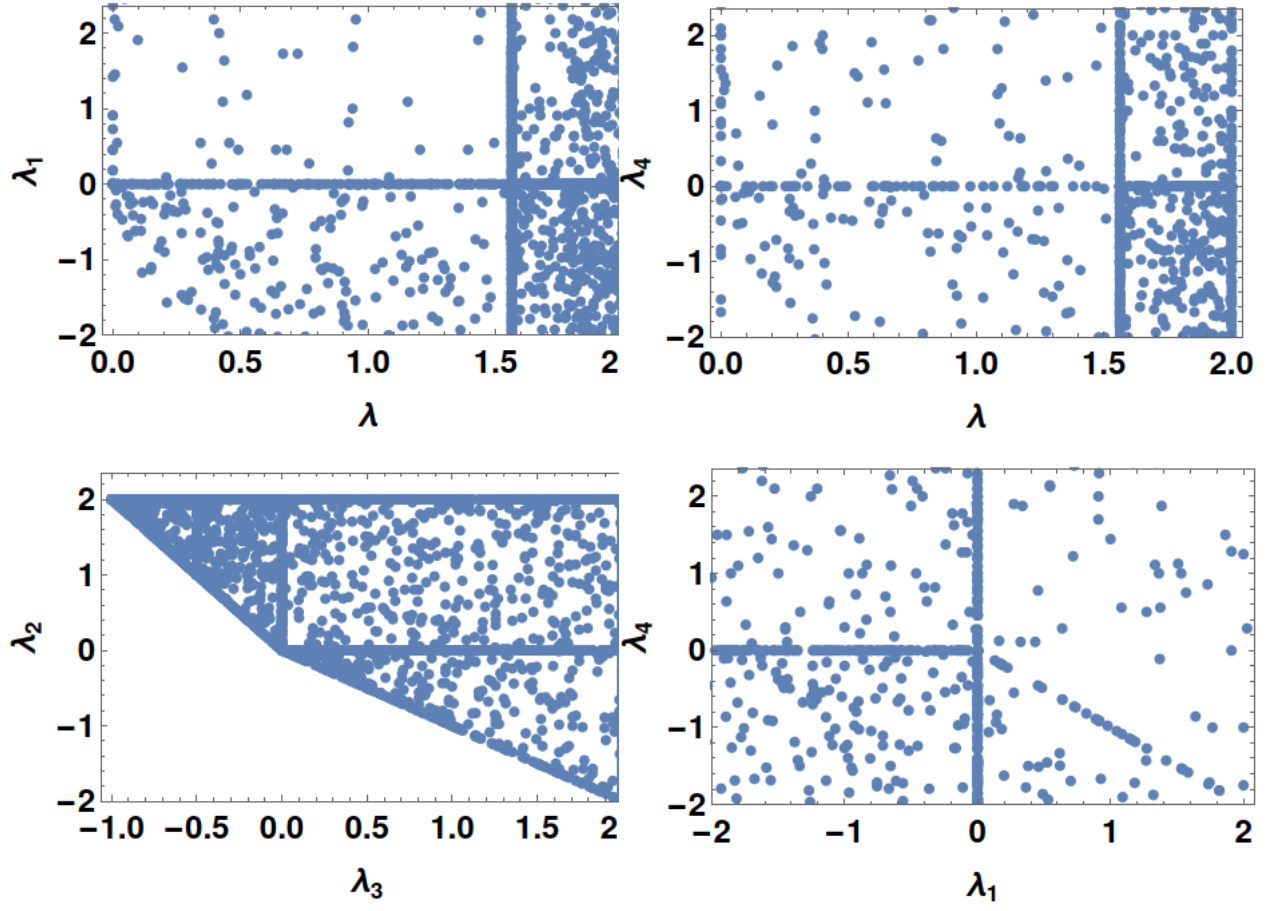


Figure 1.1: Some possible values for the quartic couplings of the potential using unitarity and BFB conditions.

2 Low Scale Type II Seesaw

2.1 Introduction

As was discussed in the introduction and in the last chapter, type II seesaw is the most versatile among canonical seesaw mechanisms. This versatility is associated with the possibility of this mechanism generates tiny masses for neutrinos with different energy scales. Explicitly breaking of the lepton number at low energy scales is well motivated, since spontaneously breaking of the lepton number is at low scales, too. Hence, v_3 is responsible for generate Majorana mass for neutrinos $M_L \bar{\nu}_L^C \nu_L$ that violates lepton number by 2, as $\mu \Phi^T i \sigma^2 \Delta^\dagger \Phi$ did. Nonetheless, it is theoretically motivating to study a relation between v_3 and μ close to unity can (relating these lepton number violation energy scales). As we have discussed, the main type II seesaw relation is given by the expression $v_3 \sim \mu v_2^2 / \mu_3^2$. If this mechanism is phenomenologically viable, meaning that triplet scalars masses are close to actual experimental covering range, or $\mu_3 \sim v_2$. If this is true, consequently $\mu \sim v_3$ in which lepton number is explicitly broken in the same scale that is spontaneously broken [47]. This case can encompass left-right symmetric extensions of the SM (conformal and $B - L$ symmetry), with additional interesting phenomenology at the LHC, cf. refs. [48, 49], or can also be studied in its minimal version.

Therefore, to analyse the ratio μ/v_3 , one needs to study its relation with triplet scalars mass and compare with recent experimental data. Nonetheless, v_3 value may be estimated according to the neutrino masses. For $m_\nu = Y_L v_{3(\Delta)} \sim 0.1 \text{ eV}$ and assuming principles of naturalness ($Y_L \lesssim 1$) it is natural to estimate v_3 to lie at eV scales. So, assuming the last statement and that scalar triplet has masses close to TeV energy scales, we should say that $\mu \sim eV$ by the seesaw relation. So, our investigation will focus on the ratio between μ and v_3 , which we will call ϵ . One type of process that can relate the masses of charged triplet scalars (and consequently this ϵ parameter) are lepton flavor violation processes (LFV).

The discussion mentioned above will be addressed in Section (2.2) of this chapter. Another interesting aspect of the type II seesaw mechanism at low energies is its similarity to the inverse seesaw mechanism (ISS). This subject will be worked out carefully in the Section (2.3). Finally, we will contextualize the Higgs Metastability problem and how minimal type II seesaw may solve this problem, in Section (2.4). There is another naturalness problem, related to Higgs mass correction at one-loop. However, as discussed by

[50], these two problems cannot be solved simultaneously in the minimal type II seesaw. This is the last subject of this chapter, in Section (2.5), with a brief discussion in Section (2.6).

2.2 ϵ -Parameter and LFV processes

As we have saw, type II seesaw relation is written as $v_3 \sim \mu v_2^2/\mu_3^2$. From another point of view, looking at the scalar triplet mass, this interesting relation can also be seen as $\mu_3^2 \sim \mu v_2^2/v_3$. It is natural, in t'Hooft sense, to assume that $\mu \sim v_3$, and consequently $\mu_3 \sim v_2$, as discussed in the last chapter. Since μ_3 depends on the ratio μ/v_3 and not from μ and v_3 individual absolute values, it is immediate to ask what possible values these parameters may assume. Firstly, v_3 is superiorly limited by the ρ -parameter in such a way that $v_3 < 2.3 \text{ GeV}$, as we have discussed in the previous chapter. Inferiorly, v_3 is limited by neutrino masses. In minimal type II seesaw, v_3 has a direct relation with m_ν ($v_3 = m_\nu/Y_L$). In order to fulfill the perturbativity condition, Yukawa triplet couplings (from now, we will only refer as Yukawa couplings) obey the relation $Y_L < 4\pi$. Conversely, actual constraints for neutrinos masses are around $m_\nu \lesssim 0.1 \text{ eV}$. These two constraints directly implies that $v_3 > \mathcal{O}(10^{-2} \text{ eV})$. Therefore, there is an 11-order range for possible values for v_3 , $10^{-2} \text{ eV} - 2.3 \text{ GeV}$. Consequently, for low scale type II seesaw, μ must be limited in the same range as v_3 [51].

After this brief discussion about v_3 and μ possible values, once again we will appeal to the naturalness principle. If $v_3 \sim 1 \text{ GeV}$, then the Yukawa couplings are unnaturally tiny ($Y_L \sim 10^{-10}$). However, considering $v_3 \sim 1 \text{ eV}$, we don't need a fine tuning in this sector ($Y_L \sim 0.1$). Based upon the assumption that the Yukawa couplings are higher as possible (respecting perturbativity), v_3 at eV scales it is a foreseeable consequence. This choice has many phenomenological consequences. One of them are Lepton Flavor Violation processes (LFV). Since Y_{Lij} are close to one, the triplet Higgs states can predominantly induces LFV processes such as $\mu \rightarrow 3e$, $\tau \rightarrow 3\mu$, $\tau \rightarrow e2\mu$, etc at tree-level, and at one-loop level decays like $\mu \rightarrow e\gamma$, $\tau \rightarrow e\gamma$ and $\tau \rightarrow \mu\gamma$ can also happen. None of the above mentioned LFV decay processes have been observed in experiments and stringent experimental upper bounds have been put on the decay branching ratios of these processes [52].

Therefore, in this model LFV processes depends on neutrino Yukawa couplings and masses of triplet Higgs states, as discussed above. Nonetheless, Yukawa couplings can be determined from neutrino masses and mixing angles as well as from the vev of scalar triplet Higgs. Hence, by determining the Yukawa couplings, the experimental limits on LFV processes can put constraints on triplet scalars masses. However, as we have discussed, these masses are totally determined by the ϵ parameter. Consequently, LFV processes can put constraints on v_3 , for small ϵ .

In order to find limits for ϵ we must use stringent experimental constraints in LFV.

The main processes that contribute are the decays $\mu \rightarrow \gamma e$ and $\mu \rightarrow eee$. Their branching ratios should respect these experimental values

$$\begin{aligned} BR(\mu \rightarrow \gamma e) &< 4.2 \times 10^{-13} [53], \\ BR(\mu \rightarrow eee) &< 1.0 \times 10^{-12} [54]. \end{aligned} \quad (2.1)$$

These constraints relate the model parameters with $m_{\Delta^{++}} \simeq m_{\Delta^+}$ as [32, 55]

$$\begin{aligned} BR(\mu \rightarrow \gamma e) &= \frac{27\alpha |(Y_L)_{11}(Y_L)_{12} + (Y_L)_{13}(Y_L)_{32} + (Y_L)_{12}(Y_L)_{22}|^2}{64\pi G_F^2 m_{\Delta^{++}}^4}, \\ BR(\mu \rightarrow eee) &= \frac{|(Y_L)_{11}|^2 |(Y_L)_{12}|^2}{4G_F^2 m_{\Delta^{++}}^4} BR(\mu \rightarrow e\bar{\nu}\nu). \end{aligned} \quad (2.2)$$

where α is the fine structure constant and $G_F = 1.1663787 \times 10^{-5} \text{ GeV}^{-2}$ and $BR(\mu \rightarrow e\bar{\nu}\nu) \simeq 100\%$.

In order to analyse these expressions carefully, we need to find the direct dependence between the Yukawa couplings and v_3 . Fixing $m_1 = 0$ and applying the experimental mean values of the mixing angles in neutrino mass normal ordering hierarchy scenario ($m_1 = 0 < m_2 < m_3$), Eqs. (1.12), (1.14) and (1.13) lead us to

$$\begin{aligned} Y_{11}^L &= \frac{1}{v_3} 6.26559 \times 10^{-3} \text{ eV}, \\ Y_{12}^L &= -\frac{1}{v_3} 1.15733 \times 10^{-2} \text{ eV}, \\ Y_{13}^L &= \frac{1}{v_3} 7.1017 \times 10^{-3} \text{ eV}, \\ Y_{22}^L &= \frac{1}{v_3} 2.30257 \times 10^{-2} \text{ eV}, \\ Y_{23}^L &= -\frac{1}{v_3} 1.88369 \times 10^{-2} \text{ eV}, \\ Y_{33}^L &= \frac{1}{v_3} 2.78919 \times 10^{-2} \text{ eV}. \end{aligned} \quad (2.3)$$

With these Yukawa couplings in hand, we can substitute these expressions in Eq. (2.2). It is possible to infer that theoretically, after assuming the assumptions above, a ratio between these two main LFV branching ratios is close 0.17 ($BR(\mu \rightarrow \gamma e)/BR(\mu \rightarrow eee) \approx 0.17$). Their experimental limits are close, too (difference of only one order). After considering experimental errors, we can state that these two experimental limits impose the same constraints (in the $v_3 \times m_{\Delta^{++}}$ plane).

Now, after explicitly write the Yukawa couplings as a function of the triplet vev, $Y_L = Y_L(v_3)$, we will explore tree-level doubly-charged scalar mass parameter dependence,

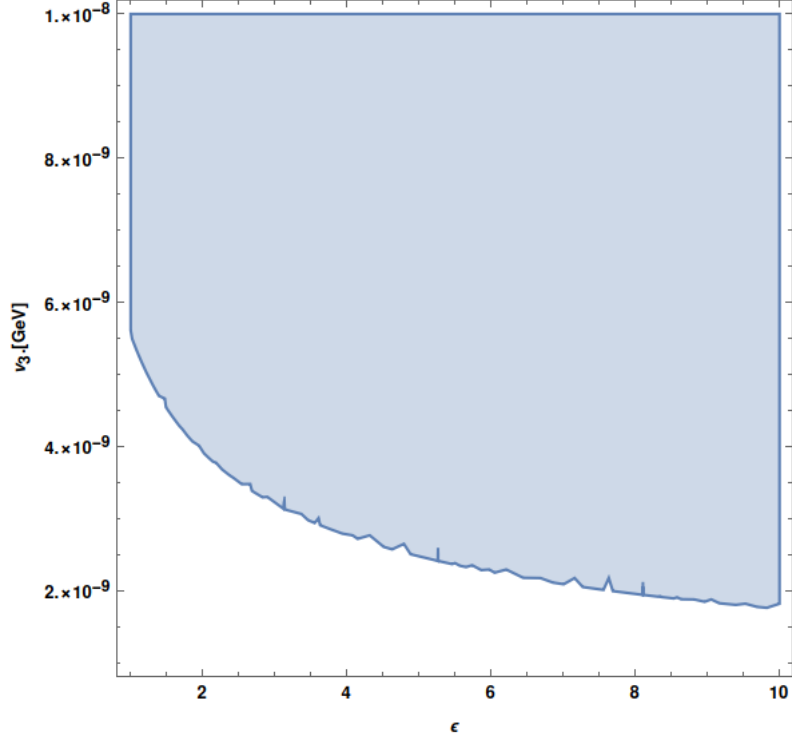


Figure 2.1: This plot represents how the vev v_3 changes compared to the ϵ -parameter, supposing that the doubly and singly-charged particles are degenerated in mass.

Eq. (1.36). Considering degenerescence between triplet charged scalars is the same as ignore the λ_4 parameter, since $|m_{\Delta^{++}}^2 - m_{H^+}^2| \approx \frac{1}{4}\lambda_4 v_2^2$. Then, it is possible to write the doubly-charged scalar mass at tree-level as

$$m_{\Delta^{++}}^2 \approx \frac{\epsilon v_2^2}{\sqrt{2}}. \quad (2.4)$$

As we have discussed before, this doublet scalar vev v_2 is very close to the standard-Higgs one, $v_2 \approx 246 \text{ GeV}$. Now, these branching ratios have a direct constraint between v_3 and ϵ -parameter. Explicitly, in the process $\mu \rightarrow \gamma e$, the branching ratio constraint leads toward the relation

$$\frac{4.76379 \times 10^{-10}}{v_3^4 \epsilon^2} < 4.2 \times 10^{-13}. \quad (2.5)$$

Following the train of thought, we want to choose the lowest possible value for the triplet vev (seeking a natural value for the Yukawa couplings). For ϵ -parameter minor than 10, we have found a more stringent constraint in v_3 parameter space. The triplet vev must obey $v_3 > 2 \text{ eV}$, as can be seen in Fig. (2.1) .

With this new limit in low scale type II seesaw, we will choose the most natural value for v_3 that respects LFV processes constraints. From now on in this Section, we

will work with $v_3 = 3 \text{ eV}$. We wrote in a table some values for Yukawa couplings in three different triplet vevs. It is important to mention that for these choices, μ lies between $6 - 30 \text{ eV}$. As was discussed in previous chapter, t'Hooft naturalness leads to small μ values. Then, our choice was natural in t'Hooft sense in two ways ($\mu \rightarrow \text{eV}$ and $Y_L \rightarrow 1$). Setting these parameters (v_3 and μ) at low energy scales, will lead to a phenomenological richer type II seesaw. We will investigate some physical consequences in the next chapter.

Y_{ij}^L	$v_3 = 3 \text{ eV}$	$v_3 = 6 \text{ eV}$	$v_3 = 9 \text{ eV}$
Y_{11}^L	0.00208853	0.00104427	0.000696177
Y_{12}^L	-0.00385776	-0.00192888	-0.00128592
Y_{13}^L	0.00236723	0.00118362	0.000789078
Y_{22}^L	0.00767522	0.00383761	0.00255841
Y_{23}^L	-0.00627895	-0.00313948	-0.00209298
Y_{33}^L	0.00929729	0.00464865	0.0030991

Table 2.1: This table represent different neutrino Yukawa coupling values after fixing the triplet vev in the values 3 eV , 6 eV and 9 eV . After looking at how these Yukawa couplings evolves, it became clear that it is important to keep v_3 small as possible if it is wanted natural Yukawa couplings.

2.3 Low scale type II seesaw and Inverse Seesaw mechanism

Another interesting aspect that we may investigate is the proximity of the low scale type II seesaw and the Inverse seesaw mechanism (ISS). Firstly, we will fully introduce ISS. Implementing minimal ISS mechanism requires the addition of three right-handed neutrinos N_{iR} and three standard model singlet neutral left-handed fermions S_{iL} to three SM active neutrinos ν_{iL} , as in [56]. In order to allow that these nine neutrinos develop exactly the following bilinear terms

$$\mathcal{L} = -\bar{\nu}_L m_D N_R - \bar{S}_L M N_R - \frac{1}{2} \bar{S}_L \mu_{ISS} S_L^C + H.c., \quad (2.6)$$

where m_D , M and μ_{ISS} are generic 3×3 mass matrices. These masses can be represented as a 9×9 matrix in the basis (ν_L, N_R^C, S_L) :

$$M_\nu = \begin{pmatrix} 0 & m_D^T & 0 \\ m_D & 0 & M^T \\ 0 & M & \mu_{ISS} \end{pmatrix}. \quad (2.7)$$

It is important to note that μ_{ISS} is the only term that explicitly breaks lepton number. Using the same naturalness principles as in chapter 1, μ_{ISS} lies at low energies. In this scenario M represents a Dirac mass term, however it is associated with another

energy scale, a hidden sector that is choose to be at TeV scales to be phenomenological viable in actual experiments[56]. m_D is our usual Dirac mass generated after EWSB of the standard-like Higgs. Lastly, μ_{ISS} is the Majorana mass of the LH fermion and explicitly violates $B - L$ global symmetry. On considering the hierarchy $\mu_{ISS} \ll m_D \ll M$, the diagonalization of the neutrino mass matrix provides the following effective neutrino mass matrix for active neutrinos:

$$m_\nu \approx m_D^T (M^T)^{-1} \mu_{ISS} M^{-1} m_D. \quad (2.8)$$

This relation can be written in a simpler form as

$$m_\nu \approx \frac{m_D^2 \mu_{ISS}}{M^2}, \quad (2.9)$$

that has the same form as the low scale type II seesaw

$$v_3 \approx \frac{v_2^2 \mu}{\mu_3^2}. \quad (2.10)$$

This similarity is incredible, since they are very different physical scenarios. In low scale type II seesaw case, there are only three neutrinos, left-handed. Is added in the SM six degrees of freedom (six spin-0 fields), related to the six scalar fields $H, A, H^+, H^-, \Delta^{--}, \Delta^{++}$. Doubly charged scalars have unique signature, the heavy Higgs is a particle that can decay in two photons and lastly singly charged scalars contributes to electron-neutrino scattering amplitude. In the Inverse Seesaw case, there are nine neutrinos, six left-handed and three right-handed. Adding three right-handed fermions and three left-handed fermions, in general increases twelve degrees of freedom of the Lagrangian. However, in ISS case, these fermions are Majorana particles. The last fact cut off these new degrees of freedom by half, i.e., in this case there are six degrees of freedom, too. Considering its couplings hierarchy, there is a small chance to measure directly these new Majorana particles, compared to the low scale type II seesaw case.

Another property of ISS mechanism is that the coupling μ_{ISS} explicitly violates $B - L$ symmetry. This parameter is very similar to the μ -parameter of low scale type II seesaw, since they are lepton number explicitly broken parameters at low energy scales ($eV - keV$). To justify smallness of μ_{ISS} , we can use the naturalness principle. In 331 models this small coupling can be associated with a spontaneous symmetry breaking of a scalar field. Then, $B - L$ symmetry is recovered[56].

The versatility of type II seesaw is quite impressive! Its continuously connects two completely different seesaw scenarios, the type I seesaw and the ISS. Therefore it has very different physical realization from both scenarios. The low scale version of this mechanism is natural in t'Hooft sense and the lepton number violation coupling is

dynamically justified. Neutrinos masses are generated by SSB of the triplet scalar and there is not right-handed neutrinos in this mechanism and consequently no Dirac mass terms.

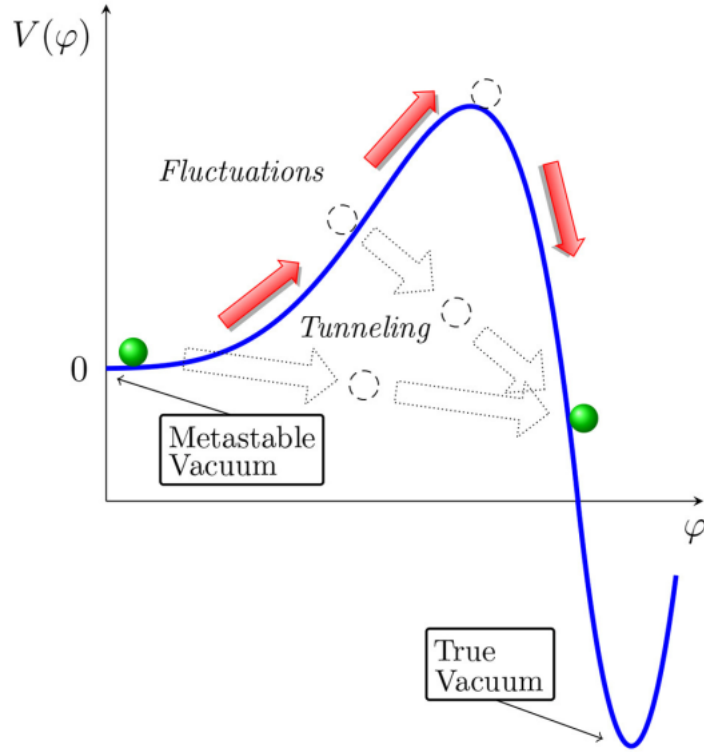


Figure 2.2: This figure represents three different ways in which the false vacuum transits to the true vacuum. To transit using Quantum and Thermal fluctuations, the false ground state climbs the potential barrier, going to the true vacuum. However, Tunneling this potential barrier is the most effective way for this transition.

2.4 False Vacuum and Higgs Metastability

2.4.1 False Vacuum vs True Vacuum

If the potential is BFB, then it is guaranteed that a true vacuum exists. A true vacuum is the the ground state of a quantum (and classical) potential. Consequently, tunneling to a lower energy state it is not possible. Alternatively, a false vacuum, defined first in [57] and more detailed in [58, 59], is a local minima of the potential, but it is not a global one. Therefore, if the potential rests in a false vacuum it is allowed to transit from this state to a true vacuum state in three different ways, as indicated by Fig. 2.2[59]. It is viable to climb the barrier of the potential via quantum or thermal fluctuations. Tunneling through this energy barrier it is permitted, too. Qualitatively, a false vacuum can decay to the true vacuum.

Between these three possibilities, the more frightening transition is via quantum tunneling. Frightening because the vacuum state can propagate through a potential barrier no matter its height. Following [57, 60], we will try to explain this process intuitively. Let the potential of a scalar field ϕ , $V(\phi)$, possess two relative minima, only one of which, ϕ_- is an absolute minimum, as in Fig 2.3. Classically and quantically, ϕ_- corresponds to the true vacuum state. The state $\phi = \phi_+$ is a stable classical equilibrium state. Although,

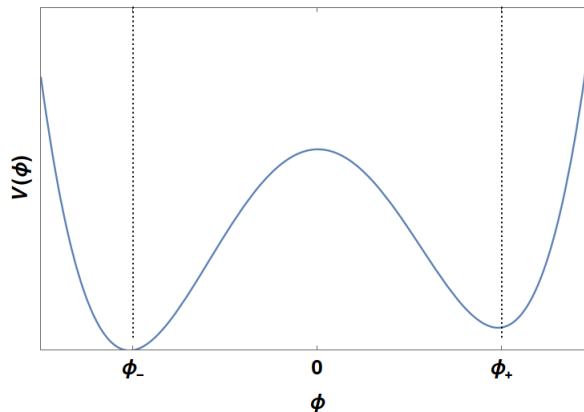


Figure 2.3: Here we represent a projection of an inclined “mexican hat”, in which ϕ_- is the true vacuum of this potential and ϕ_+ is a local minima, but not a global one.

it is rendered unstable by quantum effects, as discussed before. As described in [57], if the vacuum rests in ϕ_+ , quantum fluctuations (instanton effects) can form a bubble of true vacuum, ϕ_- .

If the bubble is too small, the gain in volume energy caused by the manifestation of this bubble is compressed by its positive surface tension (domain walls), and the bubble shrinks to nothing (volume energy goes with R^3 and surface tension with R^2). Then, there is a critical radius R_c whereby the total energy of this process is zero. Nonetheless, if a bubble is formed large enough ($R > R_c$), it is energetically favorable for this bubble to grow. Once this occurs, the bubble expands throughout the universe until it converts false vacuum to true.

This process requires some time to proceed. Calculations of this time were made first in [57, 60]. They call this calculation as a “semi-classical approach”. Its indicates that the decay rate of the false vacuum depends on two parameters A and B in such a way that [61]

$$\Gamma \sim Ae^{-B}, \quad (2.11)$$

in natural units.

The phase factor B is proportional to the difference of the action between the false vacuum and the true one, ΔS . If this difference is high, then $\Gamma \ll 1$. Knowing that the time decay is inversely proportional to the decay rate, then $t_D = 1/\Gamma \gg 1$, and the typical time of this decay would become long as the cosmological time. We will discuss later these implications in the SM picture. Another interpretation for the B phase parameter is that B is the integral of the radial momentum of the walls through the potential barrier[60]. As before, this interpretation imposes a very small value for $e^{-B} \sim 10^{-730}$ [60]. Now that we saw what is the semi-classical point of view behind vacuum transitions, we need to understand how quantically these fields behave.

2.4.2 The Callan-Symanzik Equation

To connect the above discussion with Higgs Metastability, we must add a very important feature of Quantum Fields Theories, the evolution of coupling constants. As commented before, studying the BFB inequalities is a necessary condition for the vacuum stability, but not sufficient. Opposing classical field theories, quantum field theories have a very singular feature. Due to quantum corrections, tree-level couplings can change their behavior at high (and low) momenta. A natural question that arises is whether the coupling associated with the highest-order potential coupling is negative at some energies. If this is true for an arbitrary potential, it would not have a global minimum, therefore it would not acquire a true vacuum. These quantum corrections of the potential plus tree-level terms can be seen as an effective potential of the model, in the Coleman-Weinberg formalism [62].

However, this formalism depends on the cutoff scale. To be more general and precise we will use another formalism, called Renormalization Group [58, 27, 59]. The term "Group" has no relation to Group Theories, it only refers to a set of parameters that changes according to the scale of the renormalization of the model. The parameters of a renormalizable theory are determined by a set of renormalization conditions, which are applied at a certain momentum scale. Then, by looking at how the parameters of this arbitrary theory depends on the renormalization scale, we can find out the evolution of the coupling constants.

Following [27], we will show how the Callan-Symanzik equation can be derived in the ϕ^4 -theory. After, we will obtain the β -function of the Higgs quartic self-coupling λ via computational packages. To start, we must define the Lagrangian of the ϕ^4 -theory as

$$\mathcal{L} = \frac{1}{2}(\partial_\mu\phi)^2 - \frac{1}{2}m_0^2\phi^2 - \frac{\lambda_0}{4!}\phi^4, \quad (2.12)$$

in such a way that ϕ is a non renormalized scalar field, λ_0 and m_0 are the bare quartic coupling and the field's bare mass, respectively. To rescale this field in a renormalizable way, we must separate infinite (Z) and non infinite (ϕ_r) parts, as the following transformation (see Appendix B)[27]

$$\phi = Z^{1/2}\phi_r. \quad (2.13)$$

This transformation modifies the correlation functions values by a factor of $Z^{1/2}$ for each field and it is dependent on the arbitrary renormalization scale M . Studying these changes in correlation functions are the key point, since they derive the (1PI) diagrams, essential in our analysis (see Appendix B). This means that

$$\langle \Omega | T\phi_r(x_1)\dots\phi_r(x_n) | \Omega \rangle = Z^{n/2} \langle \Omega | T\phi(x_1)\dots\phi(x_n) | \Omega \rangle, \quad (2.14)$$

such that $|\Omega\rangle$ is the vacuum state ket and T is the time-ordering operator.

In this procedure, we will rescale all the couplings and the field ϕ of the Lagrangian, separating infinite (nonphysical) and finite (physical) parameters. Applying the transformation (2.13) in the Lagrangian, we obtain

$$\mathcal{L} = \frac{1}{2}Z(\partial_\mu\phi_r)^2 - \frac{1}{2}m_0^2Z\phi_r^2 - Z^2\frac{\lambda_0}{4!}\phi_r^4, \quad (2.15)$$

and the infinite terms can be absorbed by the counterterms

$$\delta_Z = Z - 1, \quad \delta_m = m_0^2Z - m^2, \quad \delta_\lambda = \lambda_0Z^2 - \lambda. \quad (2.16)$$

The more easy ϕ^4 -theory is massless (physical mass $m = 0$), and it can be shown that if $m^2 \rightarrow 0$ would lead to singularities in the counterterms[27]. To avoid this, particle's mass will be proportional to a renormalizable energy scale M in such a way that the renormalization conditions at a space-like momentum p with $p^2 = -M^2$ are given by

$$\begin{aligned} (1PI) &= 0 & \text{at } p^2 &= -M^2, \\ \frac{d}{dp^2}(1PI) &= 0 & \text{at } p^2 &= -M^2, \\ (p_1, p_2, p_3, p_4)_{amp} &= -i\lambda & \text{at } (p_1 + p_2)^2 &= (p_1 + p_3)^2 = (p_1 + p_4)^2 = -M^2, \end{aligned} \quad (2.17)$$

(Appendix B for more details).

These conditions define the two- and four- point Green's functions at a certain point and remove all ultraviolet divergences. It can be seen that the scale of renormalization M can vary freely, which varies the Green's functions $G^{(n)}$. Then, we can derive the same formalism for a different renormalization scale M' , using a new renormalized quartic coupling λ' and a new rescaling factor Z' . Then, it is viable to associate all the different renormalization scales with the Green's functions in a invariant scale equation commonly called Callan-Symanzik equation. In simple terms, a shift in the renormalization scale M leads to a shift in ϕ and λ ,

$$\begin{aligned} M &\rightarrow M + \delta M, \\ \lambda &\rightarrow \lambda + \delta\lambda, \\ \phi_r &\rightarrow (1 + \delta\eta)\phi_r, \end{aligned} \quad (2.18)$$

where $\delta\eta = \delta\phi_r/\phi_r$ is the perturbation in the renormalized field ϕ_r . Rescaling the field ϕ shifts the Green's function, since

$$G^{(n)}(x_1, \dots, x_n) = \langle \Omega | T \phi_r(x_1) \dots \phi_r(x_n) | \Omega \rangle_{connected}, \quad (2.19)$$

it is clear that in first order perturbation theory the Green's functions becomes

$$G^{(n)} \rightarrow (1 + n\delta\eta)G^{(n)}. \quad (2.20)$$

We can think of $G^{(n)}$ as a function of the renormalization scale M and the coupling λ , such that $G^{(n)}(M, \lambda)$. The differential form of $G^{(n)}$ can be written as

$$dG^{(n)} = \frac{\partial G^{(n)}}{\partial M} \delta M + \frac{\partial G^{(n)}}{\partial \lambda} \delta \lambda = n\delta\eta G^{(n)}, \quad (2.21)$$

or, more explicitly

$$\left(\frac{\partial}{\partial M} \delta M + \frac{\partial}{\partial \lambda} \delta \lambda - n\delta\eta \right) G^{(n)} = 0. \quad (2.22)$$

It is conventional to write this equation with the dimensionless parameters

$$\beta \equiv \frac{M}{\delta M} \delta \lambda, \quad \gamma \equiv -\frac{M}{\delta M} \delta \eta. \quad (2.23)$$

Then, its final form can be written as

$$\left(M \frac{\partial}{\partial M} + \beta \frac{\partial}{\partial \lambda} + n\gamma \right) G^{(n)}(x_1, \dots, x_n; M, \lambda) = 0. \quad (2.24)$$

Even $G^{(n)}$ depending on the renormalization scale, the parameters β and γ does not. This is so because the Green's function is renormalized (Eq. 2.19), consequently these dimensionless parameters cannot depend on the cutoff scale. Since these two parameters cannot vary with the cutoff scale and by dimensional analysis they are not energy quantities, the ratio $M/\delta M$ is independent from M . These functions depends only from the couplings of the model. Therefore, all Green's function of massless ϕ^4 -theory must satisfy this equation.

The physical intuition of the Callan-Symanzik Equation is that the scale M does not impact the observables of the theory. We can define the theory at any other scale and obtain the same answer. It is fundamental to understand that exists two universal

$$G^{(4)} = \text{tree-level} + \text{one-loop bubble} + \dots + \text{one-loop crossed} + \mathcal{O}(\lambda^3)$$

Figure 2.4: The Green's function $G^{(4)}$ at one-loop perturbation theory. We need to calculate each of these diagrams to find the β -function of the quartic coupling λ .

functions $(\beta(\lambda), \gamma(\lambda))$ related to the shifts in the coupling constant and field strength, respectively, that compensate for the shift in the renormalizable scale M . Interpreting physically Eq. (2.23) shows us that the β -function is associated with a shift in the quartic coupling constant, and the γ -function as the shift in the field normalization. As we are not interested in observing shifts in the field, we will deepen our investigation in the β -function and understand its physical interpretation, not only in the ϕ^4 -theory, but in an arbitrary model. In agreement with this formalism, we will finally calculate how coupling constants evolves with energy.

2.4.3 β -function interpretation

Here, we need to interpret the physical meaning of these dimensionless functions to make the connection between our previous discussion about false vacuum and the β -function. This function is proportional to the shifting in the coupling constant when the renormalization scale is changed. Here we will “compute” the ϕ^4 -theory β_λ -function at one-loop and interpret this result physically.

Quantum corrections of the coupling λ depends on the 4-point correlation function, here as Green's function $G^{(4)}$, as in Fig. (2.4). This Green's function depends on s , t , and u diagrams. They can be written as

$$G^{(4)}(s, t, u, M) = [-i\lambda + \Gamma(s) + \Gamma(t) + \Gamma(u) - i\delta_\lambda] \prod_{i=1}^4 \frac{i}{p_i^2}. \quad (2.25)$$

Using the Renormalization Conditions in Eq. (2.18), and after explicit calculations of these diagrams in [27]

$$G^{(4)}(-M^2, -M^2, -M^2) = [-i\lambda + 3i(-i\lambda)^2 V(-M^2) - i\delta_\lambda] \prod_{i=1}^4 \frac{i}{p_i^2} = -i\lambda \prod_{i=1}^4 \frac{i}{p_i^2}, \quad (2.26)$$

that implies

$$\delta_\lambda = \frac{3\lambda^2}{2(4\pi)^{d/2}} \int_0^1 dx \frac{\Gamma(2 - \frac{d}{2})}{(x(1-x)M^2)^{2-d/2}}. \quad (2.27)$$

In the limit as $d \rightarrow 4$, it becomes

$$\delta_\lambda = \frac{3\lambda^2}{2(4\pi)^2} \left[\frac{1}{2-d/2} - \log M^2 + \text{finite} \right], \quad (2.28)$$

where the finite terms are independent of M . Now, we can apply the Callan-Symanzik equation in to the Green's function, since the only dependence of $G^{(4)}$ comes from δ_λ . The first term of this equation is

$$M \frac{\partial G^{(4)}}{\partial M} = \frac{3\lambda^2}{2(4\pi)^2} \prod_{i=1}^4 \frac{i}{p_i^2}. \quad (2.29)$$

At one-loop $\gamma = 0$. Then, the remaining term is, in first order

$$\frac{\partial G^{(4)}}{\partial \lambda} = -i + \mathcal{O}(\lambda), \quad (2.30)$$

and finally the β -function

$$\beta(\lambda) = \frac{3\lambda^2}{16\pi^2} + \mathcal{O}(\lambda^3). \quad (2.31)$$

It is notorious the difficulties of this type of calculation. There is a more easy way to find out the β -function only with the counterterms[27]. However, we will not dive deeply in this subject. As we have saw, β -function is the rate of change of the renormalized coupling at the scale M corresponding to a fixed bare coupling. This can be associated with the rate of the renormalization group flow of the coupling constant λ . Then, a positive sign for the β -function indicates a renormalized coupling that increases at large momenta and decreases at small momenta. We can solve explicitly the Callan-Symanzik equation for the coupling λ as [27]

$$\frac{d}{d \log(p/M)} \bar{\lambda}(p; \lambda) = \beta(\bar{\lambda}), \quad \bar{\lambda}(M; \lambda) = \lambda. \quad (2.32)$$

Integrating with the equation (2.31), this λ parameter becomes

$$\bar{\lambda}(p) = \frac{\lambda}{1 - (3\lambda/16\pi^2) \log(p/M)}. \quad (2.33)$$

As expected, a positive value for the β -function should imply an effective coupling that becomes stronger in large momenta and weaker at low momenta. One can investigate

what happens for decreasing or null β -functions. If these are the cases, when the β -function is decreasing, the coupling becomes weaker at large momenta and stronger at low momenta. For the null β -function, the effective coupling does not vary with momenta.

Nonetheless, it can be shown that if we add fermions in ϕ^4 -theory (known as Yukawa theory), then it is possible for λ to become negative at high momenta [58]

$$\mathcal{L}_{Yukawa\ theory} = \mathcal{L}_{\phi^4} + i\bar{\psi}\gamma_\mu\partial^\mu\psi + y_f\phi\bar{\psi}\psi + H.c., \quad (2.34)$$

in such a way that ψ represents a fermion. The β_λ function takes on the following expression[58]

$$16\pi^2\beta_\lambda = 12\lambda^2 + 12\lambda y_f^\dagger y_f - 12y_f^\dagger y_f y_f^\dagger y_f. \quad (2.35)$$

In this case, the β_Y function of the Yukawa coupling is strictly positive ($16\pi^2\beta_{y_f} = 9/2 y_f^3$). Then, it is clear that, for small initial λ values and large initial y_f values, it is probable that the β_λ function is negative at high energies.

2.4.4 $\beta_{\lambda_{SM}}$ -function of the Standard Model

As seen in the previous subsection, it is an extremely arduous task to calculate β -functions for more complex models. For this reason, we seek to do these calculations in a mathematical package called SARAH-4.14.3[63]. According to this software and corroborated by the paper [58], the main contribution of the one-loop $\beta_{\lambda_{SM}}$ -function (λ_{SM} as the quartic coupling of the Higgs) is written as

$$16\pi^2\beta_{\lambda_{SM}} \approx \frac{27}{100}g_Y^4 + \frac{9}{10}g_Y^2g^2 + \frac{9}{4}g^4 - 9g^2\lambda_{SM} - \frac{9}{4}g_Y^2\lambda_{SM} + 12\lambda_{SM}^2 \quad (2.36) \\ + 12\lambda_{SM}y_t^\dagger y_t - 12y_t^\dagger y_t y_t^\dagger y_t,$$

where y_t is the Yukawa Top coupling, g_Y and g are the $U(1)_Y$ and $SU(2)_L$ gauge couplings, respectively and λ_{SM} is the quartic self-coupling of the Higgs.

For quark top mass much larger than the Higgs mass, $\beta_{\lambda_{SM}}$ is negative and λ_{SM} is weaker at high momenta. If λ_{SM} becomes negative, then the potential is not BFB at high energies. As was discussed at the beginning of this section, if the vacuum is in a position of local but not global minimum, it is possible a transition from the false vacuum to the true vacuum. For negative λ_{SM} , this global minimum state is $-\infty$. Another possibility is if the energy barrier is so thick that the decay time of this vacuum becomes greater than the cosmological time. We will call this region Metastable.

It is possible to distinguish between three regions, where the vacuum is completely

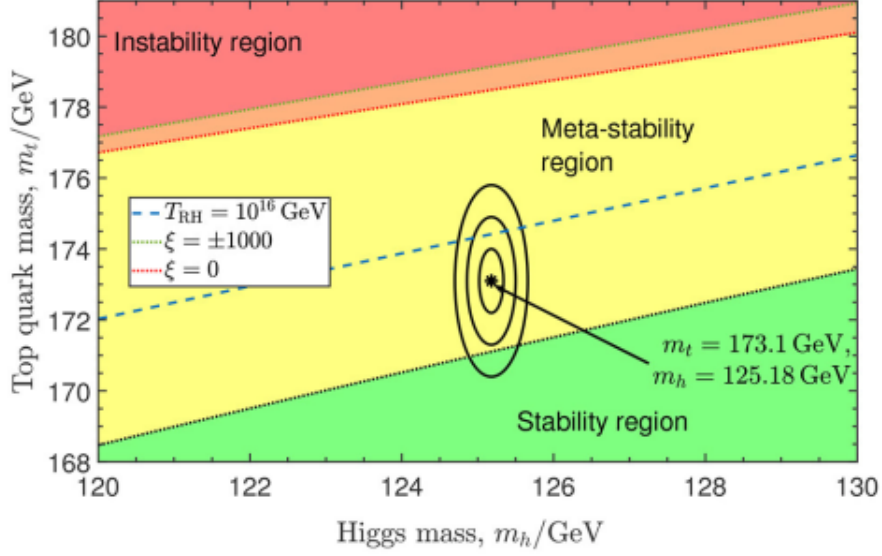


Figure 2.5: This plot represents the stability of the SM vacuum state in the Higgs and top masses. Ellipses show the 1σ , 2σ , 3σ confidence intervals for m_t and m_h around their central values. In the green region, the current vacuum is absolutely stable, in the yellow region it is metastable, and in the red region it is so unstable that it would not have survived until the present day. These blue and red dotted line are associated with cosmological constraints, assuming values for the Reheating temperature T_{RH} . This ξ parameter is associated with gravitational corrections in the vacuum state of the universe. More detailed explanation in the cited paper.

stable, totally unstable and metastable, as in Fig. (2.5)[59].

Our current best estimates of the Higgs and top quark masses are [46]

$$m_t = 173.1 \pm 0.9 \text{ GeV}, \quad m_h = 125.18 \pm 0.16 \text{ GeV}, \quad (2.37)$$

place the Standard Model squarely in the metastable region [64].

Then a question arises. Is it possible that the contribution of the new scalar triplets will make the Higgs vacuum totally stable? The answer is: Yes. However, as we will see in the next section, when solving this problem, another problem related to naturalness arises, in such a way that it is not possible to solve both at the same time.

2.5 Two problems that cannot be solved simultaneously in this Triplet Extension

2.5.1 Vacuum Stability at High Scales

At $\Lambda \approx 10^8 - 10^{10} \text{ GeV}$ scale energies, the quartic coupling of the Standard Higgs λ_{SM} becomes negative, as we already discussed. This transforms the previously stable vacuum into a metastable one. If we introduce physics beyond Standard Model (BSM) at low energy scales than Λ , it is possible to make λ_{SM} always positive. For the potential of

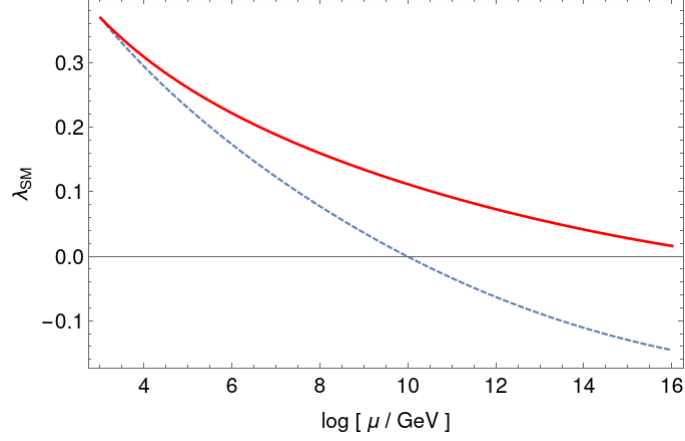


Figure 2.6: The dashed blue line represents the SM prediction. In the triplet model, the red thick line, $\lambda_4 = 0.5$. Commonly the other parameters are taken as $\lambda_1 = \lambda_2 = \lambda_3 = 0.1$. We have observed that this model can have a stable vacuum at high scales.

Eq. (4.3), positive contributions to the $\beta_{\lambda_{SM}}$ function arise ($\lambda \approx \lambda_{SM}$) due to the quartic interactions between the Higgs and the scalar triplet, λ_4 and λ_1 .

Using SARAH-4.14.3[63], the one-loop $\beta_{\lambda_{SM}}$ function is

$$\begin{aligned} \beta_{\lambda_{SM}} \approx & \frac{27}{100}g_Y^4 + \frac{9}{10}g_Y^2g^2 + \frac{9}{4}g^4 - \frac{9}{4}g_Y^2\lambda - 9g^2\lambda + 12\lambda^2 + \frac{3}{2}\lambda_1^2 + \frac{3}{2}\lambda_1\lambda_4 \quad (2.38) \\ & + \frac{5}{8}\lambda_4^2 + 12\lambda y_t^\dagger y_t - 12y_t^\dagger y_t y_t^\dagger y_t. \end{aligned}$$

Analysing this beta function, we can find that, if λ_4 and/or λ_1 are relatively large, then the quartic coupling λ_{SM} is always positive at high scales as in Fig. (2.6) and this vacuum is always stable. Otherwise, this potential has a metastable vacuum as the SM.

2.5.2 One-loop Higgs Mass Correction

Higgs mass one-loop correction, according to [50, 65], depends directly from the triplet mass μ_3 and the quartic couplings λ_1 and λ_4

$$\delta m_h^2 \approx -\frac{3}{16\pi^2}(\lambda_1 + \lambda_4)\mu_3^2 \log \frac{M_{Pl}^2}{\mu_3^2}, \quad (2.39)$$

where $M_{Pl} = 2.4 \times 10^{18} \text{ GeV}$ is the chosen cutoff.

By naturalness principles in t'Hooft sense, Higgs one-loop mass correction should be much smaller its at tree-level, $\delta m_h^2/M_h^2 \ll 1$. For mass corrections to be small as possible, it is necessary that the coupling between the Higgs and the scalar triplet be very tiny

$$\frac{\delta m_h^2}{M_h^2} \approx -\frac{3}{16\pi^2}(\lambda_1 + \lambda_4) \frac{\mu_3^2}{m_h^2} \log \frac{M_{Pl}^2}{\mu_3^2} \ll 1. \quad (2.40)$$

Then, it is natural to limit $\lambda_1, \lambda_4 \ll 1$. Therefore, as we have already seen these quartic couplings are required to be large enough for the Higgs vacuum to be fully stable at high energies. Furthermore, these two problems cannot be solved simultaneously in this model. As we will explore in chapter 4, there is one model that solves these two problems simultaneously. This is the called 123 model.

2.6 Discussion

In this chapter we have complained about some aspects of the low energy scale type II seesaw mechanism. Firstly, LFV process have guided us to constraint the ϵ -parameter. Secondly, we have discussed how close low scale type II seesaw is to the ISS mechanism. However, phenomenological scenarios between these two mechanisms are very different, even though the seesaw relationship between couplings are very similar. In the last two sections, we have commented about false vacuum, renormalization group equations and the metastability of the standard Higgs. Then, in minimal type II seesaw, the naturalness problem (related to the one-loop mass correction of the Higgs) and vacuum stability at high scales cannot be performed simultaneously, since these two problems are solved by the same couplings in very different parametric region. In the next chapter we will study the main phenomenological properties of this model, as the doubly charged constraints and the main decays of neutral triplet scalars.

3 Phenomenology of the Low Scale Type II Seesaw Mechanism

One attractive feature of HTM is the presence of the doubly-charged Higgs boson, and its distinguishing decay modes. Depending on the Yukawa coupling value Y_Δ (or the triplet vev), the doubly-charged Higgs boson can decay into same-sign dilepton, same-sign gauge bosons, or even via a cascade decay [35, 66, 67]. If such couplings are sufficiently large (v_Δ small), it will decay predominantly into same-sign charged leptons, which is a clear signature of Lepton Flavor Violation (LFV), discussed in chapter 2. Such signal at colliders are a generic high energy analogue of the neutrinoless double beta decay as a probe of LFV. Besides, if Y_Δ are very small (v_Δ large), doubly-charged scalars will decay predominantly in same sign W bosons.

Another interesting aspect to explore in HTM is its singular contribution to electron-neutrino scattering due singly-charged scalar. $\nu - e$ scattering is a precision test of the SM because do not involve QCD contributions. However, such experiment has many sources of unavoidable background (we will discuss about this later) and it can only be tested in a restricted energy range. We will explore how H^+ contributes for the differential cross section of such scattering process, comparing it with actual data.

Additionally, for completeness, we will obtain the interactions and branching ratios for the remaining triplet scalar particles components(A and H). We will searched for another scalars signatures in experiments, like the heavy Higgs H decay in gauge bosons and active neutrinos. A particular case that we are interested is the diphoton decay of H . Thus, for the massive CP-odd scalar, we will calculate the symbolic expression for its principal decay rate (for small v_Δ).

A last comment is about notation. In past chapters we have adopted v_3 as the triplet scalar vev and μ_3 as the triplet scalar mass. However, specially in this chapter we have adopted the substitution $3 \rightarrow \Delta$. Then, v_Δ as the triplet scalar vev, M_Δ as the triplet scalar mass and v as the doublet scalar vev.

This chapter is organized as follows. In Section 3.1 we develop the decay channels of doubly-charged scalar, while in Section 3.2 we study the contribution of the H^+ to electron-neutrino scattering processes. In Section 3.3 we briefly discuss the decay rate of the CP-odd scalar particle, while in Section 3.4 we develop heavy Higgs decays. The last section of this chapter we present our final remarks.

3.1 Doubly-charged scalar branching ratios

As commented above, a characteristic feature of type II seesaw is the presence of the doubly-charged scalar $\Delta^{\pm\pm}$. Its decay into leptonic and bosonic states gives unique signatures in the colliders. In this section we will investigate these signatures and the parametric dependence of each decay mode. To do this, we need to find the main vertices responsible for $\Delta^{\pm\pm}$ tree-level decay,

$$\begin{aligned} V(\Delta^{++}l_i^-l_j^-) &= \frac{Y_{Lij}}{\sqrt{2}}, \\ V(\Delta^{++}W^-W^-) &= -\sqrt{2}iv_\Delta g^2 g_{\mu\nu}. \end{aligned} \quad (3.1)$$

Since $Y_{Lij} = \frac{m_{\nu ij}}{v_\Delta} \approx \frac{0.1 \text{ eV}}{v_\Delta}$, these two vertices are inversely proportional. This fact will resonate in the decay rate final formula. The relevant decay widths were calculated with the help of **CalcHEP v 3.8.6** tool[68]. It is possible to find the following expression for the Total Decay Width (Γ) of the double-charged scalar

$$\begin{aligned} \Gamma(\Delta^{++} \rightarrow All) &\approx \Gamma(\Delta^{++} \rightarrow l_i^+l_j^+) + \Gamma(\Delta^{++} \rightarrow W^+W^+) \\ &= \frac{1}{(1 + \delta_{ij})8\pi} \sqrt{(m_{\Delta^{++}}^2 - 4m_{l_j}^2)(m_{\Delta^{++}}^2 - 4m_{l_i}^2)} Y_{Lij}^2 + \\ &\quad \frac{g^4 v_\Delta^2}{8\pi m_{\Delta^{++}}} \sqrt{1 - 4/r_W(r_W^4/4 - r_W^2 + 3)}, \end{aligned} \quad (3.2)$$

such that $r_W = m_{\Delta^{++}}/m_W$ [66][35].

Specifically for the case where neutrino mass hierarchy is normal ordered (NO) and the lightest neutrino mass is zero ($m_1 = 0$), it can be inferred the branching fraction of the leptonic and bosonic modes using Eq.2.3. Figures 3.1, 3.2, 3.3 and 3.4 represents decay modes **vs** triplet mass $M_\Delta = m_{\Delta^{++}}$. Each figure is related to a different triplet vev value.

For small triplet vevs, $v_\Delta = 1 - 100 \text{ eV}$, Δ^{++} predominantly decays into the same-sign leptonic states $\Delta^{++} \rightarrow l_i^+l_j^+$ (Figs. 3.1 and 3.2). In this case, its most relevant decays are $\Delta^{++} \rightarrow \tau^+\tau^+$, $\Delta^{++} \rightarrow \tau^+\mu^+$ and $\Delta^{++} \rightarrow \mu^+\mu^+$, due to hierarchy $Y_{L11}^2 \ll Y_{L22}^2 < Y_{L33}^2$. For our choice ($m_1 = 0$) the dominance of the leptonic decay mode is balanced with the gauge boson mode $\Delta^{++} \rightarrow W^+W^+$ around the triplet vev $\sim 1 \text{ keV}$, slightly lower than predictions of the papers [66][35], where $v_\Delta \sim 100 \text{ keV}$. Whereas for larger v_Δ , the gauge boson mode becomes dominant (Figs. 3.3 and 3.4).

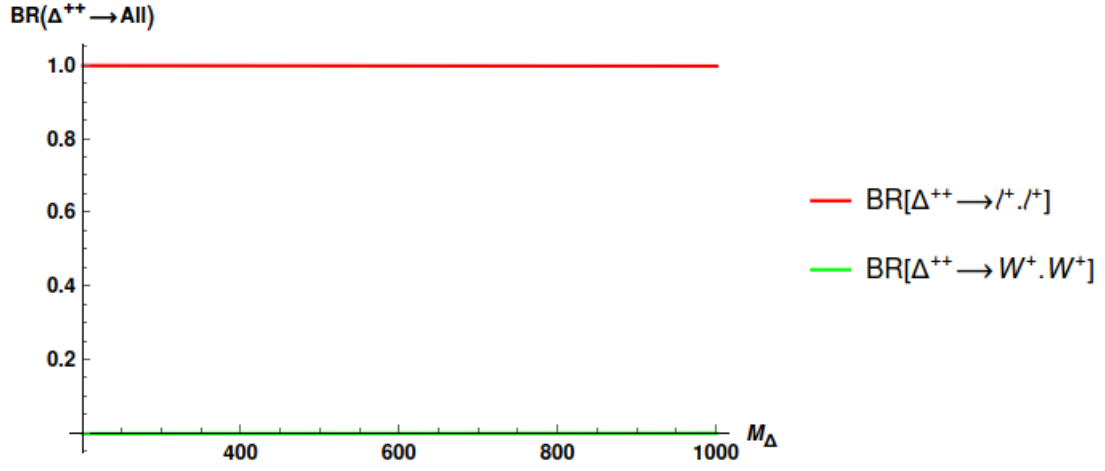


Figure 3.1: For $v_3 = 1 \text{ eV}$, leptonic decays are totally predominant in the doubly charged scalar channel. We have fixed $m_{\nu 1} = 0$ in Normal Hierarchy, using Eq. 2.3.

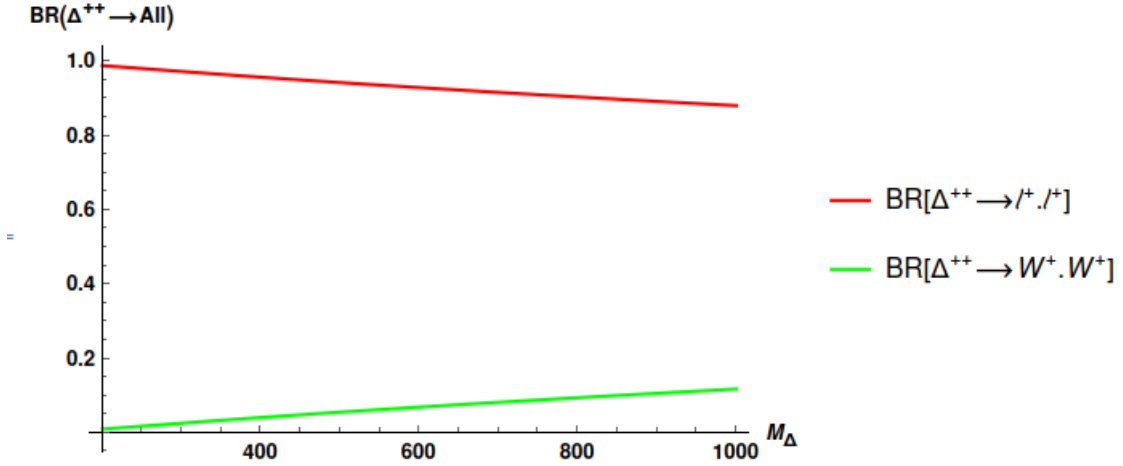


Figure 3.2: For $v_3 = 100 \text{ eV}$, leptonic decays are predominant in the doubly charged scalar channel. We have fixed $m_{\nu 1} = 0$ in Normal Hierarchy, using Eq. 2.3.

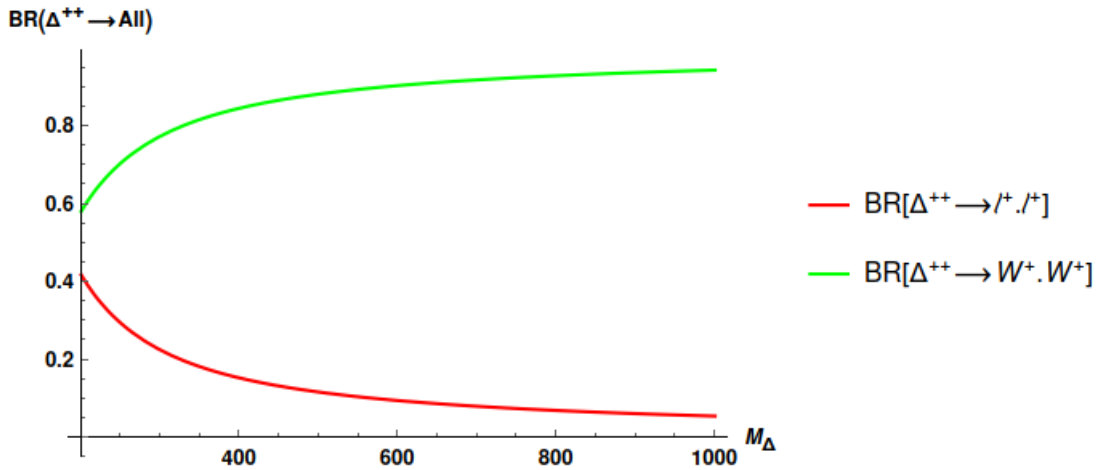


Figure 3.3: For $v_3 = 1 \text{ keV}$, W boson decays are predominant in the doubly charged scalar channel. We have fixed $m_{\nu 1} = 0$ in Normal Hierarchy, using Eq. 2.3.

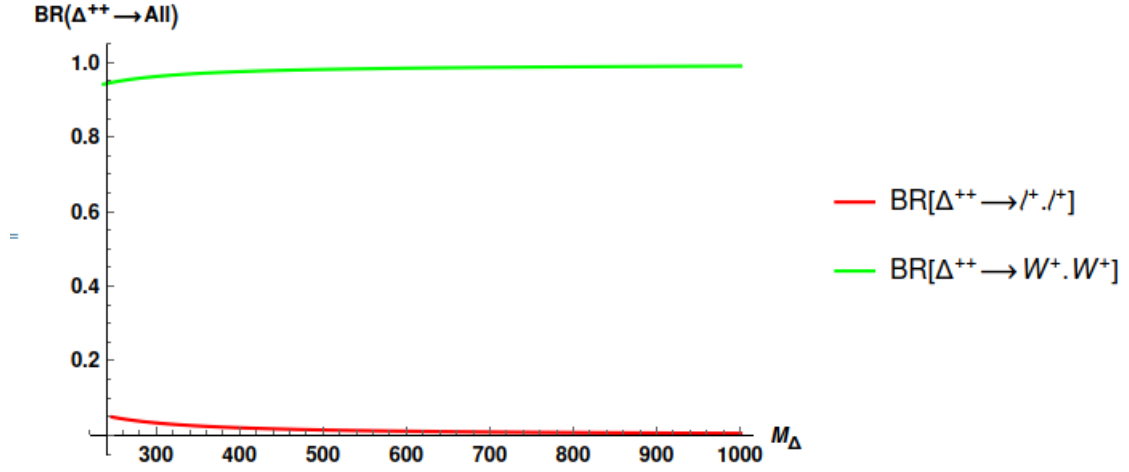


Figure 3.4: For $v_3 = 10 \text{ keV}$, W boson decays are totally predominant in the doubly charged scalar channel. We have fixed $m_{\nu 1} = 0$ in Normal Hierarchy, using Eq. 2.3.

3.2 Neutrino-Electron Scattering in Type II Seesaw

Lately, the study of elastic collisions between electrons and neutrinos have become of great interest. This type of collision offers a clean probe of contributions from the Standard Model and deviations of these values can be related to new physics, such as Dark Photons [69]. We know that in the Standard Model the diagrams that generate these processes at tree level only have W and Z bosons as intermediaries. There are no hadronic complications, so that deviations from SM expectations are directly accessible. Following the line of reasoning of [70] and [71] we will investigate the contribution of the simply-charged scalar for this collision.

The study of neutrino-electron scattering is experimentally challenging due to its tiny cross-section, which forces one to pursue very intense sources and large targets. An important comment that should be made is about irreducible backgrounds for this type of experiment. The neutrino-nucleon scattering cross-section, as said in [70], is generally three orders of magnitude larger and serves as a large potential source of background. Mainly in ν_e and $\bar{\nu}_e$ sources, charged current neutrino-nucleon reaction $\nu_e N \rightarrow e X$ can yield a final state that is often consistent with a single recoil electron. Such backgrounds, however, can still be reduced with Kinematics constraints. For example, electrons produced by neutrino-electron scattering are constrained by kinematics to have small transverse momenta, whereas the electron distribution in most background events is much broader (due nucleon masses). Therefore, an experiment with good transverse energy resolution can significantly constrain this class of background events. More simply, for collisions with energies much greater (or much smaller) than the resting energy of the electrons (0.511 MeV), background associated with neutrino-nucleon collisions are much greater than the signal of neutrino-electron collisions.

Our goal its to find the differential cross section as a function of the electron's recoil energy T and the neutrino beam energy E_ν . Precisely,

$$\frac{d\sigma_{\nu_\alpha e^- \rightarrow \nu_\alpha e^-}}{dT} = \frac{d\sigma(E_\nu, T)}{dT}. \quad (3.3)$$

In SM, the contributions are from the diagrams of the Fig. 3.5. The total cross section as a function of T and E_ν is[71]

$$\frac{d\sigma}{dT}_{SM} = \frac{g^4 m_e}{16\pi m_W^4 E_\nu^2} (a^2 E_\nu^2 + b^2 (E_\nu - T)^2 - ab m_e T), \quad (3.4)$$

in such a way that a and b are listed in Table 3.1.

In type II seesaw, the relevant contribution of the singly-charged scalar H^+ is due to the interaction

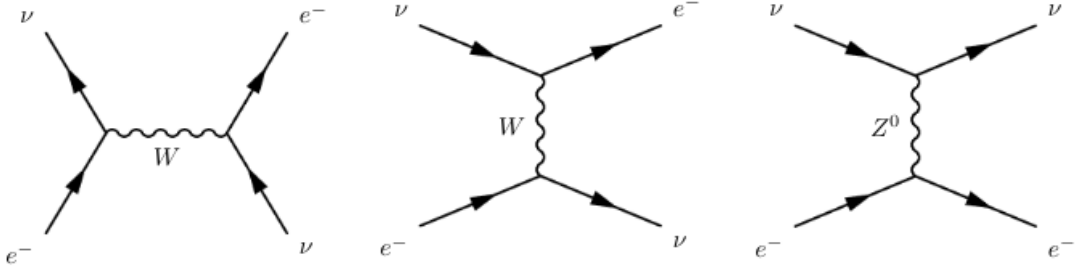


Figure 3.5: Feynman Diagrams responsible for the neutrino-electron scattering.

<i>Process</i>	<i>a</i>	<i>b</i>
$\nu_e - e^- \rightarrow \nu_e - e^-$	$s_w^2 + 1/2$	s_w^2
$\bar{\nu}_e - e^- \rightarrow \bar{\nu}_e - e^-$	s_w^2	$s_w^2 + 1/2$
$\nu_\alpha - e^- \rightarrow \nu_\alpha - e^-$	$s_w^2 - 1/2$	s_w^2
$\bar{\nu}_\alpha - e^- \rightarrow \bar{\nu}_\alpha - e^-$	s_w^2	$s_w^2 - 1/2$

Table 3.1: Here we have some values for the parameters a and b for each process that contributes for the $e - \nu$ scattering

$$V(H^+ l_i^- \nu_{lj}) = \frac{Y_{Lij}}{\sqrt{2}}. \quad (3.5)$$

Using the package **FeynCalc**, we calculate the cross section of the singly-charged diagram in Fig. 3.6. The total amplitude is the sum of SM, H^+ and mixing between these two terms,

$$|\mathcal{M}_{tot}|^2 = |\mathcal{M}_{SM}|^2 + |\mathcal{M}_{mix}|^2 + |\mathcal{M}_{H^+}|^2, \quad (3.6)$$

however we will focus only in the $|\mathcal{M}_{H^+}|^2$ amplitude. Then, it is possible to define the differential cross section contribution beyond SM (BSM)

$$\frac{d\sigma}{dT_{BSM}} = \frac{|\mathcal{M}_{H^+}|^2}{32\pi m_e |\mathbf{p}_1|^2}. \quad (3.7)$$

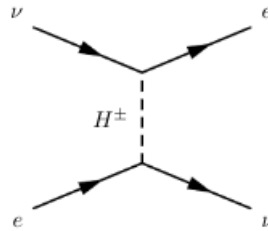


Figure 3.6: New Feynman diagram that predominantly contributes for the $e - \nu$ scattering.

After some calculations it is possible to find the following expression for the differential cross section of the diagram in Fig. 3.6

$$\begin{aligned} \frac{d\sigma}{dT}_{BSM} &= \frac{|\sum_i Y_{L1i}^2|^2 m_e}{64\pi E_\nu^2 (2E_\nu m_e + m_e^2 - m_{H^+}^2)^2} (2E_\nu^2 + m_e E_\nu - 2E_\nu T + 2m_e T - 3m_e^2) \\ &\approx \frac{|\sum_i Y_{L1i}^2|^2 m_e}{64\pi E_\nu^2 m_{H^+}^4} (2E_\nu^2 + m_e E_\nu - 2E_\nu T + 2m_e T - 3m_e^2). \end{aligned} \quad (3.8)$$

Comparing Eqs. 3.4 and 3.8 it is clear that the numerator part depending on the recoil energy of the electron and the neutrino beam energy are similar in each equation. Then, to know the contribution of new physics, we should define the r -parameter as

$$r = \frac{|\sum_i Y_{L1i}^2|^2}{g^4} \frac{m_W^4}{4m_{H^+}^4} \approx \frac{(d\sigma/dT)_{BSM}}{(d\sigma/dT)_{SM}}. \quad (3.9)$$

In the limit of Yukawa natural values, $Y_L/g \lesssim 1$,

$$r \approx \frac{m_W^4}{4m_{H^+}^4}. \quad (3.10)$$

The last result simply means that the new physics interference in $\nu - e$ scattering cross section it is proportional to the ratio between W boson mass (SM physics) and H^+ scalar mass (BSM physics). This is expected, because if H^+ is much more heavier than Z and W bosons, then it will not be possible to detect its interference (Fig. 3.7).

However, we can make the substitutions $Y_{L1j} = M_{\nu 1j}/v_\Delta$, $m_W = gv/2$ and $m_{H^+}^2 = \frac{\mu v^2}{\sqrt{2}v_\Delta}$, and see r parametric dependence. r can be written as

$$r \approx \frac{|\sum_i M_{\nu 1i}^2|^2}{32\mu^2 v_\Delta^2} = \frac{|\sum_i M_{\nu 1i}^2|^2}{32\epsilon v_\Delta^4}. \quad (3.11)$$

If v_Δ or the ϵ -parameter are high valued, r -parameter becomes insignificant. However, even for small $v_\Delta \sim 1$ eV and $\epsilon = 1$ it makes r -parameter tiny ($r \rightarrow 10^{-5}$). Then, we can conclude that the minimal extension of the SM that generates low scale type II seesaw with natural Y_L values is the model that contributes the most for the neutrino-electron scattering cross section. However, their contribution is still very small.

3.3 CP-odd scalar decay

The CP-odd triplet scalar is not phenomenological appealing. However, a relevant fact is that, if there is not explicitly lepton number violation in the scalar sector ($\mu \rightarrow 0$)

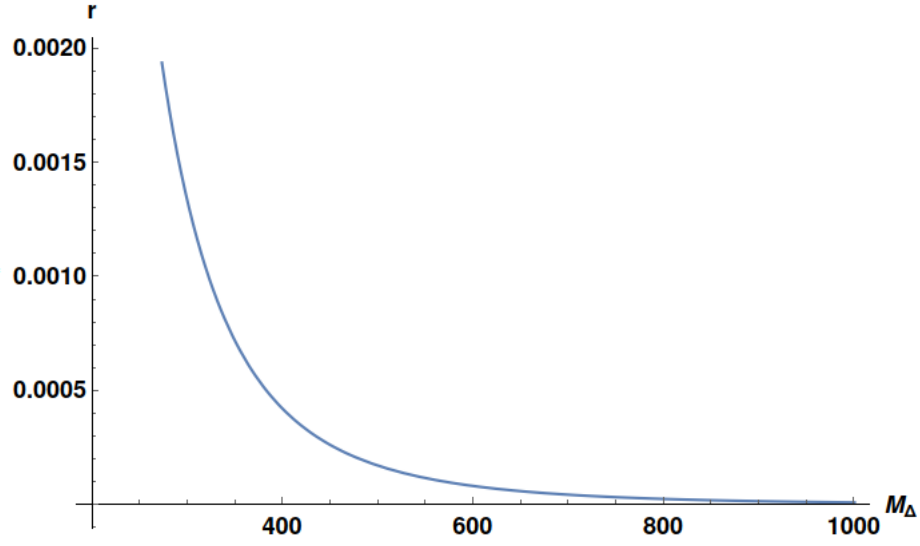


Figure 3.7: Here we can see that r becomes irrelevant for current experiments, if triplet scalar masses are high above TeV scales.

A 's mass is zero. Then, lepton number global symmetry implies a pseudoscalar A . The same happens in the model 123 of chapter 4. In that model, a Majoron J is massless (unless the potential explicitly broke lepton number). We'll go into more detail in the next chapter.

The main two-body decay of the CP-odd scalar is in a standard-like Higgs and a Z boson. This is possible only if $m_A > 216 GeV$. The vertex responsible for this decay is given by

$$V(AhZ) \approx \frac{gv_\Delta}{2c_w v} (P_A - P_h)_\mu. \quad (3.12)$$

Then, having in possession the vertex and with the help of **CalcHEP v 3.8.6** tool[68] we find the total decay of this scalar

$$\Gamma(A \rightarrow hZ) \approx \frac{g^2 v_\Delta^2}{16\pi c_w^2 v^2} \frac{((m_A - m_Z)^2 - m_h^2)^{3/2} ((m_A + m_Z)^2 - m_h^2)^{3/2}}{m_A^3 m_Z^2}. \quad (3.13)$$

As we have discussed, ρ -parameter suppress the ratio $v_\Delta/v \ll 1$. Then, this decay is very suppressed by this term and even more if $v_\Delta \sim eV$. In this energy range, the decays into neutrinos and anti-neutrinos are the most relevant for large Yukawa couplings and in the low mass region[66]. Notice that the decay $A \rightarrow Zh$ is higher for large values of v_Δ .

Then, a natural question appears. Is this A CP-odd scalar long lived? For $v_\Delta = 3 eV$ and $m_A = 390 GeV$ ($\epsilon \approx 3.5$), the total decay rate is approximated by $\Gamma_A \approx 5.5 \times 10^{-20} GeV$. Transforming in seconds, we have the decay time of A , that is $t_A \approx 10^{-5} s$ (Quark Epoch).

3.4 CP-even scalar decays and diphoton decay

The diphoton heavy Higgs decay channel provides an interesting opportunity to test some alternatives to the SM that could be realized at the Electroweak scale, and hence, be promptly probed at the current phase of LHC. An excess of diphoton signals can be directly associated with physics Beyond Standard Model. In some SEM extensions an excess of diphoton signals can be realized by addition of heavy fields and actual data can help us to limit some parameters of the triplet scalar extension, mainly the $H \rightarrow \gamma\gamma$ decay. As we will see in the end of this section, in the case of eV triplet vevs, the contribution of the heavy Higgs scalar to this type of decay is negligible. Firstly, let's investigate tree-level decays of the heavy CP-even scalar H . The most relevant vertices for the heavy Higgs two-body decay are

$$\begin{aligned}
V(Hhh) &\approx -\frac{\mu}{\sqrt{2}} + \frac{v_\Delta}{2}(-3\lambda + 5\lambda_1 + 5\lambda_4), \\
V(H\nu_{li}\nu_{lj}) &= \frac{Y_{Lij}}{\sqrt{2}}, \\
V(HZZ) &\approx 4v_\Delta \frac{g^2}{c_w^2} g_{\mu\nu}, \\
V(HW^+W^-) &\approx v_\Delta g^2 g_{\mu\nu}.
\end{aligned} \tag{3.14}$$

Then, having in possession the vertex and with the help of **CalcHEP v 3.8.6** tool[68] we find the main decay modes of this scalar

$$\begin{aligned}
\Gamma(H \rightarrow hh) &\approx \sqrt{1 - 4\frac{m_h^2}{m_H^2}} \frac{(2\mu + \sqrt{2}(3\lambda - 5(\lambda_1 + \lambda_4))v_\Delta)^2}{124\pi m_H}, \\
\Gamma(H \rightarrow \nu_i\nu_j) &= \frac{m_H Y_{Lij}^2}{16\pi(1 + \delta_{ij})}, \\
\Gamma(H \rightarrow ZZ) &\approx \frac{g^4 \sqrt{1 - 4m_Z^2/m_H^2} (m_H^4 - 4m_H^2 m_Z^2 + 12m_Z^4) v_\Delta^2}{16\pi m_H m_Z^4 c_w^4}, \\
\Gamma(H \rightarrow W^+W^-) &\approx \frac{g^4 \sqrt{1 - 4m_W^2/m_H^2} (m_H^4 - 4m_H^2 m_W^2 + 12m_W^4) v_\Delta^2}{64\pi m_H m_W^4}.
\end{aligned} \tag{3.15}$$

For small triplet vev, it is clear that two neutrinos decay is dominant in these processes, due natural values for the Yukawa couplings. If $v_\Delta > 1 \text{ MeV}$, its decay in two standard-like Higgs, two Z bosons and two W bosons are dominant. Now, we will find explicitly the heavy Higgs diphoton decay rate.

Following the papers [72, 73, 74], we can write an effective Lagrangian for the heavy Higgs-diphoton interaction by first specifying the relevant interactions of the heavy Higgs field H with scalars (ϕ_i) and gauge bosons (W, Z) in a general fashion as[75]

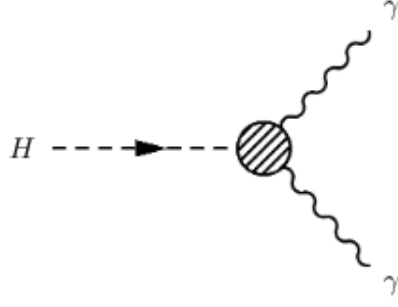


Figure 3.8: Total diphoton decay of the Heavy Higgs.

$$\mathcal{L}_{int} = -g_{\phi_i \phi_i H} \phi_i^* \phi_i H + g^2 v_\Delta W^\mu W_\mu H + g^2 W^\mu W_\mu H^2 - \lambda_i \phi_i^* \phi_i H^2, \quad (3.16)$$

where G_F is the Fermi constant, m_W is the W boson mass, and g , λ_i the Electroweak and scalars quartic couplings, respectively. The coupling parameter, $g_{\phi_i \phi_i H}$, it is proportional to the neutral scalars mix among themselves and they are generally proportional to v_3 (after SSB of Δ^0).

From the interaction Lagrangian, we can obtain the following effective Lagrangian for the $H - \gamma - \gamma$ coupling [75],

$$\mathcal{L}_{eff} = \sum_i \frac{\alpha Q_i^2 F_i}{8\pi} (\sqrt{2} G_F)^{1/2} H F^{\mu\nu} F_{\mu\nu}, \quad (3.17)$$

Q_i is the ratio of the electric charge of the corresponding field to the positron one, and the form factors F_i are given by,

$$\begin{aligned} F_W &= [2 + 3\tau_W + 3\tau_W(2 - \tau_W)I^2] \frac{v_\Delta g^2}{2v}, \\ F_{\phi_i} &= [\tau_{\phi_i}(1 - \tau_{\phi_i}I^2)] \frac{g_{\phi_i \phi_i H}^2}{m_{\phi_i}^2}, \end{aligned} \quad (3.18)$$

in such a way that $\tau_i \equiv 4m_i^2/m_H^2$ and I is given by

$$I \equiv \left\{ \begin{array}{ll} \arcsin\left(\sqrt{\frac{1}{\tau_i}}\right), & \text{for } \tau_i \geq 1, \\ \frac{1}{2}[\pi + i \ln\left[\frac{1 + \sqrt{1 - \tau_i}}{1 - \sqrt{1 - \tau_i}}\right]], & \text{for } \tau_i \leq 1 \end{array} \right\}. \quad (3.19)$$

Then, using the effective Lagrangian it is achievable to find the general expression for diphoton decay rate (as in [75])

$$\Gamma(H \rightarrow \gamma\gamma) = \frac{\alpha^2 m_H^3 G_F}{128\sqrt{2}\pi^3} \left| \sum_i Q_i^2 F_i \right|^2. \quad (3.20)$$

In the triplet with hypercharge extension of the SM, the new particles that contribute for diphoton decay are the singly- and doubly-charged scalars. Imposing the hierarchy between the vevs $v_\Delta \ll v$ and after some approximations, our first step is to find the couplings between the charged scalars and heavy Higgs

$$\begin{aligned} g_{H^+H^-H} &\approx 2((\lambda_2 + \lambda_3) - (\lambda_1 + \lambda_4))v_\Delta, \\ g_{\Delta^{++}\Delta^{--}H} &\approx 2(\lambda_2 - \lambda_1)v_\Delta \approx \frac{1}{2}g_{H^+H^-H}. \end{aligned} \quad (3.21)$$

Imposing mass degenerescence between H^\pm and $\Delta^{\pm\pm}$, we can find the approximate value of $\Sigma_i Q_i^2 F_i$ calculating the Form Factors. Here, $\tau_\Delta \approx 4$ and $I_\Delta \approx \pi/6$ and term $\tau_\Delta(1 - \tau_\Delta I^2) \approx -1/2$. Since $Q_{\Delta^{++}} = 2$ and $Q_{H^+} = 1$, the scalar form factors can be written as

$$4F_{\Delta^{++}} + F_{H^+} \approx 8F_{\Delta^{++}} \approx -4 \frac{g_{\Delta^{++}\Delta^{--}H}^2}{m_H^2} \approx -16 \frac{v_\Delta^2 (\lambda_2 - \lambda_1)^2}{m_H^2}. \quad (3.22)$$

Another contribution for this loop diagram is due to the W boson. To simplify our arguments, we must define the R_W parameter in such a way that

$$R_W = 2 + 3\tau_W + 3\tau_W(2 - \tau_W)I^2. \quad (3.23)$$

This parameter is interesting since can be divided in two parts, $M_\Delta < 321 \text{ GeV}$ and $M_\Delta > 321 \text{ GeV}$. These two situations are represented in Fig. 3.9. Analysing these plots it is plausible to state that $8.5 < R_W < 12.5$ for $200 \text{ GeV} < M_\Delta < 1000 \text{ GeV}$,

$$F_W = R_W \frac{g^2 v_\Delta}{2v} \rightarrow 8.5 \left(\frac{g^2 v_\Delta}{2v} \right) < F_W < 12.5 \left(\frac{g^2 v_\Delta}{2v} \right). \quad (3.24)$$

Analysing these form factors, we can see that the contribution of the charged scalars are negligible compared to the contribution of the W boson, since the first it is a second order perturbation (v_Δ^2/v^2) quantity and the second it is a first order perturbation quantity (v_Δ/v). Then, $\Sigma_i Q_i^2 F_i \approx F_W$ and the diphoton decay rate of the heavy Higgs is approximated by

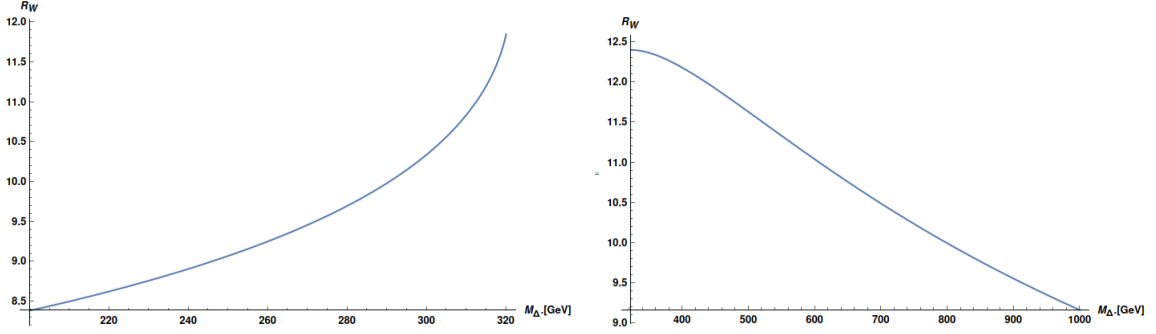


Figure 3.9: Here we divided in two regions to understand completely the behavior of the R_W parameter.

$$\Gamma(H \rightarrow \gamma\gamma) \approx R_W^2 \frac{\alpha^2 m_H^3 G_F^2 m_W^2 v_\Delta^2}{16\sqrt{2}\pi^3 v^2}. \quad (3.25)$$

Since we choose to study only small triplet vevs, we made numerical calculations for all these decays. After fixing $v_\Delta = 3 \text{ eV}$ and $m_H = 390 \text{ GeV}$, the decays of the heavy Higgs in the bosons are

$$\begin{aligned} \Gamma(H \rightarrow \text{All}) &\approx 1.04 \text{ MeV}, \\ \Gamma(H \rightarrow hh) &\approx 10^{-18} \text{ MeV}, \\ \Gamma(H \rightarrow \gamma\gamma) &\approx 10^{-23} \text{ MeV}, \\ \Gamma(H \rightarrow ZZ) &\approx 10^{-16} \text{ MeV}, \\ \Gamma(H \rightarrow W^+W^-) &\approx 10^{-17} \text{ MeV}. \end{aligned} \quad (3.26)$$

The only relevant decay channels are from Majorana neutrinos,

$$\begin{aligned} \Gamma(H \rightarrow \nu_\tau \nu_\tau) &\approx 3.355 \times 10^{-1} \text{ MeV}, \\ \Gamma(H \rightarrow \nu_\tau \nu_\mu) &\approx 3.079 \times 10^{-1} \text{ MeV}, \\ \Gamma(H \rightarrow \nu_\mu \nu_\mu) &\approx 2.300 \times 10^{-1} \text{ MeV}, \\ \Gamma(H \rightarrow \nu_\mu \nu_e) &\approx 1.120 \times 10^{-1} \text{ MeV}, \\ \Gamma(H \rightarrow \nu_\tau \nu_e) &\approx 3.755 \times 10^{-2} \text{ MeV}, \\ \Gamma(H \rightarrow \nu_e \nu_e) &\approx 1.711 \times 10^{-2} \text{ MeV}. \end{aligned} \quad (3.27)$$

3.5 Final Remarks

Here in this chapter our main goal was to explore the viable parametric space of the model HTM. Then, our choice in the last chapter in adopting $v_\Delta \sim 1 \text{ eV}$ have leaded

us to explore its consequences at diphoton decay, $e - \nu$ scattering and the decay of the doubly-charged scalar. The results that we have found were very plausible and many of them can be applied for the next model that we will present in the following chapter.

4 123 Model

4.1 Introduction

We have complained in previous chapters that the explicitly lepton number violation parameter (μ) is responsible for the type II seesaw relation $v_3 \sim \mu v_2^2/\mu_3^2$. This μ coupling at low energy scales can naturally be seen as an effective coupling, associated with a spontaneous lepton number breaking interaction. Therefore, a simple way to build such effective coupling is associate it to a singlet scalar field (σ) that interacts with the triplet (Δ) and doublet the (Φ) scalars[76, 77, 78, 79, 80]. From now on, we shall refer to this case as the 123 model.

In such new scenario, we perform the interaction $\kappa(\Phi^T \Delta \Phi \sigma^\dagger + H.c.)$, with σ carrying lepton number equal to the scalar triplet. Then, it is possible to preserve the global symmetry $B - L$ of the Lagrangian, for $\mu = \kappa \langle \sigma \rangle$. However, due to σ singlet field carrying a lepton number, it becomes viable a Yukawa interaction between this singlet scalar field and some neutral fermion that carries a lepton number, too.

Therefore, it is natural to add right-handed neutrinos in this 123 model. In this case, neutrino Lagrangian yields the most general neutrino mass matrix involving Majorana and Dirac mass terms for both neutrinos. Hence, when we assume that the lepton number is spontaneously violated at low-energy scales, right-handed neutrinos acquire light masses and may explain the recent MiniBooNE experimental results[81] by means of neutrino oscillation.

This discussion resulted in the paper published in the journal Physics Review D[82]. Here, we will derive the complete set of conditions that guarantee the potential of the 123 model to be bounded from below (BFB), as in chapter 1. However, for this model, we will probe every step using the method called "Spherical Parametrization". As in chapter 2, we will investigate the case were lepton number violation is at low energy scales. However, as we have commented above, in 123 model lepton number is spontaneously broken.

We will obtain the spectrum of scalars of the model and discuss the stability of the vacuum by evaluating the evolution of the self-coupling of the standard-like Higgs up to Planck scales. The discussion in section "Two problems that cannot be solved simultaneously" in chapter 2 will guide us and we will probe that this puzzle can be solved with 123 model.

Therefore, this model is particularly interesting because it encompasses a Majoron

(due explicitly lepton number conservation) and a light CP-even scalar in their spectrum of scalars. We will investigate phenomenological aspects of this model and discuss the contributions of these scalars for the invisible decay channels of the standard-like Higgs and of the neutral gauge boson Z . We will also obtain the constraints that lepton flavor violating puts over the parameters of the potential, as was explored in chapter 2. Regarding neutrino physics, we provide a solution, i.e., a set of values for the Yukawa couplings, that recovers the standard neutrino sector and provides at least one right-handed neutrino with mass resting on the eV scale and robustly mixed with the standard neutrinos in such a way that it accommodates MiniBooNE current results by means of neutrino oscillation and is in agreement with cosmological data.

This chapter is organized as follows. In chapter 4.2 we develop the main aspect of the model including neutrino masses, while in chapter 4.3 we develop the scalar sector. In chapter 4.4 we discuss the stability of the vacuum. In chapter 4.5 we present our final remarks.

4.2 The 1-2-3 model

The leptonic sector of the model is composed of the standard content plus right-handed neutrinos in the singlet form,

$$L_i = \begin{pmatrix} \nu_i \\ \ell_i \end{pmatrix}_L \sim (\mathbf{1}, \mathbf{2}, -1); \quad \ell_{i_R} \sim (\mathbf{1}, \mathbf{1}, -2); \quad \nu_{i_R} \sim (\mathbf{1}, \mathbf{1}, 0); \quad (4.1)$$

where $i = e, \mu, \tau$.

The scalar sector is composed of the standard Higgs doublet, Φ , one Higgs triplet, Δ , and one Higgs singlet, σ , presented below,

$$\Delta = \begin{pmatrix} \Delta^0 & \frac{\Delta^+}{\sqrt{2}} \\ \frac{\Delta^+}{\sqrt{2}} & \Delta^{++} \end{pmatrix} \sim (\mathbf{1}, \mathbf{3}, 2); \quad \Phi = \begin{pmatrix} \phi^0 \\ \phi^- \end{pmatrix} \sim (\mathbf{1}, \mathbf{2}, -1); \quad \sigma \sim (\mathbf{1}, \mathbf{1}, 0). \quad (4.2)$$

The quark sector is the standard one.

The most general potential involving this scalar content that conserves lepton number is composed of the following terms

$$\begin{aligned} V(\sigma, \Phi, \Delta) = & \mu_1^2 \sigma^* \sigma + \mu_2^2 \Phi^\dagger \Phi + \mu_3^2 \text{tr}(\Delta^\dagger \Delta) \\ & + \lambda_1 (\Phi^\dagger \Phi)^2 + \lambda_2 [\text{tr}(\Delta^\dagger \Delta)]^2 + \lambda_3 \Phi^\dagger \Phi \text{tr}(\Delta^\dagger \Delta) \\ & + \lambda_4 \text{tr}(\Delta^\dagger \Delta \Delta^\dagger \Delta) + \lambda_5 (\Phi^\dagger \Delta^\dagger \Delta \Phi) + \\ & \beta_1 (\sigma^* \sigma)^2 + \beta_2 \Phi^\dagger \Phi \sigma^* \sigma + \beta_3 \text{tr}(\Delta^\dagger \Delta) \sigma^* \sigma - \\ & \kappa (\Phi^T \Delta \Phi \sigma^* + H.c.). \end{aligned} \quad (4.3)$$

4.3 The Yukawa Sector

With such lepton and scalar content, the Yukawa interactions that generate mass for all neutrinos of the model is given by

$$\mathcal{L}_Y^\nu = \frac{1}{2} Y_{ij}^L L_i^T \Delta L_j + Y_{ij}^D \bar{L}_i \tilde{\phi} \nu_{Rj} + \frac{1}{2} Y_{ij}^R \bar{\nu}_{Ri}^C \nu_{Rj} \sigma + H.c.. \quad (4.4)$$

The Yukawa interactions of the charged fermions are the standard ones.

When the neutral scalars of the model develop vevs other than zero, i.e, $\langle \sigma \rangle = \frac{v_1}{\sqrt{2}}$, $\langle \phi \rangle = \frac{v_2}{\sqrt{2}}$ and $\langle \Delta \rangle = \frac{v_3}{\sqrt{2}}$, the Yukawa interactions in Eq. (4.4) provide the following mass terms for the neutrinos,

$$\mathcal{L}_{mass}^{D+M} = \frac{1}{2} \bar{\nu}_L^C M_L \nu_L + \bar{\nu}_L M_D \nu_R + \frac{1}{2} \bar{\nu}_R^C M_R \nu_R + H.c., \quad (4.5)$$

with $\nu_L = (\nu_{eL} \ \nu_{\mu L} \ \nu_{\tau L})^T$ and $\nu_R = (\nu_{eR} \ \nu_{\mu R} \ \nu_{\tau R})^T$.

Considering the basis $\nu = (\nu_L \ \nu_R^C)^T$, we can simplify Eq. (4.5) to

$$\mathcal{L}_{mass}^{D+M} = \frac{1}{2} \bar{\nu}^C M^{D+M} \nu + H.c., \quad (4.6)$$

and the 6×6 symmetric mass matrix is given by

$$M^{D+M} = \begin{pmatrix} M_L & M_D^T \\ M_D & M_R \end{pmatrix}, \quad (4.7)$$

where $M_L = Y^L \langle \Delta \rangle$, $M_D = Y^D \langle \phi \rangle$ and $M_R = Y^R \langle \sigma \rangle$. M^{D+M} is the most general neutrino mass matrix. It involves Dirac and Majorana mass terms for both left- and right-handed neutrinos. 123 is the simplest model that generates this mass matrix in the case of spontaneous violation of the lepton number.

The relation between the flavor basis, ν , and the physical ones, $N = (N_1 \ N_2 \ N_3 \ N_4 \ N_5 \ N_6)^T$, is given by $N = U \nu$ with U being the unitary matrix that diagonalizes M^{D+M} ,

$$U^T M^{D+M} U = M = \text{diag}(M_1 \ M_2), \quad (4.8)$$

where $M_1 = \text{diag}(m_1 \ m_2 \ m_3)^T$ and $M_2 = \text{diag}(m_4 \ m_5 \ m_6)^T$. We will develop the idea of light sterile neutrinos in next sections. First, we need to explore SSB of this model.

4.4 Spontaneous Symmetry Breaking

First, we expand the neutral scalar fields around their respective VEVs,

$$\begin{aligned}\sigma &= \frac{v_1}{\sqrt{2}} + \frac{R_1 + I_1}{\sqrt{2}} \\ \phi^0 &= \frac{v_2}{\sqrt{2}} + \frac{R_2 + I_2}{\sqrt{2}} \\ \Delta^0 &= \frac{v_3}{\sqrt{2}} + \frac{R_3 + I_3}{\sqrt{2}},\end{aligned}\tag{4.9}$$

and obtain the set of minimum conditions required by the potential above to allow spontaneous breaking of the symmetries of the model which include the global B-L symmetry,

$$\begin{aligned}v_1(\mu_1^2 + \beta_1 v_1^2 + \frac{1}{2}\beta_2 v_2^2 + \frac{1}{2}\beta_3 v_3^2) - \frac{1}{2}\kappa v_2^2 v_3 &= 0 \\ v_2(\mu_2^2 + \lambda_1 v_2^2 + \frac{1}{2}\lambda_3 v_3^2 + \frac{1}{2}\lambda_5 v_3^2 + \frac{1}{2}\beta_2 v_1^2 - \kappa v_1 v_3) &= 0 \\ v_3(\mu_3^2 + \lambda_2 v_3^2 + \frac{1}{2}\lambda_3 v_2^2 + \lambda_4 v_3^2 + \frac{1}{2}\lambda_5 v_2^2 + \frac{1}{2}\beta_3 v_1^2) - \frac{\kappa v_1 v_2^2}{2} &= 0.\end{aligned}\tag{4.10}$$

Upon analyzing this set of constraints, observe that the first and third relations yield

$$v_1 \approx \frac{\mu_3}{\mu_1} v_3.\tag{4.11}$$

The parameters μ_1 , μ_3 and v_1 are free to take any value while v_3 is constrained by the ρ -parameter, as discussed in chapter 1. Then, the direct proportionality among v_1 and v_3 provided by Eq. (4.11) hints that $v_1 < v_2$ which implies that right-handed neutrinos may be light particles, too. Assuming phenomenologically viable triplet scalars ($\mu_3 \sim TeV$) with $v_3 \sim eV$ as we have explored in chapter 2, it is clear that

$$v_1 \approx \frac{(MeV)^2}{\mu_1}.\tag{4.12}$$

Then, a natural scale for v_1 is when $\mu_1 \sim MeV$, and consequently $v_1 \sim MeV$. This is why we will assume $v_1 = 10^{-1} MeV$ as a standard value for this vev.

4.5 Scalar sector

We saw in the previous section that the scenario we are developing here is capable of accommodating neutrino physics including short-baseline (SBL) anomalies as LSND and MiniBooNE. This provides a strong reason for we go deep into the development of such case. Thus, in this section we perform a careful analysis of the spectrum of scalars of the model that is in consonance with previous section which means to consider the vevs

respecting the hierarchy $v_3 \ll v_1 \ll v_2$.

4.5.1 Spectrum of scalars

We start developing the CP-even sector. Considering the basis $(R_1 \ R_3 \ R_2)$, the potential above together with the minimum conditions provide,

$$M_R^2 = \begin{pmatrix} 2\beta_1 v_1^2 + \frac{1}{2}\kappa v_2^2 \frac{v_3}{v_1} & \beta_3 v_1 v_3 - \frac{1}{2}\kappa v_2^2 & \beta_2 v_1 v_2 - \kappa v_2 v_3 \\ \beta_3 v_1 v_3 - \frac{1}{2}\kappa v_2^2 & 2(\lambda_2 + \lambda_4)v_3^2 + \frac{1}{2}\kappa v_2^2 \frac{v_1}{v_3} & (\lambda_5 + \lambda_3)v_2 v_3 - \kappa v_1 v_2 \\ \beta_2 v_3 v_2 - \kappa v_2 v_1 & (\lambda_5 + \lambda_3)v_2 v_3 - \kappa v_1 v_2 & 2\lambda_1 v_2^2 \end{pmatrix}. \quad (4.13)$$

The complexity of this mass matrix prevent us to achieve a closed analytic form of the eigenvalues/eigenvectors. In this case the better we can do is a simplification based on our assumptions regarding the parameter space. In this way, according to the hierarchy of the VEVs we assumed here, this matrix may be approximated by

$$M_R^2 \approx \begin{pmatrix} \frac{1}{2}\kappa v_2^2 \frac{v_3}{v_1} & -\frac{1}{2}\kappa v_2^2 & \sim 0 \\ -\frac{1}{2}\kappa v_2^2 & \frac{1}{2}\kappa v_2^2 \frac{v_1}{v_3} & \sim 0 \\ \sim 0 & \sim 0 & 2\lambda_1 v_2^2 \end{pmatrix}. \quad (4.14)$$

This means that R_2 decouple from the other ones, while R_1 and R_3 mix among themselves to form H_1 and H_3 according to the following relation

$$\begin{pmatrix} H_1 \\ H_3 \end{pmatrix} = U_R \begin{pmatrix} R_1 \\ R_3 \end{pmatrix}; \quad R_2 = H_2, \quad (4.15)$$

where

$$U_R \approx \begin{pmatrix} 1 & \epsilon \\ -\epsilon & 1 \end{pmatrix}; \quad \epsilon \approx \frac{v_3}{v_1}. \quad (4.16)$$

The masses are given by,

$$m_{H_1}^2 \approx \frac{2\beta_2^2 v_1^2}{\kappa}, \quad m_{H_3}^2 \approx \frac{\kappa v_1 v_2^2}{2v_3}, \quad m_{H_2}^2 \approx 2\lambda_1 v_2^2. \quad (4.17)$$

Observe that, for the hierarchy of the VEVs assumed here, we have that H_2 will play the role of the standard Higgs while H_3 is a heavy Higgs, with mass around TeV scale, and H_1 is a light one with mass at eV scale.

In the CP-odd sector, things are much simple and the mass matrix in the basis

(I_1, I_2, I_3) is given by

$$M_I^2 = \begin{pmatrix} \frac{1}{2}\kappa v_2^2 \frac{v_3}{v_1} & \kappa v_2 v_3 & \frac{1}{2}\kappa v_2^2 \\ \kappa v_2 v_3 & 2\kappa v_1 v_3 & \kappa v_1 v_2 \\ \frac{1}{2}\kappa v_2^2 & \kappa v_1 v_2 & \frac{1}{2}\kappa v_2^2 \frac{v_1}{v_3} \end{pmatrix}. \quad (4.18)$$

Its diagonalization leads to a Goldstone boson, G , that is dominantly I_2 and will be eaten by the standard gauge boson Z ; a massless pseudo-scalar, J , which we call the Majoron and a heavy pseudo-scalar, A , which is dominantly I_3 . The relation among these pseudo-scalars with the basis is given by

$$\begin{pmatrix} J \\ G \\ A \end{pmatrix} = U_I \begin{pmatrix} I_1 \\ I_2 \\ I_3 \end{pmatrix}, \quad (4.19)$$

where U_I is given by

$$U_I \approx \begin{pmatrix} 1 & -2\frac{v_3^2}{v_1 v_2} & -\epsilon \\ 0 & 1 & -2\frac{v_3}{v_2} \\ \epsilon & 2\frac{v_3}{v_2} & 1 \end{pmatrix}. \quad (4.20)$$

For the case of interest here, the Majoron is related to the basis in the following way,

$$J \approx I_1 - 2\frac{v_3^2}{v_2 v_1} I_2 - \epsilon I_3, \quad (4.21)$$

which allow we conclude that it is dominantly singlet. In this case its coupling to the standard neutrinos may be approximated by $\sim i g_{\alpha\beta} \bar{\nu}_\alpha \gamma_5 \nu_\beta J$ where $g_{\alpha\beta} = Y_{L_{\alpha\beta}} \epsilon$. For $\epsilon = 10^{-5}$ and for the values of $Y_{L_{\alpha\beta}}$ given in Eq. (4.41) we have $g_{e\mu} \sim 10^{-8}$. This value for $g_{e\mu}$ is in agreement with supernova bounds, $\beta\beta 0\nu$ decay and neutrino decays as discussed in [83]. Another source of constraint on Majoron arises from star cooling which, for our hierarchy of vevs, put the following constraint over them (see Eq. (36) of the first paper in Ref. [77])

$$\frac{2v_3^2}{v_1 v_2} \leq 10^{-6}, \quad (4.22)$$

which is completely obeyed by our choice in Eq. (4.39). In what concern long-range force, the Majoron is so weakly coupled to matter that it may have well escaped detection [84, 85].

The mass of the pseudo-scalar A take the following expression,

$$m_A^2 \approx \frac{\kappa v_1 v_2^2}{2v_3}, \quad (4.23)$$

which allow we conclude that it is a heavy particle even for the set of VEVs considered here.

In what concern the charged scalars, in considering the basis (Δ^+, ϕ^+) , we have the following mass matrix for these scalars

$$M_{H^\pm}^2 = \begin{pmatrix} \kappa v_1 v_3 - \frac{1}{2} \lambda_5 v_3^2 & \frac{1}{2\sqrt{2}} v_2 (\lambda_5 v_3 - 2\kappa v_1) \\ \frac{1}{2\sqrt{2}} v_2 (\lambda_5 v_3 - 2\kappa v_1) & \frac{1}{4v_3} v_2^2 (2\kappa v_1 - \lambda_5 v_3) \end{pmatrix}. \quad (4.24)$$

We can easily diagonalize this matrix and find the physical fields

$$\begin{pmatrix} G^\pm \\ H^\pm \end{pmatrix} = U_\pm \begin{pmatrix} \phi^\pm \\ \Delta^\pm \end{pmatrix}, \quad (4.25)$$

$$U_\pm \approx \begin{pmatrix} 1 & \frac{\sqrt{2}v_3}{v_2} \\ -\frac{\sqrt{2}v_3}{v_2} & 1 \end{pmatrix}. \quad (4.26)$$

We see that there are not any relevant mixing between the charged fields. G^\pm is the Goldstone while H^\pm is the simply charged scalar whose mass expression is given by

$$m_{H^\pm}^2 = \frac{1}{4v_3} (2\kappa v_1 - \lambda_5 v_3) (v_2^2 + 2v_3^2) \approx \frac{\kappa v_1 v_2^2}{2v_3}. \quad (4.27)$$

Observe that it must be heavy for the choice of the VEVs used here.

The doubly-charged scalar acquires the following mass expression

$$m_{\Delta^\pm}^2 = \frac{1}{2v_3} (\kappa v_1 v_2^2 - 2\lambda_4 v_3^2 - \lambda_5 v_2^2 v_3) \approx \frac{\kappa v_1 v_2^2}{2v_3}, \quad (4.28)$$

which must be heavy, too.

Thus, we see have that, although the VEVs v_1 and v_3 are much smaller than v_2 , we have that the scalars that belong to the triplet Δ are heavier than the standard-like Higgs and their masses are practically determined by the parameter κ . This is a consequence of the hierarchy of the VEVs. It is curious that the same hierarchy among the VEVs does the opposite with regard to the scalars belonging to the singlet σ . The scenario predicts a light scalar H_1 . The heavy scalars may be probed at the LHC, while the massless J and light H_1 will contribute to the invisible decay channels of the Higgs and Z .

4.5.2 Some constraints

The coupling constants κ , β_2 , $\lambda_{3,5}$ will play an important role in the RGE-evolution of the quartic coupling of the standard-like Higgs λ_1 . Thus, information on these parameters in the form of constraints is mandatory in order to we conclude if the vacuum of the 1-2-3 model in the regime of low energy scale is stable or not. But before we address this issue, let us investigate the contributions of the light scalars to the invisible decay of the standard neutral gauge boson Z .

In what concern the invisible decay of Z , the Lagrangian of interest is given by

$$\mathcal{L}_{R_3 I_3 Z} \supset -\frac{g}{c_w} Z^\mu [R_3 \partial_\mu I_3 - I_3 \partial_\mu R_3]. \quad (4.29)$$

Because R_3 mix with R_1 to compose H_1 and I_3 mix with I_1 to compose J , we have that this Lagrangian generates an interaction among Z , H_1 and J modulated by the following vertex

$$V_{ZH_1(P_1)J(P_2)} \approx \frac{g\epsilon^2}{c_w} (P_1 - P_2)_\mu, \quad (4.30)$$

where g is the $SU(2)$ coupling constant and $c_w = \cos(\theta_w)$ with θ_w being the Weinberg angle. ϵ is given in Eq. (4.16). The current data gives $\Gamma(Z)_{inv} = 500.1 \pm 1.9$ MeV [46]. Because $M_{H_1} \ll M_Z$, the vertex above provides the following expression for the decay width $Z \rightarrow H_1 J$,

$$\Gamma(Z \rightarrow JH_1) = \frac{M_Z \epsilon^4 G_F}{16\sqrt{2}\pi} (M_Z - \frac{M_{H_1}^2}{M_Z})^2 \approx \frac{M_Z^3 \epsilon^4 G_F}{16\sqrt{2}\pi}. \quad (4.31)$$

The expression for the decay width of Z in two neutrinos is given by

$$\Gamma(Z \rightarrow \bar{\nu}\nu) = \frac{G_F M_Z^3}{12\sqrt{2}\pi}. \quad (4.32)$$

On substituting the current values of the standard parameters that enter in the expression above, i.e., $M_Z = 91.18$ GeV, $G_F = 1.1663787 \times 10^{-5}$ GeV⁻² we obtain $\Gamma(Z \rightarrow \bar{\nu}\nu) \approx 166$ MeV. In view of this, the window for new physics is established by $\Gamma(Z)_{inv} - 3 \times \Gamma(Z \rightarrow \bar{\nu}\nu) \approx 2.1$ MeV. In other words, all new contributions to the invisible decay of Z must lie within 2.1 MeV.

Observe that Eqs. (4.31) and (4.32) provide

$$\frac{\Gamma_{Z \rightarrow JH_1}}{\Gamma_{Z \rightarrow \bar{\nu}\nu}} \approx 0.75\epsilon^4 \rightarrow \Gamma_{Z \rightarrow JH_1} \approx 124.5\epsilon^4 \text{ MeV}. \quad (4.33)$$

According to this we have that $\Gamma_{Z \rightarrow JH_1}$ must be smaller than 2.1 MeV. Once $\frac{v_3}{v_1} = \epsilon$, at

the end of the day we get

$$\epsilon < 0.36 \rightarrow v_1 > 2.77v_3. \quad (4.34)$$

This result confirms the hierarchy among the VEVs we are considering here.

In order to check that our scenario obeys the constraint put by the invisible decay of Z as discussed above, see that for $v_1 = 10^5$ eV and $v_3 = 1$ eV, we get $\Gamma(Z \rightarrow JH_1) = 124.5 \times 10^{-20}$ MeV which is much smaller than 2.1 MeV. The other possible contribution to $\Gamma(Z)_{inv}$ is $\Gamma(Z \rightarrow JJJ)$. However we must have that $\Gamma(Z \rightarrow JH_1) > \Gamma(Z \rightarrow JJJ)$ because the later decay is obtained from the first by means of the decay $H_1 \rightarrow JJ$. Thus, we conclude here that the invisible Z decay is not a threat to our model.

Now let us extract constraints over the parameters of the potential by means of the invisible Higgs decay channels and the LFV process $\mu \rightarrow e\gamma$.

Let us consider the contributions that our case give to the invisible decay of the standard-like Higgs H_2 . We consider the following contributions $\Gamma(H_2 \rightarrow H_1H_1)$ and $\Gamma(H_2 \rightarrow JJ)$. Their decay widths take the expression[78]

$$\Gamma(H_2 \rightarrow H_1H_1) \approx \frac{\beta_2^2 v_2}{128\sqrt{2}\pi} \quad \text{and} \quad \Gamma(H_2 \rightarrow JJ) \approx \frac{(\lambda_3 + \lambda_5)^2 v_2}{128\sqrt{2}\pi}. \quad (4.35)$$

The prediction for the total decay width of the standard Higgs is around 4 MeV with $\sim 20\%$ being invisible decay rates($BR(H_2 \rightarrow inv) = 0,26 \pm 0,17$). All this allows we conclude that β_2 , λ_3 and λ_5 are constrained to lie around 10^{-2} or smaller.

Thus we conclude here that the 1-2-3 model in the regime of low energy scale, although has a Majoron, which is a massless pseudo-scalar, and a light CP-even scalar it is a safe model in what concern the invisible decay of the standard neutral gauge boson Z . As a nice fact we have that our particular case gives reasonable contribution to the invisible decay of the standard Higgs through the channels $\Gamma(H_2 \rightarrow H_1H_1)$ and $\Gamma(H_2 \rightarrow JJ)$. In other words, our case may be constrained by future improvement of the data concerning Higgs physics.

In what concern LFV processes, the muon decay channel $\mu \rightarrow e\gamma$ provides the strongest constraint on the parameters of the potential. This is so because in our case $BR(\mu \rightarrow 3e) \sim \frac{BR(\mu \rightarrow e\gamma)}{160}$, see Eq. (70) of Ref. [86].

In one-loop order we have the following expression for the branching ratio of this process[87]

$$BR(\mu \rightarrow \gamma e) \approx \frac{27\alpha \left| (Y_L)_{11}(Y_L)_{12} + (Y_L)_{13}(Y_L)_{32} + (Y_L)_{12}(Y_L)_{22} \right|^2}{64\pi G_F^2 M_{\Delta^{++}}^4}, \quad (4.36)$$

where α is the fine structure constant and $G_F = 1.1663787 \times 10^{-5} \text{ GeV}^{-2}$.

On substituting the expression of the mass of the doubly charged scalar given in Eq. (4.28), we have that for the fixed values of Y_L 's given in Eq. (4.41) and of the VEVs given in Eq. (4.39), the upper bound $BR(\mu \rightarrow \gamma e) < 5.7 \times 10^{-13}$ [53] translates in the following lower bound over κ

$$\frac{7 \times 10^{-19}}{\kappa^2} < 5.7 \times 10^{-13} \rightarrow \kappa > 1.1 \times 10^{-3}. \quad (4.37)$$

In addition to this lower bound over κ , there is a natural upper bound over κ , too, that arise from the constraint that all dimensionless parameters in any scalar potential are required to be less than $\sqrt{4\pi}$ in order to fulfill the perturbativity condition. In summary, have

$$1.1 \times 10^{-3} < \kappa < \sqrt{4\pi}. \quad (4.38)$$

With this set of constraints in hand, we are ready to analysis the RGE-evolution of the quartic coupling of the standard-like Higgs λ_1 .

4.6 Light Sterile Neutrinos

A strong reason for the existence of light right-handed neutrinos is the explanation of short-baseline neutrino results (LSND and MiniBooNE)[81][88] by means of neutrino oscillation. In this case, the adequate value for v_1 is one that accommodates at least one right-handed neutrino with mass around eV with robust mixing with the standard neutrinos and that is in conciliation with cosmology. We follow this line of reasoning here.

The current scenario of neutrino physics involving MiniBooNE and LSND experimental results may be accommodated within our model with the following set of values for the VEVs,

$$v_1 = 10^{-1} \text{ MeV}; \quad v_2 = 246 \text{ GeV}; \quad v_3 = 1 \text{ eV}, \quad (4.39)$$

and the following set of values for the Yukawa couplings,

$$Y_D = \begin{pmatrix} 3,6 \times 10^{-13} & 5,74 \times 10^{-13} & 5,74 \times 10^{-14} \\ -2,21 \times 10^{-13} & -3,45 \times 10^{-10} & 5,75 \times 10^{-13} \\ -7,07 \times 10^{-13} & 5,75 \times 10^{-12} & 5,75 \times 10^{-13} \end{pmatrix}; \quad (4.40)$$

$$Y_L = \begin{pmatrix} 6,20 \times 10^{-3} & -4,11 \times 10^{-3} & -1,25 \times 10^{-2} \\ -4,11 \times 10^{-3} & 3,90 \times 10^{-1} & 1,95 \times 10^{-2} \\ -1,25 \times 10^{-2} & 1,95 \times 10^{-2} & 3,83 \times 10^{-2} \end{pmatrix}; \quad (4.41)$$

$$Y_R = \begin{pmatrix} 1,40 \times 10^{-5} & 4,75 \times 10^{-12} & 4,52 \times 10^{-12} \\ 4,75 \times 10^{-12} & 10^{-1} & 5,08 \times 10^{-15} \\ 4,52 \times 10^{-12} & 5,08 \times 10^{-15} & 10^{-1} \end{pmatrix}. \quad (4.42)$$

On substituting all of these values into M^{D+M} , given in Eq. (4.7), we have that

its diagonalization provides

$$\begin{aligned} m_1 &= 2 \times 10^{-4} \text{ eV}; \quad m_2 = 8,6 \times 10^{-3} \text{ eV}; \quad m_3 = 5 \times 10^{-2} \text{ eV}; \\ m_4 &= 1,4 \text{ eV}; \quad m_5 = 10^4 \text{ eV}; \quad m_6 = 10^4 \text{ eV}. \end{aligned} \quad (4.43)$$

The mixing matrix, U , responsible for the diagonalization of M^{D+M} and relating the basis ν to N , as in Eq. (4.8), is given by

$$U = \begin{pmatrix} 0,83 & 0,54 & -0,12 & 0,045 & 10^{-5} & 10^{-6} \\ -0,25 & 0,59 & 0,72 & -0,03 & -6 \times 10^{-3} & 10^{-5} \\ 0,44 & -0,6 & 0,69 & -0,09 & 10^{-4} & 10^{-5} \\ -0,045 & 0,03 & 0,09 & 1 & \sim 0 & \sim 0 \\ 10^{-6} & 10^{-4} & 10^{-4} & \sim 0 & 1 & \sim 0 \\ 10^{-6} & 10^{-5} & 10^{-4} & \sim 0 & \sim 0 & 1 \end{pmatrix}. \quad (4.44)$$

The values of m_1 , m_2 and m_3 given in Eq. (4.43) and the upper left 3×3 submatrix of U accommodate the current solar and atmospheric neutrino oscillation data. A nice thing to observe is that the mixing angles among N_4 with ν_μ and N_4 with ν_e , together with the mass value of m_4 , are in such a way that they allow the explanation of neutrino anomalies suggested by the data from short-baseline (SBL) neutrino experiments by means of neutrino oscillation. Finally, observe in U that N_5 and N_6 practically decouple from the other neutrinos. In other words, this case recovers the 3+1 sterile neutrino scenario.

A problem with models involving an eV sterile neutrino is that they create tension with current cosmological data[89, 90, 91]. We will discuss this point at the end of this chapter.

4.7 Vacuum Stability

Now that we have developed the scalar sector by finding the spectrum of scalars for a particular set of values of the VEVs and obtained some constraints over the parameters of the potential due to Higgs invisible decay and lepton flavor violation, it is the moment to investigate the stability of the vacuum by finding the bound from below conditions and calculating the running of the self coupling of the Higgs.

4.7.1 Bounded from below conditions

In order to assure that the scalar potential of the 1-2-3 model is bounded from below at large field strength, where the potential is generically dominated by the Quartic terms, we need to find the set of conditions that guarantee that the parameters of the Quartic Couplings of the potential are positive when the fields go to infinity. We find the whole set of conditions and paved the way for similar models. In this subsection, we

will derive the BFB conditions, which can be applied in the section (1.7). We follow the techniques employed in [92, 93, 94].

Firstly, we separate the quartic couplings of the potential,

$$V^4 = \lambda_1(\Phi^\dagger\Phi)^2 + \lambda_2[tr(\Delta^\dagger\Delta)]^2 + \lambda_3\Phi^\dagger\Phi tr(\Delta^\dagger\Delta) + \lambda_4 tr(\Delta^\dagger\Delta\Delta^\dagger\Delta) + \lambda_5(\Phi^\dagger\Delta^\dagger\Delta\Phi) \\ + \beta_1(\sigma^*\sigma)^2 + \beta_2\Phi^\dagger\Phi\sigma^*\sigma + \beta_3 tr(\Delta^\dagger\Delta)\sigma^*\sigma - \kappa(\Phi^T\Delta\Phi\sigma^\dagger + H.c.) \quad (4.45)$$

and then build the following parametrization:

$$\begin{aligned} r^2 &= \Phi^\dagger\Phi + tr(\Delta^\dagger\Delta) + \sigma^*\sigma, \\ \Phi^\dagger\Phi &= r^2 \cos^2\gamma \sin^2\theta, \\ tr(\Delta^\dagger\Delta) &= r^2 \sin^2\gamma \sin^2\theta, \\ \sigma^*\sigma &= r^2 \cos^2\theta, \end{aligned} \quad (4.46)$$

where $0 \leq r \leq \infty$, $0 \leq \gamma \leq \frac{\pi}{2}$ and $0 \leq \theta \leq \frac{\pi}{2}$.

We also need to develop the following parameters,

$$\begin{aligned} \zeta &= \frac{tr(\Delta^\dagger\Delta\Delta^\dagger\Delta)}{[tr(\Delta^\dagger\Delta)]^2}, \\ \xi &= \frac{\Phi^\dagger\Delta\Delta^\dagger\Phi}{\Phi^\dagger\Phi tr(\Delta^\dagger\Delta)}, \\ \alpha &= \frac{Re(\Phi^T\Delta\Phi\sigma)}{tr(\Delta^\dagger\Delta)\sigma^*\sigma + \Phi^\dagger\Phi\sigma^*\sigma + tr(\Delta^\dagger\Delta)\Phi^\dagger\Phi}, \end{aligned} \quad (4.47)$$

where $\frac{1}{2} \leq \zeta \leq 1$, $0 \leq \xi \leq 1$ and $-1 \leq \alpha \leq 1$. Two of them are already knew in the literature. The third one is a new parameter. We can see in detail in Appendix A how we can limit this parameter.

Let also define new variables x and y that must vary between 0 and 1 in the following way:

$$\begin{aligned} y &= \sin^2\theta, \\ x &= \sin^2\gamma. \end{aligned} \quad (4.48)$$

Replacing Eq. (4.48) in Eq. (4.45) we get,

$$\begin{aligned} \frac{V^4}{r^4} &= y^2[\lambda_1(1-x)^2 + \lambda_2x^2 + \lambda_3(1-x)x + \zeta\lambda_4x^2 + \xi\lambda_5(1-x)x - 2\kappa\alpha x(1-x)] \\ &+ (1-y)^2\beta_1 + (1-y)y[\beta_2(1-x) + \beta_3x - 2\kappa\alpha]. \end{aligned} \quad (4.49)$$

We manage things such that we can express these quartic terms in the following

way,

$$\begin{aligned}
\frac{V^4}{r^4} &= A_x y^2 + B_x (1-y)^2 + C_x (1-y)y \quad \text{where,} \\
A_x &= \lambda_1 (1-x)^2 + (\lambda_2 + \zeta \lambda_4) x^2 + (\lambda_3 + \xi \lambda_5 - 2\kappa \alpha) (1-x)x, \\
B_x &= \beta_1, \\
C_x &= \beta_2 (1-x) + \beta_3 x - 2\kappa \alpha.
\end{aligned} \tag{4.50}$$

We can fix $y = 0$ or $y = 1$ to obtain the cases when the quartic couplings of the potential is positive. When we do this, we obtain the following conditions

$$A_x > 0, \tag{4.51}$$

$$B_x > 0, \tag{4.52}$$

$$C_x + 2\sqrt{A_x B_x} > 0. \tag{4.53}$$

For $A_x > 0$ we need to use the same argument as before. Fixing $x = 0$ and $x = 1$ we have similar conditions for the inequalities

$$\begin{aligned}
\lambda_1 &> 0, \\
\lambda_2 + \zeta \lambda_4 &> 0, \\
\lambda_3 + \xi \lambda_5 - 2\kappa \alpha + 2\sqrt{\lambda_1 (\lambda_2 + \zeta \lambda_4)} &> 0.
\end{aligned} \tag{4.54}$$

These new conditions depends of the parameters in Eq. (4.50). They vary in different ranges, but we only need to study the boundary values of these intervals. In this case the new conditions are:

$$\begin{aligned}
\lambda_1 &> 0, \\
\lambda_2 + \lambda_4 &> 0, \\
\lambda_2 + \frac{1}{2}\lambda_4 &> 0, \\
\lambda_3 + 2\kappa + 2\sqrt{\lambda_1(\lambda_2 + \frac{1}{2}\lambda_4)} &> 0, \\
\lambda_3 + 2\kappa + 2\sqrt{\lambda_1(\lambda_2 + \lambda_4)} &> 0, \\
\lambda_3 + \lambda_5 + 2\kappa + 2\sqrt{\lambda_1(\lambda_2 + \frac{1}{2}\lambda_4)} &> 0, \\
\lambda_3 + \lambda_5 + 2\kappa + 2\sqrt{\lambda_1(\lambda_2 + \lambda_4)} &> 0, \\
\lambda_3 - 2\kappa + 2\sqrt{\lambda_1(\lambda_2 + \frac{1}{2}\lambda_4)} &> 0, \\
\lambda_3 - 2\kappa + 2\sqrt{\lambda_1(\lambda_2 + \lambda_4)} &> 0, \\
\lambda_3 + \lambda_5 - 2\kappa + 2\sqrt{\lambda_1(\lambda_2 + \frac{1}{2}\lambda_4)} &> 0, \\
\lambda_3 + \lambda_5 - 2\kappa + 2\sqrt{\lambda_1(\lambda_2 + \lambda_4)} &> 0.
\end{aligned} \tag{4.55}$$

Using the same argument for the condition in Eq. (4.52), it turns easy to see that

$$\beta_1 > 0. \tag{4.56}$$

Using the condition in Eq. (4.53) and the same fact that C_x can have $x = 0$ or $x = 1$, we obtain

$$\begin{aligned}
\beta_2 - 2\kappa\alpha + 2\sqrt{\beta_1\lambda_1} &> 0, \\
\beta_3 - 2\kappa\alpha + 2\sqrt{\beta_1(\lambda_2 + \zeta\lambda_4)} &> 0.
\end{aligned} \tag{4.57}$$

The first inequality has two different solutions while the second has four ones. At the end of the day, we have

$$\begin{aligned}
\beta_2 + 2\kappa + 2\sqrt{\beta_1\lambda_1} &> 0, \\
\beta_2 - 2\kappa + 2\sqrt{\beta_1\lambda_1} &> 0, \\
\beta_3 + 2\kappa + 2\sqrt{\beta_1(\lambda_2 + \frac{1}{2}\lambda_4)} &> 0, \\
\beta_3 + 2\kappa + 2\sqrt{\beta_1(\lambda_2 + \lambda_4)} &> 0, \\
\beta_3 - 2\kappa + 2\sqrt{\beta_1(\lambda_2 + \frac{1}{2}\lambda_4)} &> 0, \\
\beta_3 - 2\kappa + 2\sqrt{\beta_1(\lambda_2 + \lambda_4)} &> 0.
\end{aligned} \tag{4.58}$$

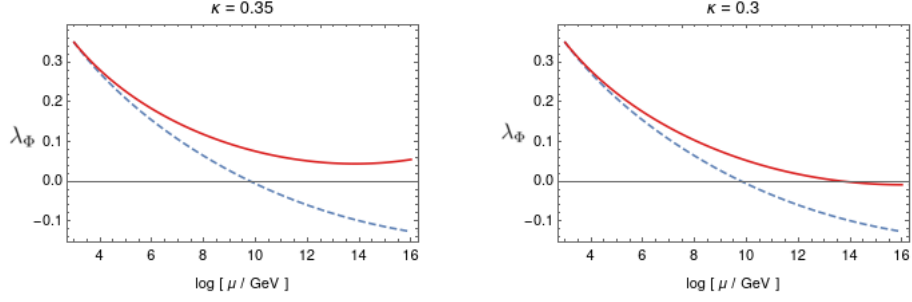


Figure 4.1: Running of $\lambda_\Phi \approx \lambda_1$ at one-loop level as a function of the energy scale μ for $\lambda_5 = \lambda_3 = \beta_2 = 0.001$ with $y_t = 0.9965$, $g_Y = 0.4627$ and $g = 0.6535$. The dotted line represents the expectation of Standard Model and the red line represents the expectation for our model for two values of κ .

So, those are the set of condition that guarantee the potential in Eq. (4.3) is bounded from below. In what follow we obtain the running of the self coupling related of the standard-like Higgs.

4.7.2 RGE-evolution of the self coupling of the standard-like Higgs

The standard model predicts that the self coupling of the Higgs becomes negative at an energy scale around $\Lambda = 10^{11}\text{GeV}$. This means that the standard model can not assure the stability of the vacuum up to the Planck scale. This must be remedied by means of new physics in the form of new particles with appropriate interactions. This issue has been extensively investigated in the literature[50, 95, 96, 97, 98, 99]. As we already mentioned in chapter 2, the minimum type 2 seesaw can solve this problem, but a natural problem appears in such a way that the two cannot be solved simultaneously. Within 123 model we show that the right behavior of the self coupling of the Higgs that guarantees absolute stability for the Electroweak Vacuum depends strongly on the coupling κ , not only of the quartic couplings between Φ and Δ (in this case, λ_3 and λ_5). We do our analysis by implementing the model in SARAH 4.13.0 [63] and evaluating the β function for $\lambda_1 \approx \lambda_{SM}$ at one-loop level.

The main contributions for the beta function of λ_1 involve the following terms

$$\begin{aligned} \beta_{\lambda_1} = & \frac{27}{100}g_Y^4 + \frac{9}{4}g^4 + \frac{9}{20}g_Y^2(g^2 - 2\lambda_1) - \frac{9}{5}g^2\lambda_1 + 12\lambda_1^2 + 12\lambda_1 y_t^\dagger y_t - 6y_t^\dagger y_t y_t^\dagger y_t + \\ & + \beta_2^2 + 3\lambda_3^2 + 3\lambda_3\lambda_5 + \frac{5}{4}\lambda_5^2 + 2\kappa^2, \end{aligned} \quad (4.59)$$

where g and g_Y are the gauge couplings of the standard gauge group $SU(2)$ and $U(1)_Y$ while y_t is the Yukawa coupling of the quark top.

Observe that the couplings β_2 , $\lambda_{3,5}$ and κ give positive contributions to the running of λ_1 . However, as showed above, the invisible Higgs decay requires β_2 , $\lambda_{3,5}$ minor than 10^{-2} which turns insignificant their contributions to the RGE-evolution. Rest us the contribution of the parameter κ . In Fig. 4.1 we show the plot of the running of λ_1 with

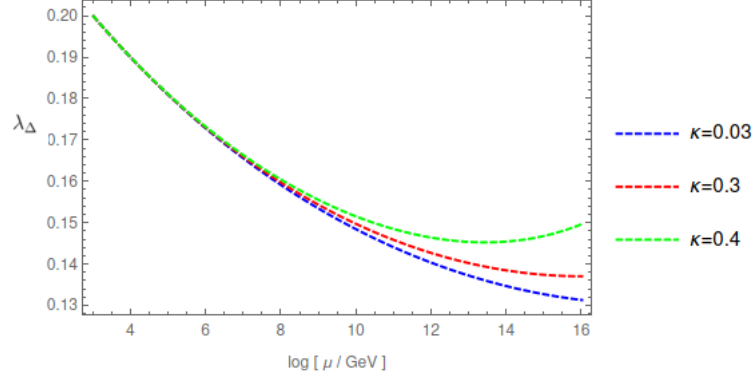


Figure 4.2: Running of $\lambda_\Delta \approx \lambda_2 + \lambda_4$ at one-loop level as a function of the energy scale μ for $\lambda_5 = \lambda_3 = \beta_2 = 0.001$ with $y_t = 0.9965$, $g_Y = 0.4627$ and $g = 0.6535$. The dotted lines represents the expectation for our model for three values of κ . The coupling β_3 is important in the same level as κ for this running.

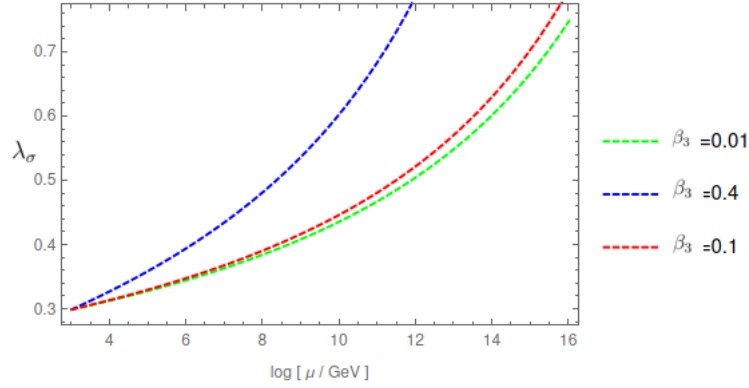


Figure 4.3: Running of $\lambda_\sigma \approx \beta_1$ at one-loop level as a function of the energy scale μ for $\lambda_5 = \lambda_3 = \beta_2 = 0.001$ with $y_t = 0.9965$, $g_Y = 0.4627$ and $g = 0.6535$. The dotted lines represents the expectation for our model for three values of β_3 .

energy scale for two possible values of κ . We see that the running of λ_1 may get positive up to Planck scale for $\kappa > 0.3$. Thus, the model may have the vacuum stable thanks to the contribution of the parameter κ .

For sake of completeness, in Figs. 4.2 and 4.3 we present the running at one-loop level of the other self-quartic couplings $\lambda_{2,4}$ and β_1 . As we can see in those plots, they do not develop negative values and are weakly influenced by κ .

4.8 Discussion

In this work we studied stability of the vacuum in the 123 model with right-handed neutrinos. We restricted our investigation to a specific case where lepton number is spontaneously broken at low energy scale. The scenario is well motivated since it yields light sterile neutrinos and may explain MiniBooNE by means of neutrino oscillation. In such a scenario, we obtained the whole set of conditions that guarantee the model is bounded from below and studied the RGE-evolution of the self-coupling of the standard-

like Higgs. As main result we have that the quartic coupling $\kappa\Phi^T\Delta\Phi\sigma^\dagger$ plays a central role in the process and stability of the vacuum requires $\kappa > 0.3$.

As interesting consequence, we remark that the model has one Majoron (J) and one light Higgs (H_1) composing the spectrum of scalar of the model. Their contributions to the invisible decay rate of the standard-like Higgs, $H_2 \rightarrow JJ$ and $H_2 \rightarrow H_1H_1$, were considered and the results are the bounds $\beta_2, \lambda_3, \lambda_5 \leq 10^{-2}$ over the couplings of the potential.

In what concern the neutrino sector, the scenario recovers the 3+1 sterile neutrino model which explain MiniBooNE experiment by means of neutrino oscillation. However, we know that light sterile neutrinos are strongly disfavored by current cosmological data involving Big Bang Nucleosynthesis(BBN) , Cosmic Microwave Background(CMB) anisotropies and Large Scale Structure(LSS)[89]. This is so because, in face of the large mixing required by MiniBooNE, neutrino oscillation may conduct sterile neutrino to thermal equilibrium with the active neutrino even before neutrinos decouple from the primordial plasma. A possible solution for this tension requires the suppression of the production of these neutrinos in the early universe. This avoids that they thermalize with the active ones at high temperature. This may be achieved by means of secret interactions[100, 101, 102, 103] which is nothing more than the interaction of the sterile neutrino with a pseudo-scalar, I ,

$$\sim g_s \bar{\nu}_S^C \gamma_5 \nu_S I. \quad (4.60)$$

The solution to the tension requires I be lighter than the lightest sterile neutrino and g_s take values in the range $10^{-6} - 10^{-5}$. Observe that our scenario recover this solution. For this, recognize that g is Y_{11}^R whose value in the matrix in Eq. (4.42) is $1,4 \times 10^{-5}$ and I is the Majoron J . In order to generate a small mass to J we just need to consider a term like: $M\sigma\sigma\sigma$ in the potential. This term will generate a mass term to J proportional to M . On assuming that $M < m_{N_4}$ we have a secret sector that reconciliates eV sterile neutrino with cosmology as done in [104, 105].

Conclusions and Perspectives

In this document, we have addressed the problem of neutrino masses in a well motivated Standard Model extension, HTM, virtually certain to be revealed by experiments on the 1 TeV scale. In chapter 1, we have a quick look in the main aspects of HTM, such as its potential, main interactions with gauge bosons and fermions, explicitly and spontaneously broken of lepton number and its scalar mass spectrum.

In chapter 2, we have focused on a specific realization of HTM, in which lepton number is violated at low energy scales, investigating its link between spontaneous and explicitly lepton number breaking energy scales. Using LFV processes, we have constrained the ratio ϵ with the triplet scalar mass. Another interesting aspect of such model was its similarities with the Inverse Seesaw Mechanism, that is naturally manifested at TeV scales. However, the main part of this chapter is addressed to the problem of stability of the Higgs at high energies. We have showed that HTM can become the Higgs vacuum stable, however such choice of parameters makes the one-loop Higgs mass higher than its tree-level one, which is not a natural choice. We have proposed a solution to this problem in a similar framework in chapter 4.

Nonetheless, chapter 3 was devoted to explore some phenomenological consequences of a low scale type II seesaw. We have explored the main decays of the doubly-charged scalar, varying with the triplet vev. We have observed that for low and high triplet vevs it decays predominantly in charged leptons and W gauge bosons, respectively. Another phenomenological aspect explored in this thesis were effects of the singly-charged scalar in the process $\nu - e$ scattering. Besides, the diphoton decay rate is another relevant process that we have studied, thus specifically for the heavy Higgs H . Nonetheless, we have observed that such decay is very suppressed for low triplet vev.

In the last chapter, we have extended the simple HTM by a scalar singlet σ that can become the Higgs stable at high energies and at the same time have a small mass correction for the one-loop Higgs mass. Such proposal not only solves the Higgs stability problem, but also explains LSND and MiniBooNE results in a cosmological viable framework. Such model, known as 123 Model, have a rich scalar structure. When studying the bounded from below conditions of the potential, we have developed a parameter α and explained in which values this parameter is permitted to take. In the near future we plan to extend this model, promoting the global symmetry $B - L$ in a local one. Thus, connecting neutrino physics and dark matter, exploring signatures at neutrino detectors, and tease out the correlation

between neutrino mass ordering and lepton flavor violation.

Appendices

A Proof that α is limited between $[-1,1]$ interval

Here we will give a hint for the proof of the limitation of the parameter α . The definition of this parameter is

$$\alpha = \frac{Re[\Phi^T \Delta \Phi \sigma]}{\Phi^\dagger \Phi \sigma^\dagger \sigma + tr[\Delta^\dagger \Delta] \Phi^\dagger \Phi + tr[\Delta^\dagger \Delta] \sigma^\dagger \sigma}. \quad (A.1)$$

We can expand this parameter in terms of the components of the fields. We have that

$$\begin{aligned} \text{Numerator} &= Re[\phi^0 \Delta^0 \phi^0 \sigma + \sqrt{2} \phi^0 \Delta^+ \phi^- \sigma + \phi^- \Delta^{++} \phi^- \sigma], \\ \text{Denominator} &= (\phi^{0\dagger} \phi^0 + \phi^+ \phi^- + \sigma^\dagger \sigma) (\Delta^{0\dagger} \Delta^0 + \Delta^+ \Delta^- + \Delta^{++} \Delta^{--}) \\ &\quad + \sigma^\dagger \sigma (\phi^{0\dagger} \phi^0 + \phi^+ \phi^-). \end{aligned} \quad (A.2)$$

Then, we can study term by term to see what is the behavior of this parameter, e.g., to see if it is limited or not. As an example, we choose the first term of the Numerator and expand the fields in the real and imaginary parts. Using the following expansion

$$\begin{aligned} \phi^0 &= R_2 + iI_2, \\ \Delta^0 &= R_3 + iI_3, \\ \sigma &= R_1 + iI_1, \end{aligned} \quad (A.3)$$

we will obtain the Denominator terms (only the real part)

$$R_2^2 R_3 R_1 - R_2 R_3 I_2 I_1 - I_2 I_3 R_2 R_1 + I_1 I_2^2 I_3 - I_2^2 R_1 R_3 - I_1 I_2 R_2 R_3 - R_1 R_2 R_2 I_3 - R_2^2 I_1 I_3.$$

The idea here is to look closely in each real function and study their limitation range. For the first term, $R_2^2 R_3 R_1$, we have the following relation (for $R_2 \neq 0$)

$$\frac{R_2^2 R_3 R_1}{R_2^2 R_3^2 + R_1^2 R_2^2 + R_1^2 R_3^2 + (\dots)} \rightarrow \frac{R_3 R_1}{R_3^2 + R_1^2 + \frac{R_1^2 R_3^2}{R_2^2} + (\dots)} < \frac{R_3 R_1}{R_3^2 + R_1^2}. \quad (\text{A.4})$$

We can see easily that this last term is limited in the range $[-1,1]$ with polar coordinates. We use similar arguments for next terms and find that α lies in the range $[-1,1]$.

B (1PI) and Amputated diagrams - Renormalization conditions

(1PI) diagrams are one-particle irreducible diagrams. This means that (1PI) are any diagrams that cannot be split in two by removing a single line. In Fig. (B.1) we present two simple examples, the first as a (1PI) diagram and while the other is not.

However one can argue why this type of diagram is important in our previous analysis about renormalization conditions. We will present here only a short explanation that can be seen in more details in [27]. We will formulate this formalism in ϕ^4 -theory, since it is the most easy interaction QFT. As is well known, the propagator pole is related to the particle's mass. In a non-interaction picture, this propagator has the form, in momentum-space,

$$\frac{i}{p^2 - m_0^2},$$

in such a way that this mass m_0 is the same mass represented in the ϕ^4 -theory Lagrangian

$$\frac{1}{2}m_0^2\phi^2,$$

that we will call this mass as the bare mass of the scalar field ϕ .

However, in the interaction picture, we need to be more careful. Since we are in a quantum theory, we should account all possible diagrams. To do this, for the propagator, we will use (1PI) diagrams. The sum of all possible (1PI) is represented in Fig. B.2. This sum is necessary to define the new propagator pole. Let us define the sum of all possible (1PI) diagrams as

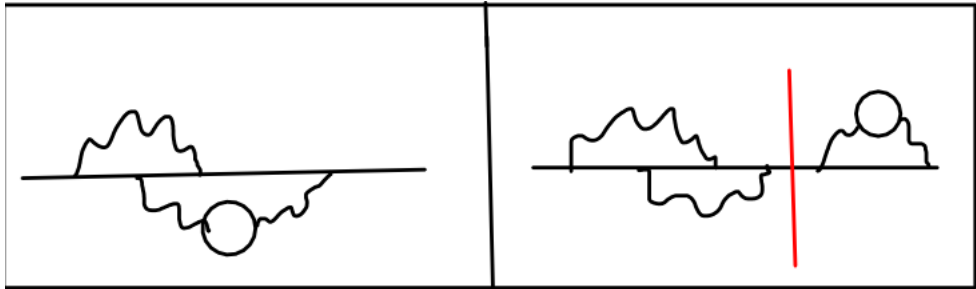


Figure B.1: The left diagram is (1PI), while the right diagram is not, because we can trace a (red)line that can divide this diagram in two.

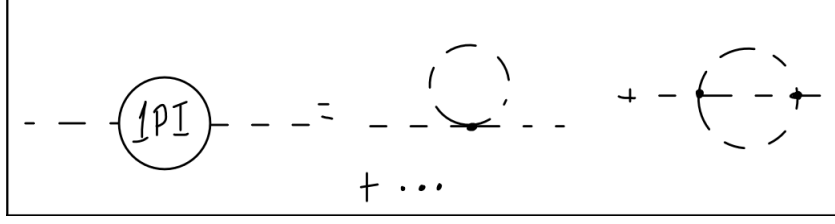


Figure B.2: The sum of $1PI$ diagrams for the simple scalar theory.

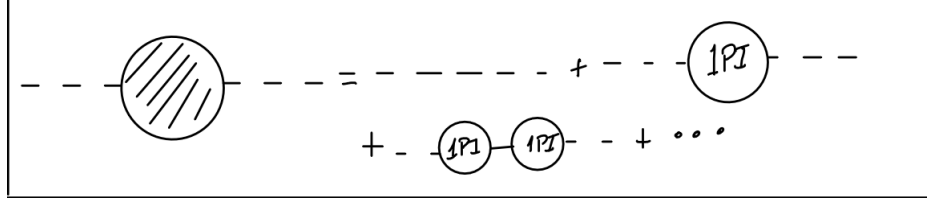


Figure B.3: Now, the total contribution is simply all combinations of $1PI$. Then, we must use the geometric series well know result, for the case in which higher orders of perturbation theory contributes less than lower orders.

$$\sum_{all\ 1PI\ diagrams} (1PI) = -i\Sigma^2(p^2). \quad (B.1)$$

Then, it is possible to write an expression for all loop contributions for ϕ 's propagator as a geometric series of $(1PI)$ diagrams, as in Fig. B.3. If this series is convergent (in other words, if this theory is perturbative), we can write all these contributions in the form

$$\frac{i}{p^2 - m_0^2} + \frac{i}{p^2 - m_0^2} (-i\Sigma^2) \frac{i}{p^2 - m_0^2} + \dots = \frac{i}{p^2 - m_0^2 - \Sigma^2(p^2)}. \quad (B.2)$$

As we have discussed, this propagator in the interaction picture needs to have its pole about the physical mass pole. Then, we came to the relation

$$\frac{i}{p^2 - m_0^2 - \Sigma^2(p^2)} \approx \frac{iZ}{p^2 - m^2}, \quad (B.3)$$

in such a way that m is the physical mass of the field ϕ and Z is the field-strength renormalization scale (as we have commented, this Z factor is the shift of the field ϕ to the renormalized field ϕ_r). Now it is possible to see the role of $(1PI)$ diagrams. The left-hand equation has a pole in the ϕ 's physical mass

$$[p^2 - m_0^2 - \Sigma^2(p^2)]|_{p^2=m^2} = 0. \quad (B.4)$$

Close to the pole, the denominator of Eq. B.2 has the form after Taylor expansion

in first order ($p^2 \rightarrow m^2$) and using Eq. B.4 to cancel the first term of the expansion

$$(p^2 - m^2) \left(1 - \frac{d\Sigma^2(p^2)}{dp^2} \Big|_{p^2=m^2} \right) + \mathcal{O}((p^2 - m^2)^2). \quad (\text{B.5})$$

Another important role of (1PI) diagrams are the determination of the field-strength renormalization scale using Eqs. B.3 and B.5

$$Z^{-1} = 1 - \frac{d\Sigma^2(p^2)}{dp^2} \Big|_{p^2=m^2}. \quad (\text{B.6})$$

Now, it is possible to redefine the field ϕ , to be a renormalized field, using two-point correlation function, with the shift of the Eq. 2.13. With this shift, the numerator of the right-hand Eq. B.3 becomes 1. Then, the Eq. B.6 can be written, after renormalization shifts of Eq. 2.16

$$\frac{d\Sigma^2(p^2)}{dp^2} \Big|_{p^2=m^2} = 0. \quad (\text{B.7})$$

There is another shift, related to m_0 . Defining the mass counterterm as (Eq. 2.16)

$$\delta_m = m_0^2 Z - m^2,$$

the tree-level propagator of the theory is simply

$$\frac{i}{p^2 - m^2}. \quad (\text{B.8})$$

With the same procedure as before, expanding all contributions of (1PI) diagrams leads to

$$[p^2 - m^2 - \Sigma^2(p^2)] \Big|_{p^2=m^2} = 0, \quad (\text{B.9})$$

or

$$[\Sigma^2(p^2)] \Big|_{p^2=m^2} = 0. \quad (\text{B.10})$$

This relation is expected, since we are only working with physical quantities and the infinities are in the counterterms (hidden in $\Sigma^2(p^2)$ term). There is no more dependence of the nonphysical quantities Z and m_0 . Eqs. B.10 and B.7 are the renormalization

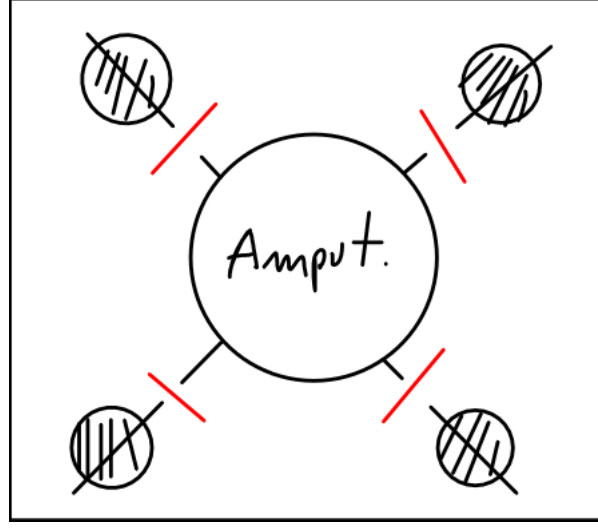


Figure B.4: The definition of an amputated 4-point diagram. We cut-off the legs of this diagram, representing this with the red lines. Then, an amputated diagram is the irreducible four-point correction.

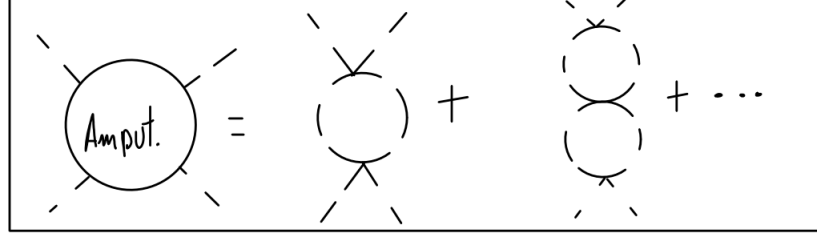


Figure B.5: Here we define an amputated diagram for the simple ϕ^4 -theory.

conditions of the propagator. In a theory where $m = 0$, these conditions cannot be used because they lead to singularities in the counterterms. To avoid such singularities, we choose an arbitrary momentum scale M and impose the renormalization conditions at a spacelike momentum p with $p^2 = -M^2$.

A last comment is about the renormalization condition related to the amputated four-point correlation function. What is the meaning of “amputated” diagram? It is a generalization of (1PI) diagrams to more external legs. Amputated diagrams are n external legs Feynman diagrams that cannot be split by two by removing a single line. Fig. B.4 represent this idea with four external legs.

When we talk about Amputated four-point Feynman diagrams, we refer to the sum of all possible diagrams that are Amputated, as in Fig. B.5. Then, it is natural to define the renormalization conditions of the quartic coupling λ of the ϕ^4 -theory in such a way that the contribution of all Amputated four-point Feynman diagrams corresponds to the physical coupling λ , as in Eq. 2.18.

Bibliography

- [1] Abdus Salam and John Clive Ward. Weak and electromagnetic interactions. Nuovo Cim., 11:568–577, 1959.
- [2] Abdus Salam and John Clive Ward. Gauge theory of elementary interactions. Phys. Rev., 136:B763–B768, 1964.
- [3] Abdus Salam and John Clive Ward. Electromagnetic and weak interactions. Phys. Lett., 13:168–171, 1964.
- [4] Abdus Salam. Weak and Electromagnetic Interactions. Conf. Proc. C, 680519:367–377, 1968.
- [5] Steven Weinberg. A Model of Leptons. Phys. Rev. Lett., 19:1264–1266, 1967.
- [6] Abdus Salam. Renormalizability of gauge theories. Phys. Rev., 127:331–334, 1962.
- [7] H. Umezawa and S. Kamefuchi. Equivalence theorems and renormalization problem in vector field theory (The Yang-Mills field with non-vanishing masses). Nucl. Phys., 23:399–429, 1961.
- [8] A. Komar and Abdus Salam. Renormalization problem for vector meson theories. Nucl. Phys., 21:624–630, 1960.
- [9] David J. Gross and Frank Wilczek. Ultraviolet Behavior of Nonabelian Gauge Theories. Phys. Rev. Lett., 30:1343–1346, 1973.
- [10] Sidney R. Coleman and Erick J. Weinberg. Radiative Corrections as the Origin of Spontaneous Symmetry Breaking. Phys. Rev. D, 7:1888–1910, 1973.
- [11] Gerard 't Hooft and M. J. G. Veltman. Regularization and Renormalization of Gauge Fields. Nucl. Phys. B, 44:189–213, 1972.
- [12] Alex Keshavarzi, Kim Siang Khaw, and Tamaki Yoshioka. Muon $g - 2$: current status. 6 2021.
- [13] João Paulo Pinheiro, C. A. de S. Pires, Farinaldo S. Queiroz, and Yoxara S. Vilamizar. Confronting the inverse seesaw mechanism with the recent muon $g-2$ result. 7 2021.

- [14] M. H. Ahn et al. Measurement of Neutrino Oscillation by the K2K Experiment. Phys. Rev. D, 74:072003, 2006.
- [15] Y. Fukuda et al. Evidence for oscillation of atmospheric neutrinos. Phys. Rev. Lett., 81:1562–1567, 1998.
- [16] S. Fukuda et al. Solar B-8 and hep neutrino measurements from 1258 days of Super-Kamiokande data. Phys. Rev. Lett., 86:5651–5655, 2001.
- [17] Y. Ashie et al. A Measurement of atmospheric neutrino oscillation parameters by SUPER-KAMIOKANDE I. Phys. Rev. D, 71:112005, 2005.
- [18] M. H. Ahn et al. Indications of neutrino oscillation in a 250 km long baseline experiment. Phys. Rev. Lett., 90:041801, 2003.
- [19] K. M. Case. Reformulation of the Majorana Theory of the Neutrino. Phys. Rev., 107:307–316, 1957.
- [20] Carlo Giunti and Chung W. Kim. Fundamentals of Neutrino Physics and Astrophysics. 2007.
- [21] R. N. Mohapatra and P. B. Pal. Massive neutrinos in physics and astrophysics., volume 60. 1998.
- [22] M. Magg and C. Wetterich. Neutrino Mass Problem and Gauge Hierarchy. Phys. Lett. B, 94:61–64, 1980.
- [23] S. L. Glashow. Partial Symmetries of Weak Interactions. Nucl. Phys., 22:579–588, 1961.
- [24] G. C. Branco and G. Senjanovic. The Question of Neutrino Mass. Phys. Rev. D, 18:1621, 1978.
- [25] Rabindra N. Mohapatra and Goran Senjanovic. Neutrino Mass and Spontaneous Parity Nonconservation. Phys. Rev. Lett., 44:912, 1980.
- [26] Steven Weinberg. Baryon and Lepton Nonconserving Processes. Phys. Rev. Lett., 43:1566–1570, 1979.
- [27] Michael E. Peskin and Daniel V. Schroeder. An Introduction to quantum field theory. Addison-Wesley, Reading, USA, 1995.
- [28] Ernest Ma. Pathways to naturally small neutrino masses. Phys. Rev. Lett., 81:1171–1174, 1998.

- [29] Peter Minkowski. $\mu \rightarrow e\gamma$ at a Rate of One Out of 10^9 Muon Decays? Phys. Lett. B, 67:421–428, 1977.
- [30] J. Schechter and J. W. F. Valle. Neutrino Masses in $SU(2) \times U(1)$ Theories. Phys. Rev. D, 22:2227, 1980.
- [31] Robert E. Shrock. General Theory of Weak Leptonic and Semileptonic Decays. 1. Leptonic Pseudoscalar Meson Decays, with Associated Tests For, and Bounds on, Neutrino Masses and Lepton Mixing. Phys. Rev. D, 24:1232, 1981.
- [32] R. Primulando, J. Julio, and P. Uttayarat. Scalar phenomenology in type-II seesaw model. JHEP, 08:024, 2019.
- [33] A. Arhrib, R. Benbrik, M. Chabab, G. Moulhaka, M. C. Peyranere, L. Rahili, and J. Ramadan. The Higgs Potential in the Type II Seesaw Model. Phys. Rev. D, 84:095005, 2011.
- [34] P. S. Bhupal Dev, Clara Miralles Vila, and Werner Rodejohann. Naturalness in testable type II seesaw scenarios. Nucl. Phys. B, 921:436–453, 2017.
- [35] Alejandra Melfo, Miha Nemevsek, Fabrizio Nesti, Goran Senjanovic, and Yue Zhang. Type II Seesaw at LHC: The Roadmap. Phys. Rev. D, 85:055018, 2012.
- [36] Pei-Hong Gu, He Zhang, and Shun Zhou. A Minimal Type II Seesaw Model. Phys. Rev. D, 74:076002, 2006.
- [37] Robert Foot, H. Lew, X. G. He, and Girish C. Joshi. Seesaw Neutrino Masses Induced by a Triplet of Leptons. Z. Phys. C, 44:441, 1989.
- [38] M. C. Gonzalez-Garcia, Michele Maltoni, and Thomas Schwetz. Updated fit to three neutrino mixing: status of leptonic CP violation. JHEP, 11:052, 2014.
- [39] Yi Cai, Tao Han, Tong Li, and Richard Ruiz. Lepton Number Violation: Seesaw Models and Their Collider Tests. Front. in Phys., 6:40, 2018.
- [40] Rodolfo A. Diaz and R. Martinez. The Custodial symmetry. Rev. Mex. Fis., 47:489–492, 2001.
- [41] Alessio Maiezza, Miha Nemevsek, Fabrizio Nesti, and Goran Senjanovic. Left-Right Symmetry at LHC. Phys. Rev. D, 82:055022, 2010.
- [42] Gerard 't Hooft. Naturalness, chiral symmetry, and spontaneous chiral symmetry breaking. NATO Sci. Ser. B, 59:135–157, 1980.
- [43] Michael Plumacher. Baryogenesis and lepton number violation. Z. Phys. C, 74:549–559, 1997.

- [44] R. N. Mohapatra and Mina K. Parida. Type II Seesaw Dominance in Non-supersymmetric and Split Susy SO(10) and Proton Life Time. Phys. Rev. D, 84:095021, 2011.
- [45] M. J. G. Veltman. Limit on Mass Differences in the Weinberg Model. Nucl. Phys. B, 123:89–99, 1977.
- [46] M. Tanabashi et al. Review of Particle Physics. Phys. Rev. D, 98(3):030001, 2018.
- [47] Stefan Antusch, Oliver Fischer, A. Hammad, and Christiane Scherb. Low scale type II seesaw: Present constraints and prospects for displaced vertex searches. JHEP, 02:157, 2019.
- [48] Alessio Maiezza, Miha Nemevšek, and Fabrizio Nesti. Lepton Number Violation in Higgs Decay at LHC. Phys. Rev. Lett., 115:081802, 2015.
- [49] Miha Nemevšek, Fabrizio Nesti, and Juan Carlos Vasquez. Majorana Higgses at colliders. JHEP, 04:114, 2017.
- [50] Ilia Gogoladze, Nobuchika Okada, and Qaisar Shafi. Higgs boson mass bounds in a type II seesaw model with triplet scalars. Phys. Rev. D, 78:085005, 2008.
- [51] Raghavendra Srikanth Hundi. Some implications of lepton flavor violating processes in a supersymmetric Type II seesaw model at TeV scale. Eur. Phys. J. C, 73(4):2396, 2013.
- [52] J. Beringer et al. Review of Particle Physics (RPP). Phys. Rev. D, 86:010001, 2012.
- [53] J. Adam et al. New constraint on the existence of the $\mu^+ \rightarrow e^+ \gamma$ decay. Phys. Rev. Lett., 110:201801, 2013.
- [54] Wilhelm H. Bertl et al. Search for the Decay $\mu^+ \rightarrow e^+ e^+ e^-$. Nucl. Phys. B, 260:1–31, 1985.
- [55] A. G. Akeroyd, Mayumi Aoki, and Hiroaki Sugiyama. Lepton Flavour Violating Decays $\tau \rightarrow \text{anti-}l \, l$ and $\mu \rightarrow e \, \gamma$ in the Higgs Triplet Model. Phys. Rev. D, 79:113010, 2009.
- [56] A. G. Dias, C. A. de S. Pires, P. S. Rodrigues da Silva, and A. Sampieri. A Simple Realization of the Inverse Seesaw Mechanism. Phys. Rev. D, 86:035007, 2012.
- [57] Sidney R. Coleman. The Fate of the False Vacuum. 1. Semiclassical Theory. Phys. Rev. D, 15:2929–2936, 1977. [Erratum: Phys.Rev.D 16, 1248 (1977)].
- [58] Marc Sher. Electroweak Higgs Potentials and Vacuum Stability. Phys. Rept., 179:273–418, 1989.

- [59] Tommi Markkanen, Arttu Rajantie, and Stephen Stopyra. Cosmological aspects of higgs vacuum metastability. Frontiers in Astronomy and Space Sciences, 5:40, 2018.
- [60] I. Yu. Kobzarev, L. B. Okun, and M. B. Voloshin. Bubbles in Metastable Vacuum. Yad. Fiz., 20:1229–1234, 1974.
- [61] Ruth Gregory and Ian G. Moss. The Fate of the Higgs Vacuum. PoS, ICHEP2016:344, 2016.
- [62] Sidney R. Coleman and Erick J. Weinberg. Radiative Corrections as the Origin of Spontaneous Symmetry Breaking. Phys. Rev. D, 7:1888–1910, 1973.
- [63] Florian Staub. SARAH 4 : A tool for (not only SUSY) model builders. Comput. Phys. Commun., 185:1773–1790, 2014.
- [64] Gino Isidori, Giovanni Ridolfi, and Alessandro Strumia. On the metastability of the standard model vacuum. Nucl. Phys. B, 609:387–409, 2001.
- [65] A. Abada, C. Biggio, F. Bonnet, M. B. Gavela, and T. Hambye. Low energy effects of neutrino masses. JHEP, 12:061, 2007.
- [66] Pavel Fileviez Perez, Tao Han, Gui-yu Huang, Tong Li, and Kai Wang. Neutrino Masses and the CERN LHC: Testing Type II Seesaw. Phys. Rev. D, 78:015018, 2008.
- [67] Pankaj Agrawal, Manimala Mitra, Saurabh Niyogi, Sujay Shil, and Michael Spannowsky. Probing the Type-II Seesaw Mechanism through the Production of Higgs Bosons at a Lepton Collider. Phys. Rev. D, 98(1):015024, 2018.
- [68] Alexander Belyaev, Neil D. Christensen, and Alexander Pukhov. CalcHEP 3.4 for collider physics within and beyond the Standard Model. Comput. Phys. Commun., 184:1729–1769, 2013.
- [69] Manfred Lindner, Farinaldo S. Queiroz, Werner Rodejohann, and Xun-Jie Xu. Neutrino-electron scattering: general constraints on Z' and dark photon models. JHEP, 05:098, 2018.
- [70] Andre de Gouvea and James Jenkins. What can we learn from neutrino electron scattering? Phys. Rev. D, 74:033004, 2006.
- [71] Selçuk Bilmiş. Probing physics beyond the standard model through neutrino-electron scatterings. PhD thesis, Middle East Technical University, 2016.
- [72] John R. Ellis, Mary K. Gaillard, and Dimitri V. Nanopoulos. A Phenomenological Profile of the Higgs Boson. Nucl. Phys. B, 106:292, 1976.
- [73] Lev B. Okun. Leptons and Quarks. North-Holland, Amsterdam, Netherlands, 1982.

- [74] John F. Gunion, Howard E. Haber, Gordon L. Kane, and Sally Dawson. The Higgs Hunter's Guide, volume 80. 2000.
- [75] A. Alves, E. Ramirez Barreto, A. G. Dias, C. A. de S. Pires, F. S. Queiroz, and P. S. Rodrigues da Silva. Probing 3-3-1 Models in Diphoton Higgs Boson Decay. Phys. Rev. D, 84:115004, 2011.
- [76] J. Schechter and J. W. F. Valle. Neutrino decay and spontaneous violation of lepton number. Phys. Rev. D, 25:774–783, Feb 1982.
- [77] Marco A. Diaz, M. A. Garcia-Jareno, Diego A. Restrepo, and J. W. F. Valle. Seesaw Majoron model of neutrino mass and novel signals in Higgs boson production at LEP. Nucl. Phys. B, 527:44–60, 1998.
- [78] Cesar Bonilla, Jorge C. Romão, and José W. F. Valle. Electroweak breaking and neutrino mass: ‘invisible’ Higgs decays at the LHC (type II seesaw). New J. Phys., 18(3):033033, 2016.
- [79] Sylvain Blunier, Giovanna Cottin, Marco Aurelio Díaz, and Benjamin Koch. Phenomenology of a Higgs triplet model at future e^+e^- colliders. Phys. Rev. D, 95(7):075038, 2017.
- [80] D. Cogollo, Ricardo D. Matheus, Têssio B. de Melo, and Farinaldo S. Queiroz. Type I + II Seesaw in a Two Higgs Doublet Model. Phys. Lett. B, 797:134813, 2019.
- [81] A. A. Aguilar-Arevalo et al. Significant Excess of ElectronLike Events in the Mini-BooNE Short-Baseline Neutrino Experiment. Phys. Rev. Lett., 121(22):221801, 2018.
- [82] João Paulo Pinheiro and C. A. de S. Pires. Vacuum stability and spontaneous violation of the lepton number at a low-energy scale in a model for light sterile neutrinos. Phys. Rev. D, 102(1):015015, 2020.
- [83] A. P. Lessa and O. L. G. Peres. Revising limits on neutrino-Majoron couplings. Phys. Rev. D, 75:094001, 2007.
- [84] Y. Chikashige, Rabindra N. Mohapatra, and R. D. Peccei. Are There Real Goldstone Bosons Associated with Broken Lepton Number? Phys. Lett. B, 98:265–268, 1981.
- [85] F. Ferrer and M. Nowakowski. Higgs and Goldstone bosons mediated long range forces. Phys. Rev. D, 59:075009, 1999.
- [86] Yoshitaka Kuno and Yasuhiro Okada. Muon decay and physics beyond the standard model. Rev. Mod. Phys., 73:151–202, 2001.

- [87] A. G. Akeroyd, Mayumi Aoki, and Hiroaki Sugiyama. Lepton Flavour Violating Decays $\tau \rightarrow \text{anti-}l \, l$ and $\mu \rightarrow e \, \gamma$ in the Higgs Triplet Model. Phys. Rev. D, 79:113010, 2009.
- [88] A. Aguilar-Arevalo et al. Evidence for neutrino oscillations from the observation of $\bar{\nu}_e$ appearance in a $\bar{\nu}_\mu$ beam. Phys. Rev. D, 64:112007, 2001.
- [89] Gary Steigman. Neutrinos And Big Bang Nucleosynthesis. Adv. High Energy Phys., 2012:268321, 2012.
- [90] N. Aghanim et al. Planck 2018 results. VI. Cosmological parameters. Astron. Astrophys., 641:A6, 2020.
- [91] Jan Hamann, Steen Hannestad, Georg G. Raffelt, and Yvonne Y. Y. Wong. Sterile neutrinos with eV masses in cosmology: How disfavoured exactly? JCAP, 09:034, 2011.
- [92] A. Arhrib, R. Benbrik, M. El Kacimi, L. Rahili, and S. Semlali. Extended Higgs sector of 2HDM with real singlet facing LHC data. Eur. Phys. J. C, 80(1):13, 2020.
- [93] Daniel A. Camargo, Alex G. Dias, T  ssio B. de Melo, and Farinaldo S. Queiroz. Neutrino Masses in a Two Higgs Doublet Model with a U(1) Gauge Symmetry. JHEP, 04:129, 2019.
- [94] Garv Chauhan. Vacuum Stability and Symmetry Breaking in Left-Right Symmetric Model. JHEP, 12:137, 2019.
- [95] Joydeep Chakraborty, Moumita Das, and Subhendra Mohanty. Constraints on TeV scale Majorana neutrino phenomenology from the Vacuum Stability of the Higgs. Mod. Phys. Lett. A, 28:1350032, 2013.
- [96] Archil Kobakhidze and Alexander Spencer-Smith. Neutrino Masses and Higgs Vacuum Stability. JHEP, 08:036, 2013.
- [97] J. N. Ng and Alejandro de la Puente. Electroweak Vacuum Stability and the Seesaw Mechanism Revisited. Eur. Phys. J. C, 76(3):122, 2016.
- [98] Ila Garg, Srubabati Goswami, K. N. Vishnudath, and Najimuddin Khan. Electroweak vacuum stability in presence of singlet scalar dark matter in TeV scale seesaw models. Phys. Rev. D, 96(5):055020, 2017.
- [99] Seyda Ipek, Alexis D. Plascencia, and Jessica Turner. Assessing Perturbativity and Vacuum Stability in High-Scale Leptogenesis. JHEP, 12:111, 2018.
- [100] Steen Hannestad, Rasmus Sloth Hansen, and Thomas Tram. How Self-Interactions can Reconcile Sterile Neutrinos with Cosmology. Phys. Rev. Lett., 112(3):031802, 2014.

- [101] Maria Archidiacono, Stefano Gariazzo, Carlo Giunti, Steen Hannestad, Rasmus Hansen, Marco Laveder, and Thomas Tram. Pseudoscalar—sterile neutrino interactions: reconciling the cosmos with neutrino oscillations. JCAP, 08:067, 2016.
- [102] Basudeb Dasgupta and Joachim Kopp. Cosmologically Safe eV-Scale Sterile Neutrinos and Improved Dark Matter Structure. Phys. Rev. Lett., 112(3):031803, 2014.
- [103] Xiaoyong Chu, Basudeb Dasgupta, Mona Dentler, Joachim Kopp, and Ninetta Saviano. Sterile neutrinos with secret interactions—cosmological discord? JCAP, 11:049, 2018.
- [104] C. A. de S. Pires. A cosmologically viable eV sterile neutrino model. Phys. Lett. B, 800:135135, 2020.
- [105] Djuna Croon, Nicolas Fernandez, David McKeen, and Graham White. Stability, reheating and leptogenesis. JHEP, 06:098, 2019.